SYNTHETIC RECOGNITION SYSTEMS: SELF-ASSEMBLY AND METAL CHELATION

by

Neil R. Branda
B. Sc., Chemistry and Biochemistry
University of Toronto

submitted to the Department of Chemistry in partial fulfillment of the requirements for the degree of
Doctor of Philosophy

at the
Massachusetts Institute of Technology
May 1994

Signature of Author.....
Department of Chemistry
May 12, 1994

Certified by.....
Professor Julius Rebek, Jr.
Thesis Supervisor

Accepted by.....
Professor Glenn A. Berchtold
Chairman, Departmental Committee on Graduate Students

This doctoral thesis has been examined by a Committee of the Department of Chemistry as follows:

Professor Peter T. Lansbury, Jr.....
Chairman

Professor Julius Rebek, Jr.....
Thesis Supervisor

Professor Glenn A. Berchtold.....

- to my loving wife, Erica -

SYNTHETIC RECOGNITION SYSTEMS: SELF-ASSEMBLY AND METAL CHELATION

by

Neil R. Branda

Submitted to the Department of Chemistry on May 12, 1994 in partial fulfillment of the requirements for the degree of Doctor of Philosophy in Chemistry

ABSTRACT

Host molecules were designed and synthesized for use in self-assembly or metal ligation. Each system was programmed by the specific tailoring of appropriate functionality:

Simple concave amides with the potential to form well-ordered three-dimensional aggregates through hydrogen bonds were prepared and crystallized. Methane-, *cis*-cyclopropane and *trans*-cyclopropanetricarboxamide crystallized into arrays of stacked columns, cyclohexane-type chairs and sheets respectively. Alternating enantiomers of an α-bridged diketopiperazine assembled into interlocking ribbons in a "zipper" motif.

An "upper-rim" amide-functionalized calix[4]arene formed a dimeric "football" aggregate through amide-amide hydrogen bonds. Association constants were 210 and 446 M^{-1} in 20% and 5% methanol/chloroform as determined from ^1H NMR titrations. Mass spectrometry showed the dimer was the only aggregate present.

A dimeric "tennis-ball" assembly was detected by mass spectrometry, VPO, crystal data and ^1H NMR studies. The dimer reversibly bound small convex organic molecules in $CDCl_3$ solutions with K_{inc} values ranging from 0.015 to 75 M^{-1}. In most cases, the encapsulated guests' resonances were directly visualized in the spectra. In DMF-d_7, there was a dynamic dimerization process observed, and the addition of guests induced the formation of the dimer. Examples include, methane and the noble gases. The encapsulation was reversibly regulated by changing the acidity of the medium.

Seven organic soluble polycarboxylates were prepared and their abilities to extract uranyl ion (UO_2^{2+}) from aqueous solutions were tested by scintillation counting. Values as high as one equivalent of UO_2^{2+} per molecule of ligand were measured.

The participation of the imide nitrogen of bicyclic Kemp's triacid derivatives was investigated using ^{18}O-labeling techniques. When both imide carbonyls are in the ring system, no participation was observed. Acyclic imide derivatives showed participation.

A series of chiral bis(2-oxazoline) ligands were prepared from a versatile carbazole diacid synthon. A crystal structure revealed that the ligands' nitrogen atoms are perfectly positioned to satisfy three of the four sites necessary to complex square planar metals such as nickel and copper. The nickel complexes exhibited high activity towards olefin epoxidation and was partially selective to *trans*-olefins, but no enantioselectivity was observed. The copper complexes were ineffective at mediating cyclopropanation reactions.

Thesis Supervisor: Dr. Julius. Rebek, Jr.
Title: Camille Dreyfus Professor of Chemistry

Table of Contents

List of Figures

List of Schemes

List of Tables

General Introduction

The ability of individual molecules to intimately recognize and discriminate between closely related partners is the foundation of basic biological functions. At one time this was thought to be only possible by large macromolecules. In nature, highly ordered structures contain the information required not only to recognize a substrate molecule but also to perform a specific chemical transformation. This information is attributed to specific non-covalent interactions regulated by arrays of functionality attached to macromolecular scaffolds. The outcome is the development of complicated molecular circuitry whose functions are dictated through weak intermolecular forces. This chemical communication between macromolecules cannot be easily deciphered by using small single-specied molecules, and bio-organic chemists have been obsessed with finding alternatives.[1]

Bio-organic chemistry is a discipline that is concerned with the application of the ideas of chemistry to the understanding of biochemical processes.[1] Such an understanding is achieved with the aid of synthetic molecular models. The design and synthesis of such biological mimics can no longer be considered a new field, and the past decade has been witness to an explosive introduction of new biomodels. The general goal is to fabricate molecules that can catalyze interesting reactions without the need for the complex backbones encountered in natural systems. These biomodels are intended to be utilitarian means of isolating and studying particular biochemical factors. They can also lead to novel catalysts and transporters, capable of functions not seen in biological systems, with comparable efficiency and selectivity. Biomodels have the advantage over naturally occuring systems in that they are structurally simpler and more compliant to chemical modification.

A major concept behind the development of biomimetics is molecular recognition. The importance of this discipline was publically recognized in 1987 when the Nobel prize for chemistry was awarded to Pedersen,[2] Cram,[3] and Lehn.[4] Molecular recognition

implies not only binding but selection and specific functions. Drug design is also a major goal in the area of *host-guest chemistry*. At present numerous research groups are devoted to the development of *supramolecules*[5] or assemblies in order provide a better understanding of natural phenomena. Targets include replication, regulation, transport, and molecular assembly.

References

(1) For a general introduction to bio-organic chemistry, see: Dugas, H. *Bioorganic Chemistry*; Springer-Verlag: New York, 1988.

(2) Pedersen, C. J. *Angew. Chem. Int. Ed. Engl.* (Nobel Lecture) **1988**, *27*, 1021-1027.

(3) Cram, D. J. *Angew. Chem. Int. Ed. Engl.* (Nobel Lecture) **1988**, *27*, 1009-1020.

(4) Lehn, J.-M. *Angew. Chem. Int. Ed. Engl.* (Nobel Lecture) **1988**, *27*, 89-112.

(5) Lehn, J.-M. *Angew. Chem. Int. Ed. Engl.* **1990**, *29*, 1304-1319.

Part I. Self-Assembly

Chapter One. Self-Assembly Through Hydrogen Bonds

1.1 Historical Introduction

Self-assembly is the spontaneous generation of higher-ordered species from many subunits, leading to the generation of long-range three-dimensional order.[1-3] The information required to create this molecular order is expressed as each component's ability to interact with another through non-covalent bonds and steric interactions or repulsions. It is the balance of these factors that allows for the finding of an energetically favourable assembly. The cooperation of magnitude, orientation and directionality of the weak interactions is paramount to the design of successful assembling systems. Investigations of simple systems are expected to provide insight into the nature of biological organization and recognition, with the development of synthetic transporters and reaction chambers a likely goal.

Biological Self-Assembly

One of the major driving forces for developing synthetic molecular assemblies is the realization that the components of biological systems possess the architectural information required for their own assembly, as well as the ability to carrying out these functions under mild conditions. Examples of natural assemblies include clathrin triskelions,[4-6] nystatin and amphotericin B barrel staves,[7,8] and viral protein coats.[9]

Viruses are one of the predominant players in the area of biological self assembly and are inspiring examples of molecular ordering and information storage. They appear in a multitude of shapes, sizes and molecular composition, but inevitably they all must undergo membrane transport to deliver their genetic material. Only then can the virus utilize the host's biochemical systems to generate further offspring and ensure its

immortality. The viral genetic material is surrounded by a three-dimensional protein shell or capsid. It is this encapsulation that allows the virus to deliver its hydrophillic nucleotides through a lipid bilayer membrane. However, a polynucleic acid cannot generate one protein molecule of substantial size to encapsulate it. Rather, it requires large superstructures formed from multiple identical self-complementary subunits. The simplest viruses have only one type of polypeptide chain which assembles into rods or closed-shell spheres around the genetic material. In higher organisms viruses are found that adopt many different protein subunits to assemble complex spherical shells.

One of the most extensively studied three-dimensional viral assemblies is used by the tobacco mosaic virus (TMV).[10-12] Each subunit is self-complementary and initially assembles into a disc-shaped 34-mer. Only in the presence of the viral RNA, does full assembly take place. The outcome is a cylindrical container of 2130 subunits (Figure 1).

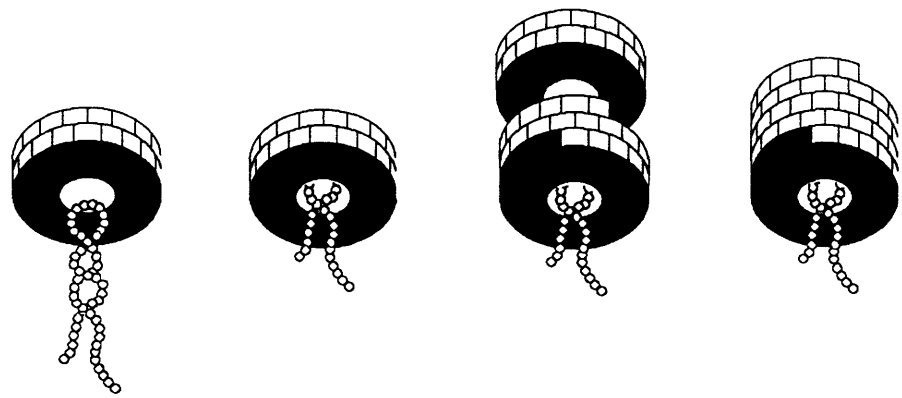

Figure 1. *Schematic representation of the self-assembly of the tobacco mosaic virus. It is not until the genetic material is present, that the formation of a 34-meric cylinder is achieved.*

Self-Assembly Through Metallic Interactions

Metal ligation is one of the interactions that has been commonly exploited by researchers over the past decade to control molecular organization. The coordination to

metals provides structural flexibility and, to some degree, directionality (as long as the structure around the metal coordination sphere is taken into consideration). Pertinent examples of assemblies brought about through metal interactions include helical polybipyridines **I**,[13-20] multicomponent cylinders **II**,[21] and metal ion-assisted helices of polypeptides.[22,23]

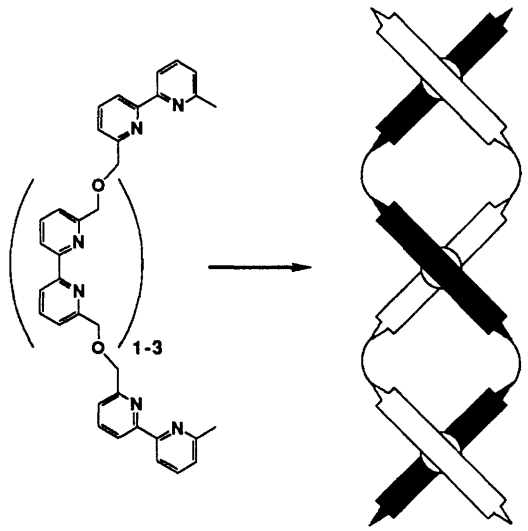

I

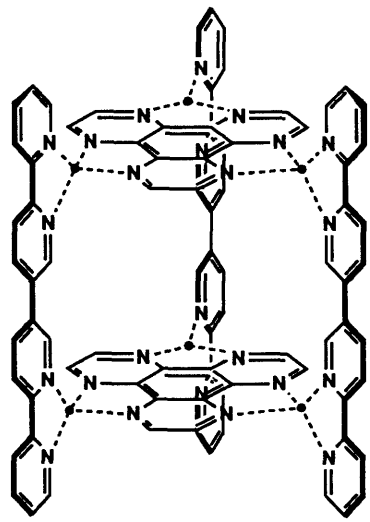

II

Self-Assembly Through Hydrogen Bonds

The predictable directionality of the hydrogen bond makes it an effective interaction for directing self-assembly.[24] The occurence of non-specific aggregates can be reduced, making the design of synthetic systems easier. Examples of synthetic systems exhibiting controlled molecular order through hydrogen bonds include molecular "boxes" composed of cyclocholates[25] or porphyrins,[26] two-component helices,[27] pyridinones,[28-32] complicated arrays of barbiturates and melamines,[3,33,34] polypeptide nanotubes,[35] and carboxylic acids.[36] Some examples are outlined below (Figure 2).

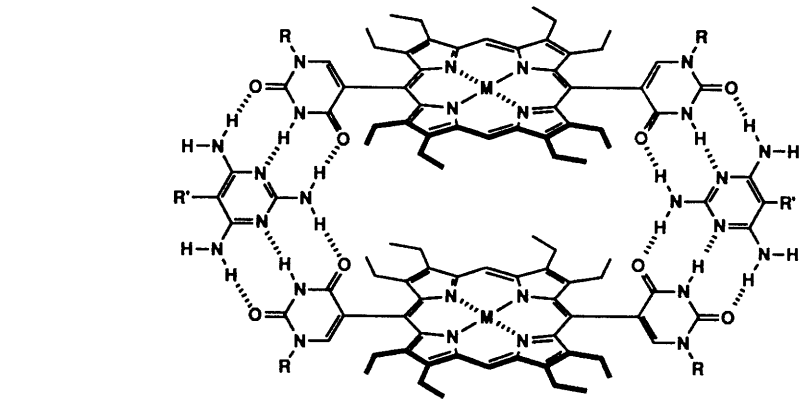

A

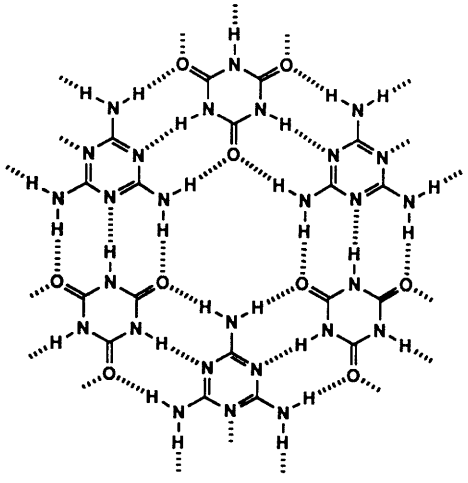

B

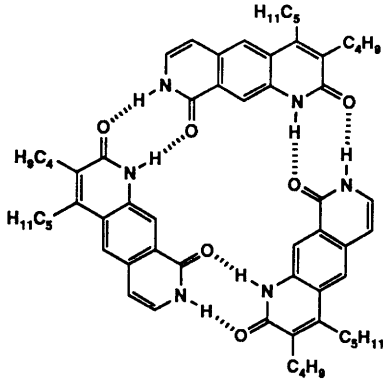

C

Figure 2. *Self-assembling porphyrin "box" (A), melamine-barbiturate mosaic (B) and pyridinone trimer (C).*

On the whole, most of the hydrogen bond donors and acceptors are provided by heteroatomic groups (amines, amides and imides, for example). However, there are also examples of self-assembled systems brought about through weaker hydrogen bonds involving sites that do not appear to be likely candidates at first glance. One example of such a system is the crystal structure of 1,3,5-tricyanobenzene (**A**) (Figure 3),[37] with "hydrogen bonding" occuring between the aromatic hydrogens and the nitriles. There are

also self-assembling systems which do not involve any hydrogens but instead use charge-transfer interactions. The molecular tapes of cyanuric chloride (**B**)[38-41] are some examples. It is noteworthy that the forces required to obtain controlled molecular organization can be far weaker than the conventional hydrogen bonds.

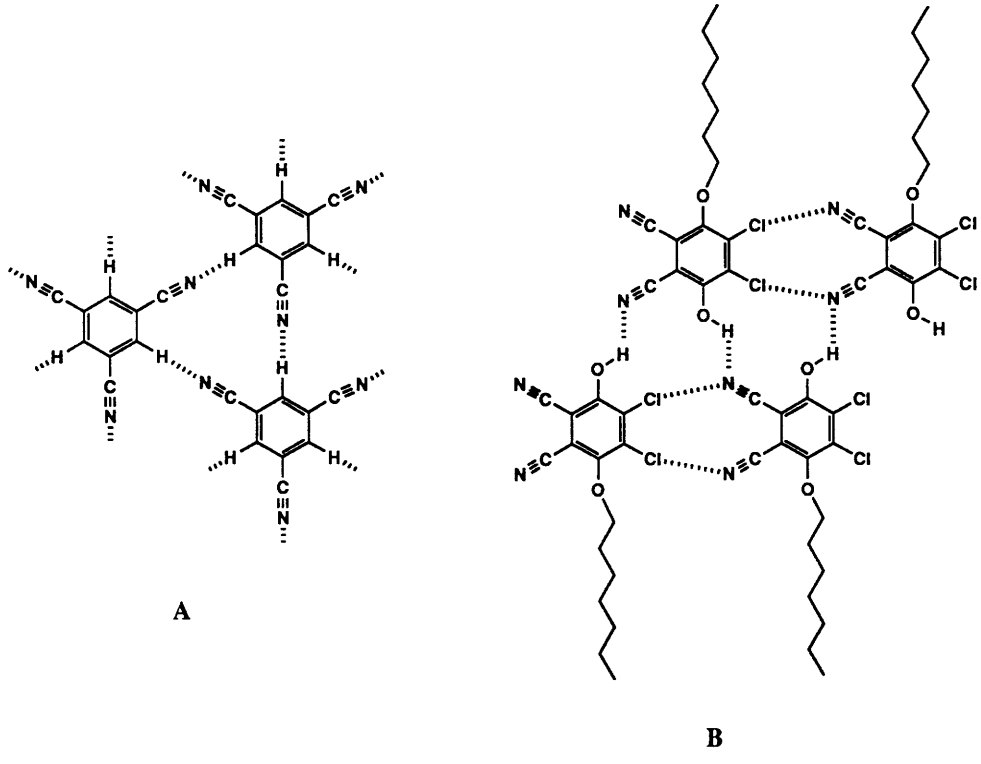

Figure 3. *Self-assembly through weak "hydrogen bonds" and charge-transfer interactions: 1,3,5-tricyanobenzene (A) and cyanuric chloride ribbon (B).*

An example that combines both metallic nucleation and hydrogen bonding interactions is the guanine quartet (a structure common in telomeric DNA).[42,43] In this instance the self-complementary Hoogsteen and Watson-Crick hydrogen bond faces are involved in hydrogen bonding (Figure 4). The presence of the metal ion is a prerequisite for the formation of the tetramer.

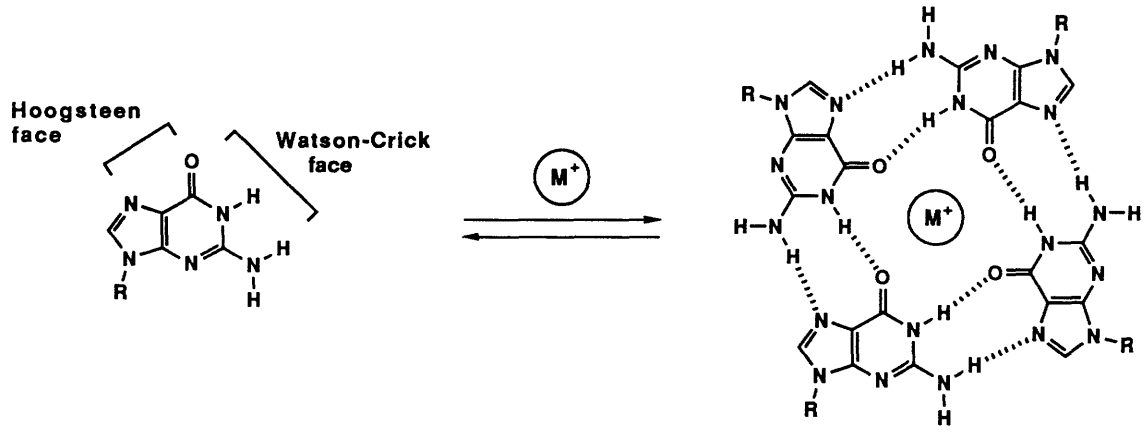

Figure 4. *A self-assembling G-quartet. The subunits interact through hydrogen bonds, although the nucleating metal ion is necessary for this formation.*

Self-Assemblies as New Materials

The macroscopic properties expressed by materials are dependent upon the chemical nature of the species involved *and* the nature of the relationship these species have with each other. It is therefore necessary, in order to prepare new materials, that both molecular and *supramolecular* considerations be examined. Historically, chemistry has been concerned mainly with the development of molecular materials through covalent synthesis, polymers being the prime examples. However, the development of larger supermolecular assemblies has prompted the investigation of molecular orientation as a solution for generating materials with novel properties.

Supermolecular assemblies can be divided into two general classes, discrete assemblies and networks. Discrete assemblies are those that lack any translational symmetry, that is, they are made up of a finite number of molecules.[44] The dimer of benzoic acid is an example. It is unlikely that discrete assemblies will possess any interesting properties as new materials because they lack macroscopic superstructure, although they are attractive as transporters and reaction chambers. Networks are assemblies that contain translational symmetry and, in theory, can be made up of an infinite

number of subunits. Network assemblies can be classified as one-dimensional rods (α-networks) with one degree of translational symmetry, two-dimensional layers (β-networks), and three-dimensional lattices (γ-networks).[44] β-networks may contain independent α-network structures, while γ-networks may be made up of both α- and β-networks. Examples of both classes of assemblies are depicted below (Figure 5).

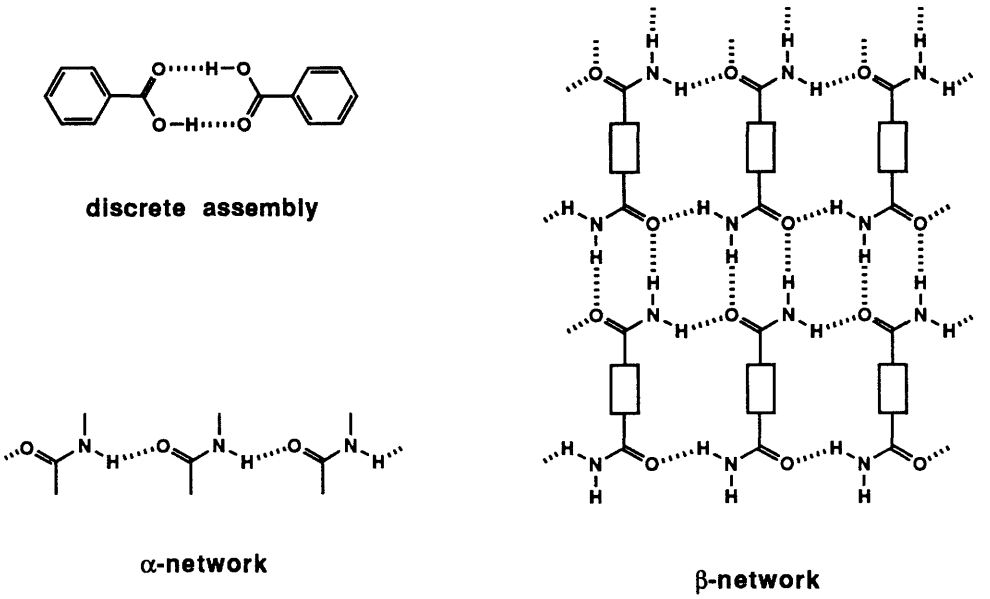

Figure 5. *Examples of discrete and network self-assembled systems.*

Lehn has reported the spontaneous assembly of "molecular tapes" through triple NH-O hydrogen bonds of 2,4,6-triaminopyridine and barbituric acid derivatives **A**.[45] This sorting of "like and unlike" species (alternating monomers) as well as left-right differentiation at the molecular level (all like units are located on the same side of the polymer's axis) is a strong argument for the idea that individual molecules that possess the correct information will assemble into a well defined and predicted geometry. The author suggests that these polymers may have interesting macroscopic properties such as optical, electronic, ionic, or magnetic.[46] Other researchers have recently reported the gel-like properties of similar species.[47]

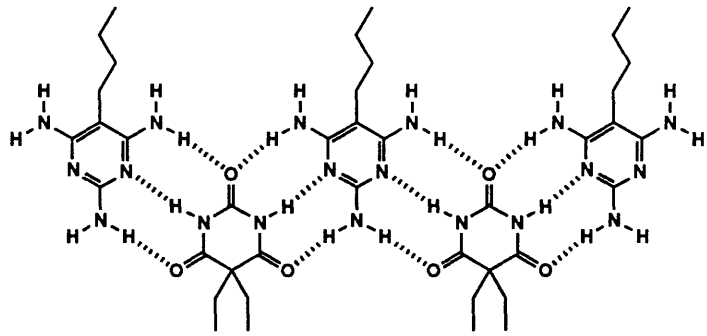

A

Much of the progress in the area of self-assemblies as new materials has revolved around the development of two-dimensional assemblies, most commonly brought about through hydrogen bonds.[44,48] The extension into the third dimension is necessary to fully realize the potential of self-assembled systems as new materials. For this persuit, three dimensional subunits are necessary.

References

(1) Lehn, J.-M. *Angew. Chem. Int. Ed. Engl.* **1990**, *29*, 1304-1319.

(2) Lindsey, J. S. *New J. Chem.* **1991**, *15*, 153-180.

(3) Whitesides, G. M.; Mathias, J. P.; Seto, C. T. *Science* **1991**, *254*, 1312-1319.

(4) Crowther, R. A.; Finch, J. T.; Pearse, B. M. F. *J. Mol. Biol.* **1976**, *103*, 785-798.

(5) Heuser, J. *J. Cell. Biol.* **1980**, *84*, 560-583.

(6) Ungewickell, E.; Branton, D. *Nature* **1981**, *289*, 420-422.

(7) Kleinberg, M. E.; Finkelstein, A. *J. Membrane Biol.* **1984**, *80*, 257-269.

(8) Yeagle, P. *The Structure of Biological Membranes*; CRC Press: London, 1992; pp 726-730.

(9) Branden, D.; Tooze, J. *The Structure of Spherical Viruses*; Garland Publishing: New York, 1991; Chapter 11, pp 161-176.

(10) Caspar, D. L. D. *Biophys. J.* **1980**, *32*, 103-135.

(11) Klug, A. *Angew. Chem. Int. Ed. Engl.* **1983**, *22*, 565-582.

(12) Namba, K.; Stubb, G. *Science* **1986**, *231*, 1401-1406.

(13) Bernardinelli, G.; Piguet, C.; Williams, A. F. *Angew. Chem. Int. Ed. Engl.* **1992**, *31*, 1622-1624.

(14) Carina, R. F.; Bernardinelli, G.; Williams, A. F. *Angew. Chem. Int. Ed. Engl.* **1993**, *32*, 1463-1465.

(15) Constable, E. C.; Hannon, M. J.; Tocher, D. A. *Angew. Chem. Int. Ed. Engl.* **1992**, *31*, 230-232.

(16) Constable, E. C. *Tetrahedron* **1992**, *48*, 10013-10059.

(17) Constable, E. C.; Edwards, A. J.; Raithby, P. R.; Walker, J. V. *Angew. Chem. Int. Ed. Engl.* **1993**, *32*, 1465-1467.

(18) Huang, C.; Lynch, V.; Anslyn, E. V. *Angew. Chem. Int. Ed. Engl.* **1992**, *31*, 1244-1246.

(19) Krämer, R.; Lehn, J.-M.; DeCian, A.; Fischer, J. *Angew. Chem. Int. Ed. Engl.* **1993**, *32*, 703-706.

(20) Lehn, J.-M.; Rigault, A. *Angew. Chem. Int. Ed. Engl.* **1988**, *27*, 1095-1097.

(21) Baxter, P.; Lehn, J.-M.; DeCian, A.; Fischer, J. *Angew. Chem. Int. Ed. Engl.* **1993**, *32*, 69-72.

(22) Ghadiri, M. R.; Soares, C.; Choi, C. *J. Am. Chem. Soc.* **1992**, *114*, 825-831.

(23) Ghadiri, M. R.; Case, M. A. *Angew. Chem. Int. Ed. Engl.* **1993**, *32*, 1594-1597.

(24) Etter, M. C. *J. Am. Chem. Soc.* **1990**, *23*, 120-126.

(25) Bonar-Law, R. P.; Sanders, J. K. M. *Tetrahedron Lett.* **1993**, *34*, 1677-1680.

(26) Drain, C. M.; Fischer, R.; Nolen, E. G.; Lehn, J.-M. *J. Chem. Soc., Chem. Commun.* **1993**, 243-245.

(27) Geib, S. J.; Vincent, C.; Fan, E.; Hamilton, A. D. *Angew. Chem. Int. Ed. Engl.* **1993**, *32*, 119-212.

(28) Ducharme, Y.; Wuest, J. D. *J. Org. Chem.* **1988**, *53*, 5787-5789.

(29) Gallant, M.; Viet, M. T. P.; Wuest, J. D. *J. Am. Chem. Soc.* **1991**, *113*, 721-723.

(30) Persico, F.; Wuest, J. D. *J. Org. Chem.* **1993**, *58*, 95-99.

(31) Simard, M.; Su, D.; Wuest, J. D. *J. Am. Chem. Soc.* **1991**, *113*, 4696-4698.

(32) Zimmerman, S. C.; Duerr, B. F. *J. Org. Chem.* **1992**, *57*, 2215-2217.

(33) Seto, C. T.; Whitesides, G. M. *J. Am. Chem. Soc.* **1990**, *112*, 6409-6411.

(34) Seto, C. T.; Whitesides, G. M. *J. Am. Chem. Soc.* **1991**, *113*, 712-713.

(35) Ghadiri, M. R.; Granja, J. R.; Milligan, R. J.; McRee, D. E.; Khazanovich, N. *Nature* **1993**, *366*, 324-327.

(36) Ebby, N.; Lapasset, J.; Pizzala, L.; Aycard, J.; Bodot, H. *Acta. Cryst.* **1985**, *C41*, 567-570.

(37) Reddy, D. S.; Goud, B. S.; Panneerselvam, K.; Desiraju, G. R. *J. Chem. Soc., Chem. Commun.* **1993**, 663-664.

(38) Desiraju, G. R.; Harlow, R. L. *J. Am. Chem. Soc.* **1989**, *111*, 6757-6764.

(39) Reddy, D. S.; Panneerselvam, K.; Pilati, T.; Desiraju, G. R. *J. Chem. Soc., Chem. Commun.* **1993**, 661-662.

(40) Pascal, R. A., Jr.; Ho, D. M. *Tetrahedron Lett.* **1992**, *33*, 4707-4708.

(41) Xu, K.; Ho, D. M.; Pascal, R. A., Jr. *J. Am. Chem. Soc.* **1994**, *116*, 105-110.

(42) Barr, R. G.; Pinnavaia, T. G. *J. Phys. Chem.* **1986**, *90*, 328-334.

(43) Williamson, J. R.; Cech, T. R. *Cell* **1989**, *59*, 871-880.

(44) Chang, Y.; West, M.; Fowler, F. W.; Lauher, J. W. *J. Am. Chem. Soc.* **1993**, *115*, 5991-6000.

(45) Lehn, J.-M.; Mascal, M.; DeCian, A.; Fischer, J. *J. Chem. Soc., Chem. Commun.* **1990**, 479-481.

(46) Lehn, J.-M.; Mascal, M.; DeCian, A.; Fischer, J. *J. Chem. Soc. Perkin Trans. 2* **1992**, 461-467.

(47) Hanabusa, K.; Miki, T.; Taguchi, Y.; Koyama, T.; Shirai, H. *J. Chem. Soc., Chem. Commun.* **1993**, 1382-1384.

(48) Zhao, X.; Chang, Y.; Fowler, F. W.; Lauher, J. W. *J. Am. Chem. Soc.* **1990**, *112*, 6627-6634.

1.2 Solid State Self-Assembly of Small Organic Molecules Through Hydrogen Bonds

Introduction

Studying self-assemblies in the solid state is advantageous because statistical mixtures of aggregates are minimized, and the structural features can be fully elucidated through the use of crystallographic visualizing techniques. The extension into solution is not unreasonable since the forces governing the formation of supramolecular assemblies in solution and the solid state are much the same (primarily electrostatics, hydrogen bonds and van der Waal's). Solid state assembly however, has the distinct disadvantage in that all the intermolecular forces must comply with the laws of crystal packing. These laws can be expressed in terms of symmetry relationships and group theory, which may not be critical for assemblies in solution. Prior to solution studies, an examination of the aggregation tendencies in the solid state would provide insight into what geometrical features are necessary to create controlled molecular order. Only then, can the species which form successful assemblies be considered as key players for investigations in solution.

In order to determine the architectural features necessary to promote self-assembling of well-defined structures, a series of small molecules was examined. Although the formation of ordered networks from smaller subunits is not yet predictable, the systematic solid state studies of Etter and coworkers[1] provide a better understanding of the preferred hydrogen bonding patterns. Taking these guidelines into consideration allows for a more facile design of potential self-assembling building blocks. A review of the literature highlighted a number of simple, synthetically accessible candidates. All molecules possess hydrogen bonding donor and acceptor sites suitable for promoting the formation of ordered three-dimensional assemblies through hydrogen bonds.

Methanetricarboxamide

The simplest system that can be envisioned is methane tricarboxamide **1**.[2-4] The trigonal arrangement of self-complementary amides onto a concave scaffold provided by the central sp^3 carbon atom suggests the formation of three-dimensional assemblies through intramolecular amide hydrogen bonds. The likely closed-shell structures, as predicted by molecular modeling,[5] are rough spheres with diameters of ~12 and ~20 Å[6] when eight or twenty subunits interact (Figure 1). The structure shows strong intermolecular hydrogen bonds (NH-O distances are 2.70 Å and angles are 164 degrees). It must be noted that one of the key features in this system is the preorganization of the amides into the desired trigonally-symmetrical species. The three intramolecular hydrogen bonds between the carbonyl oxygens and adjacent nitrogen protons are the critical element enforcing this architecture.

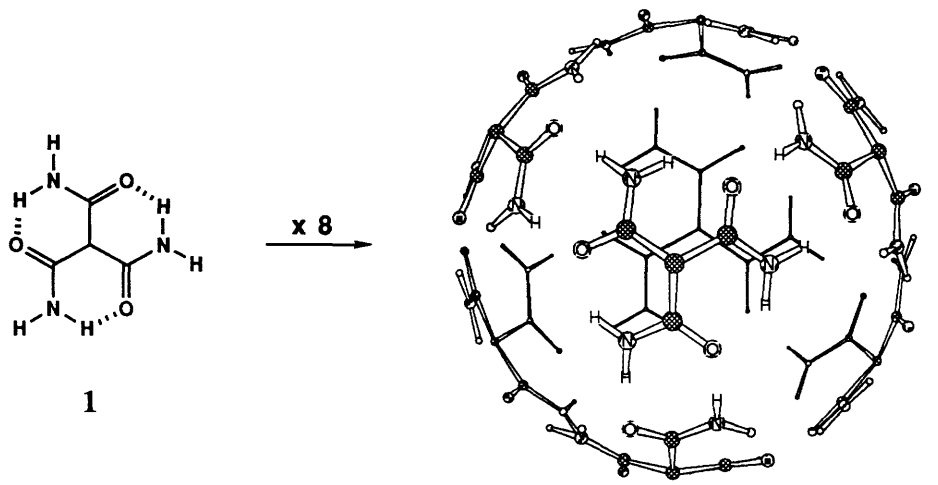

1

Figure 1. *Predicted spherical octameric assembly of methanetricarboxamide **1**, using MacroModel program with Amber force field. A spherical 20-mer was also predicted.*

Structures such as described above introduce a fundamental question with regards to self-assembly: How many hydrogen bonds are required to overcome the high entropy

price of bringing together many subunits? This question can only be solved by a thorough screening of potential self-assembling species.

Methane tricarboxamide was prepared as described in the literature.[2] Acylation of diethyl malonate afforded triethyl methanetricarboxylate[3,4] which was amidated with alcoholic ammonia. X-ray quality crystals were obtained directly from the reaction medium.

The ORTEP diagram of triamide **1** revealed that the expected intramolecular hydrogen bonds were not present (Figure 2). The molecule does exhibit a *C-3* axis of symmetry, but the amide groups were twisting into a 'propeller'-type geometry (the plane of the amides are rotated, on average, ~30 degrees from the *C-3* axis, C2-H1). Although the distances between nitrogen and oxygen atoms of adjacent amide groups appear adequate for hydrogen bonding (~3.3 Å), the rotation produces NH-O distances of ~3.5 Å which are substantially too long. This result is unexpected because the molecule was designed with the alignment of the strong intramolecular hydrogen bonding partners taken into account. The lack of this intramolecular locking gives rise to an architecture that is not attractive for producing the desired closed-shell assembly patterns. The amides of the "propeller" structure are positioned in a way that will not allow for spherical aggregation.

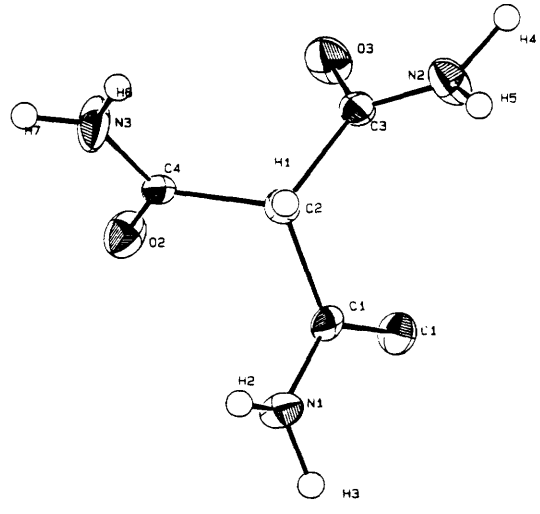

atom pair	distance (Å)
N1-O2	3.361
N2-O1	3.244
N3-O3	3.371
H2-O2	3.540
H6-O3	3.362
H5-O1	3.492

Figure 2. *ORTEP plot of methanetricarboxamide **1**. There is no evidence of intramolecular hydrogen bonding.*

An evaluation of the packing diagram of **1** (Figure 3) sheds light on the reason for the nonexistence of all intramolecular hydrogen bonds. Each subunit interacts through three hydrogen bonds to two others, resulting in a stacked column arrangement (**A**). Four structurally unique columns are vertically offset, and make up a quartet (**B**) which is repeated in all lateral directions (not shown in the figure). This packing pattern allows each monomer of **1** to hydrogen bond with two others within four laterally positioned columns. In the resulting stacked columns arrangement, ten surrounding molecules are hydrogen bonded to each monomer.

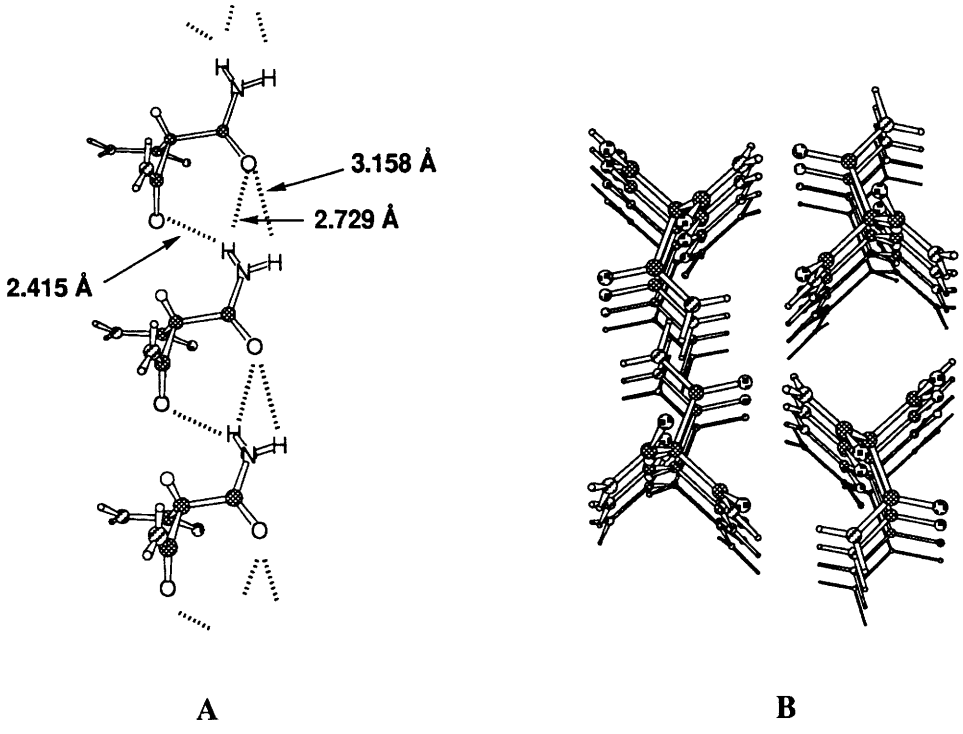

Figure 3. *Packing diagram of **1** showing the substructural columns on the left (**A**). Each of these columns is hydrogen bonded to four others (**B**).*

The sacrifice of one intramolecular hydrogen bond in order to form two intermolecular is not an unreasonable expectation in the solid state. The total sum of hydrogen bonds for each methanetricarboxamide unit is 18, and all are bifurcated (the

number of hydrogen bonds possible in the spherical closed-shell structures is 9 per subunit). In order to achieve tighter crystal lattice packing, intermolecular hydrogen bonds are favoured at the expense of the intramolecular bonds. The solid state assembly of **1** is an example of a well-ordered γ-lattice held together in all directions through hydrogen bonds.

Cyclopropanetricarboxamide

The second readily prepared molecule is cyclopropanetricarboxamide **2**, possessing similar, but more enhanced concavity as exhibited by methanetricarboxamide. Again, the intramolecular hydrogen bonds between adjacent carbonyl oxygens and nitrogen protons are critical to promote the optimal orientation of hydrogen bond donors and acceptors for intermolecular attractions. The concavity of the cyclopropane ring system provides a more optimal geometry for promoting intramolecular hydrogen bonds as compared to the methane derivative **1**. Although intramolecular NH-O distances are similar for both species (~2.6-2.7Å) the N-H-O angles for compound **2b** are more attractive to induce strong bonds (144 degrees as compared to 135 degrees for compound **1**).

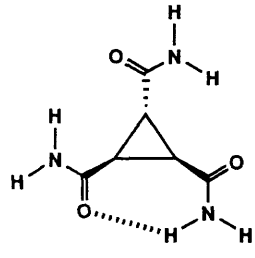

2a

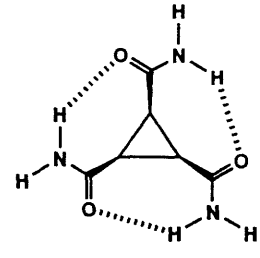

2b

Both the *cis*- and *trans*- isomers afford interesting possible self-assembling structures as elucidated by molecular modeling (Figure 4). Four molecules of the *cis*-isomer can occupy the corners of a distinct tetrahedral assembly (the inner dimensions were

estimated to be ~8.5 Å, intermolecular NH-O distances to be 2.70 Å and hydrogen bond angles to be 175 degrees). Although the more synthetically accessible *trans*-triamide **2a** does not exhibit the *C-3* symmetry required to fashion a closed-shell three-dimensional structure, modeling suggested the possibility of self-assembling into a fibrous α-network.

Trans-cyclopropanetricarboxamide **2a** was prepared as described in the literature[7,8] through the triethyl *trans*-cyclopropanetricarboxylate precursor. Amidation of this triester in aqueous ammonia resulted in the deposition of X-ray quality crystals of *trans*-amide **2a**.

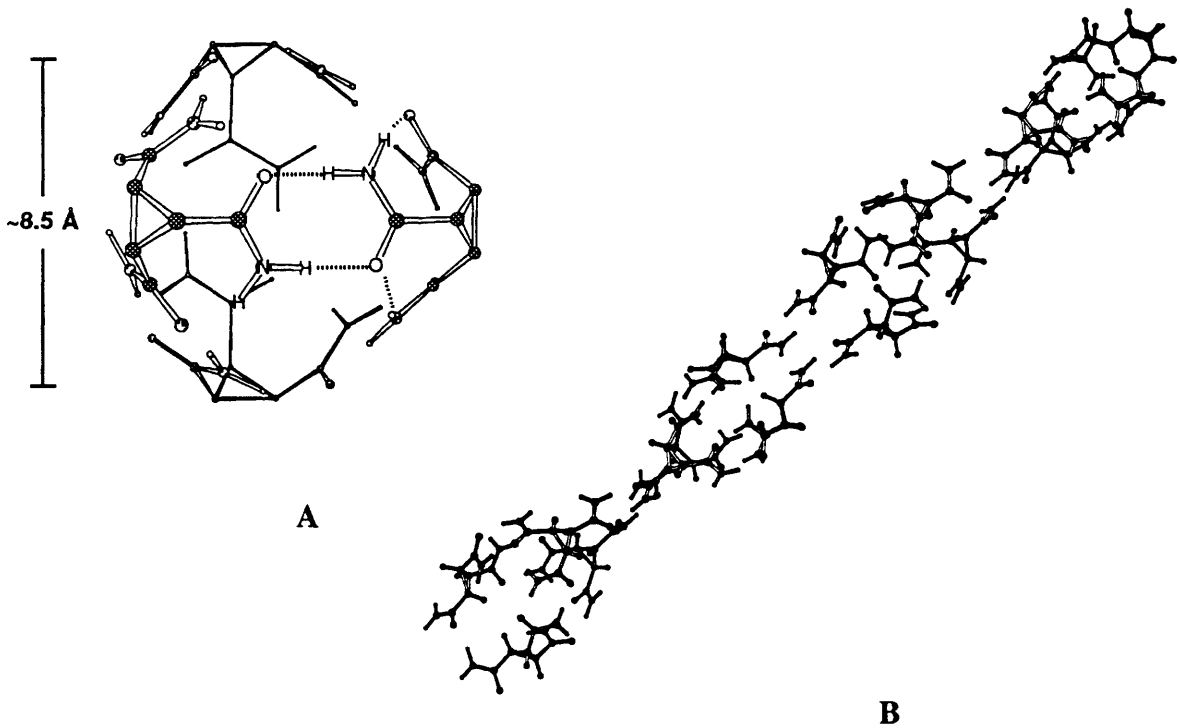

Figure 4. *Four molecules of the cis-cyclopropanetricarboxamide* ***2b*** *(A) were predicted to assemble into a closed-shell tetrahedron. A fiber assembly was predicted for trans-isomer* ***2a*** *(**B**).*

In a similar fashion to the crystal structure of methanetricarboxamide, the ORTEP diagram of **2a** reveals no internal hydrogen bonding (Figure 5). Instead, all amide groups are rotated into aligned positions, parallel to the mirror plane of a *meso*-symmetric structure.

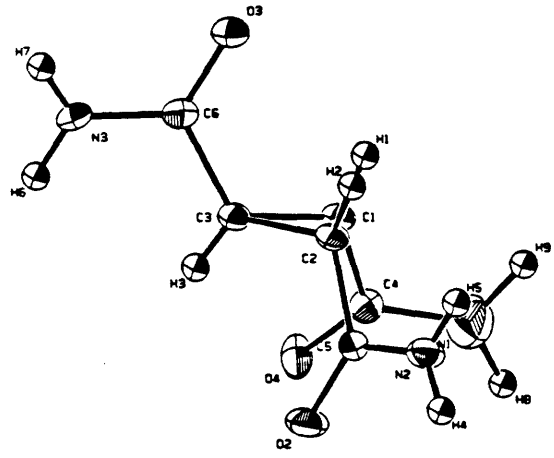

atom pair	distance (Å)
N1-O2	3.587
H8-O2	3.973
N2-O4	4.737
H4-O4	5.204

Figure 5. *ORTEP plot of trans-cyclopropanetricarboxamide* **2a**. *All amide groups are rotated out of plane resulting in a meso-structure.*

Isomer **2a** packed into an ordered arrangement with each subunit hydrogen bonded to ten surrounding molecules (Figure 6). Again, all hydrogen bonds are bifurcated and an increase in the number of these interactions was achieved by sacrificing any internal interactions (only one intramolecular hydrogen bond is possible in this case). The resulting assembly exhibited an ordered γ-network packing but lacked any interesting substructures.

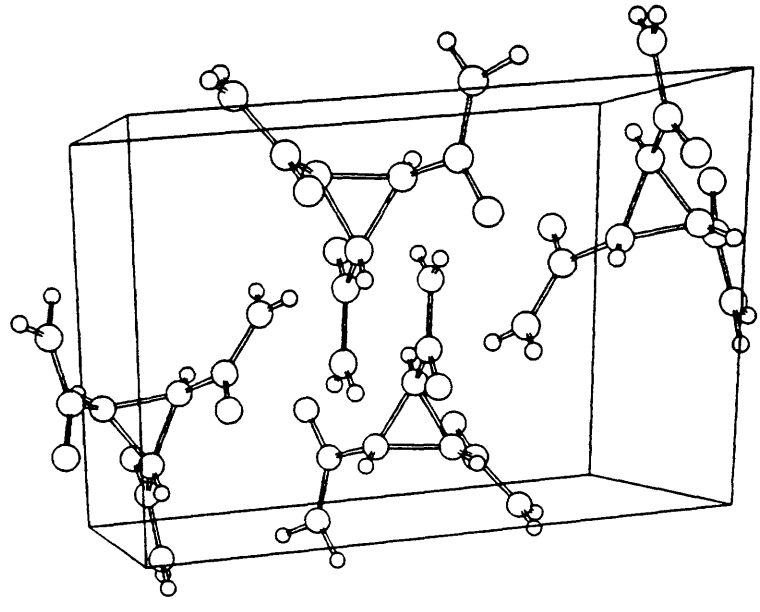

Figure 6. *Packing diagram of trans-cyclopropanetricarboxamide* **2a.**

Cis-cyclopropanetricarboxamide **2b** was prepared independently by the mild hydrolysis of the known *cis*-cyclopropanetrinitrile.[9-11] X-ray quality crystals were grown from an aqueous alcohol solution. In this instance, not all of the intramolecular hydrogen bonds were sacrificed to create a greater number of interactions with surrounding molecules (Figure 7). One of these bonds was retained, perhaps due to the enhanced concavity exhibited by the cyclopropane moiety as compared to methane.

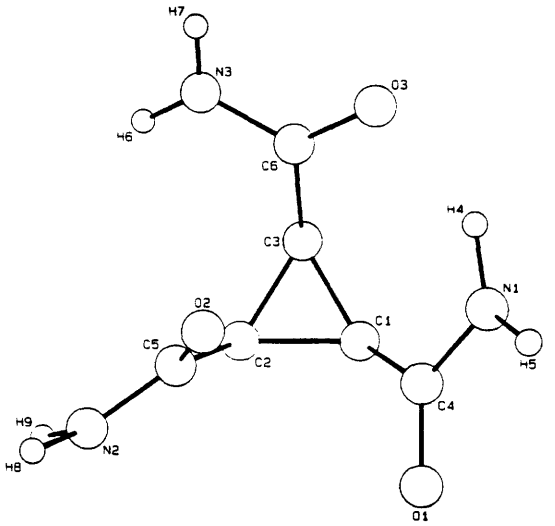

atom pair	distance (Å)
N1-O3	2.774
H4-O3	1.857
N3-O2	3.302
H6-O2	3.513
N2-O1	4.087
H8-O1	4.590

Figure 7. *Crystal structure of cis-cyclopropanetricarboxamide* ***2b****. One of the intramolecular hydrogen bonds remained.*

The resulting assembly was not a closed-shell structure, but a complicated γ-network, which on first impression appeared to lack any interesting substructures. A closer inspection of the packing diagram showed this to be untrue. When six subunits were isolated, a cyclohexane-type chair structure was realized (Figure 8). Each subunit of **2b** occupies one of the six corners of the chair skeleton with average hydrogen bond lengths of 3.24 Å. This chair-like mode of assembly was reported previously by Wuest and coworkers for polypyridinone systems.[12]

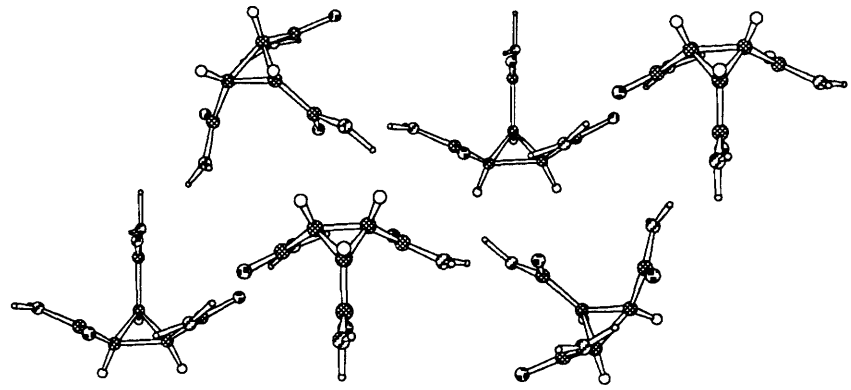

Figure 8. *Packing diagram of cis-isomer* ***2b*** *showing the cyclohexane-like chair substructure.*

Bridged Diketopiperazine

The structurally rigid bridged dilactam **3**[13,14] presents another interesting structurally unique candidate for self-assembling investigations in the solid state. The hydrogen bond donor and acceptor faces, provided by the lactams, are positioned at a 120 degree angle with respect to each other, and the covalently locked backbone eliminates the need for any intramolecular hydrogen bonds. The architecture of this system suggests the formation of discrete assemblies that, although they are not closed-shell structures, possess deep cyclindrical pockets.

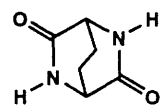

3

Molecular modeling predicted two contrasting structures that depend on the optical purity of the monomer. Alternating enantiomers of a racemic mixture were predicted to interact and result in a "zig-zag" α-network (Figure 9). Enantiomerically pure **3** modeled as a cyclic hexamer (a discrete assembly) of ~13 Å cross-section diameter and ~4.7 Å depth.

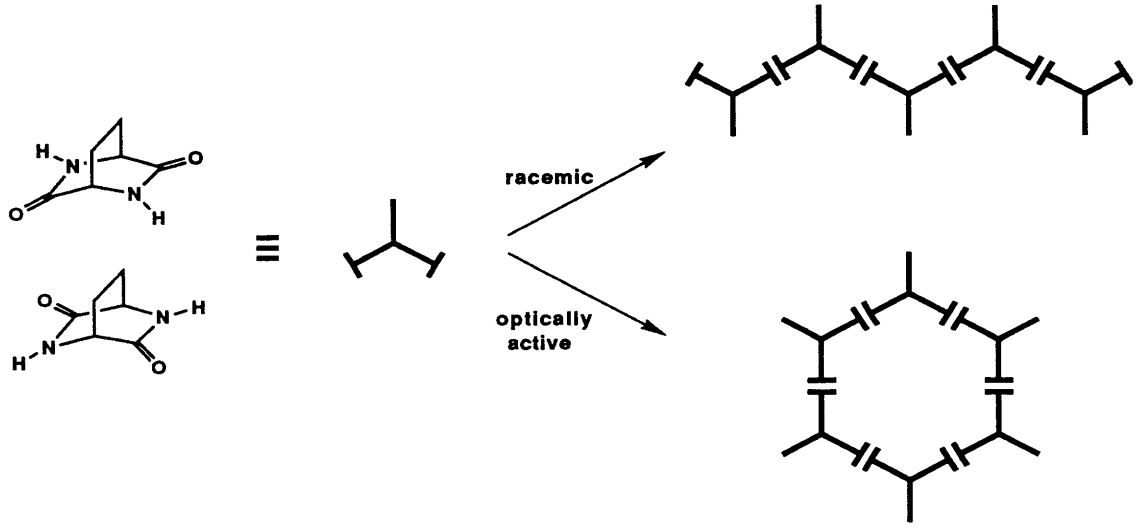

Figure 9. *The self-assembled structural motif of* ***3*** *is predicted to be dependent on the stereochemistry of the subunit.*

The dilactam **3** was prepared in racemic form by published methods.[13] X-ray quality crystals were grown from water-ethanol mixtures. Structural solution and refinement was hampered by disorder found within the crystal. Structures have not been resolved with reliability, although preliminary visualizations revealed the predicted assembly pattern. A rough packing sketch shows the existence of an array of interlocking "zig-zag" ribbons into a "zipper-like" mosaic (Figure 10). The assembly is composed of hydrogen bonded α-network ribbons held together into a γ-network by the hydrophobic interactions of the bridging methylenes.

Top view

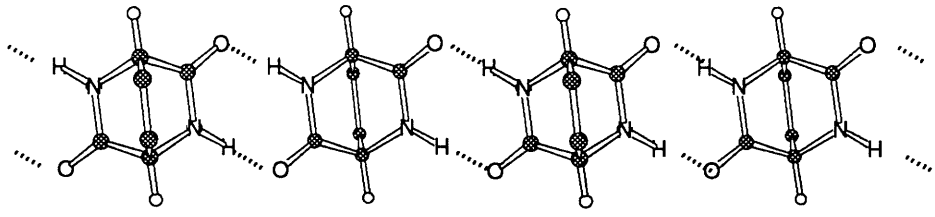

Side view

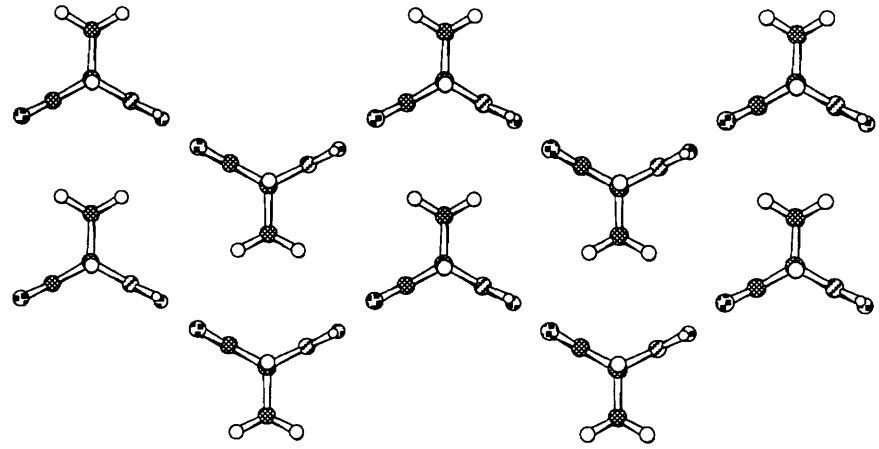

Figure 10. *Packing diagram of bis-lactam **3** showing the "zipper" mosaic.*

Discussion and Conclusions

The implications that can be drawn from these studies are as follows: 1) A completely rigid concave scaffold of hydrogen bond surfaces appears to be a prerequisite in order to obtain three dimensional assembly in the solid state. One cannot rely on an intramolecular hydrogen bond to lock the molecule into a fixed architecture. 2) The directionality provided by the hydrogen bonds must be unambiguous. There must not be other possible low energy conformations. The existence of other conformations will result in statistical mixtures, or more likely the predominance of the most energetically favourable *intermolecular* assembly. 3) A complicated γ-network at first sight might be overwhelming, but one must keep in mind the possibility that these highly symmetrical assemblies may be composed of discrete α- and β-networks. A thorough visual dissection of large arrays may lead to the isolation of interesting aggregates that are not initially obvious.

The elements of solid state interactions provide useful guidelines for developing potential self-assembling systems that are effective in solution. These guidelines cannot be

considered on their own. They must be considered with other structural occurrences that are statistically favourable in solution; however, the translational elements of the crystal data can certainly provide initial points to begin a thorough investigation for potential assemblies.

In the solid state, lattice energy is the major driving force for aggregation; therefore, the number of intermolecular interactions is maximized. In contrast, the entropy price for bringing together numerous subunits in solutions is high, and could override this driving force. The outcome is that, in solution, any intramolecular bonds will be favoured, and the formation of closed-shell structures is not unreasonable.

There is one great disadvantage of the systems discussed above. They are completely insoluble in most organic solvents. All characterization were carried out in aqueous solutions or in DMSO. This introduces a significant problem when attempting to bridge the gap between assemblies in the solid and solution states. The highly competitive nature of water and DMSO for hydrogen bonds destroys the likelihood of forming assemblies by solvating all hydrogen bond donor and acceptor sites.

Another lesson taught is the neccessity to eliminate structural ambiguity. Skeletal rigidity will provide a smaller number of structural contaminants by enforcing a more predictable (and reliable) orientation of hydrogen bond sites. This structural programming will eliminate random aggregation, and a less flexible architecture would, for this reason, certainly be desirable.

X-ray Crystallography

Crystal data was collected using a Rigaku AFC6R diffractometer and solved using Texsan-Texray Structure Analysis Package or by Mithril methods.

Methanetricarboxamide (1).

Crystal data: $C_4H_7N_3O_3$, formula weight 145.12, colourless orthorhombic plate crystals, 0.10 x 0.25 x 0.40 mm, space group Fdd2, a = 19.234(4), b = 22.534(4), c = 5.532(2) Å, V = 2398(2) $Å^3$, D_{calc} = 1.608 g/cm^3, Z = 16, $\mu(MoK\alpha)$ = 1.29 cm^{-1}, T = 23°C.

The crystals were stable at room temperature. A total of 1862 reflections were measured in ω-2θ scan mode (scan width (ω) 1.68 + 0.35 tanθ) at a rate of 16.0°/minutes, of which 931 were unique. The structure was solved by direct methods and refined with full-matrix least-squares methods. The final R factors were 3.4% and Rw = 3.8%. For atom coordinates, see appendix 1.

***Trans*-cyclopropanetricarboxamide (2a).**

Crystal data: $C_6H_9N_3O_3$, formula weight 171.16, colourless monoclinic block crystals, 0.40 x 0.50 x 0.50 mm, space group P2/n, a = 8.197(8), b = 10.564(8), c = 9.255(1) Å, β = 112.85(5), V = 738.6(3) $Å^3$, D_{calc} = 1.539 g/cm^3, Z = 4, $\mu(MoK\alpha)$ = 1.171 cm^{-1}, T = -78°C.

The crystals were stable at room temperature. A total of 1239 reflections were measured in ω-2θ scan mode (scan width (ω) 1.0 + 0.35 tanθ) at a rate of 0.79-8.24°/minutes, of which 1051 were unique. The structure was solved by direct methods and refined with full-matrix least-squares methods. Hydrogen atoms were located and refined. The final R factors were 3.8% and Rw = 5.3%. For atom coordinates, see appendix 2.

***Cis*-cyclopropanetricarboxamide (2b).**

Crystal data: $C_6H_9N_3O_3$, formula weight 171.16, colourless monoclinic parallelpiped crystals, 0.21 x 0.21 x 0.18 mm, space group $P2_1/n$, a = 5.3003(5), b = 11.538(1), c = 12.166(1) Å, β = 98.90(1), V = 735.1(2) $Å^3$, D_{calc} = 1.546 g/cm^3, Z = 4, $\mu(MoK\alpha)$ = 1.18 cm^{-1}, T = 23°C.

The crystals were stable at room temperature. A total of 989 reflections were measured in ω-2θ scan mode (scan width (ω) 0.80 + 0.35 tanθ) at a rate of 1.9-16.5°/minutes. The structure was solved by direct methods and refined with full-matrix least-squares methods. Hydrogen atoms were located and refined. The final R factors were 6.6% and Rw = 6.7%. For atom coordinates, see appendix 3.

References and Notes

(1) Etter, M. C. *J. Am. Chem. Soc.* **1990**, *23*, 120-126.

(2) Prelicz, D.; Sucharda-Sobczyk, A.; Kolodziejczyk, A. *Rocz. Chem.* **1970**, *44*, 49-59.

(3) Newkome, G. R.; Baker, G. R. *Org. Prep. Proced. Int.* **1986**, *18*, 117-144.

(4) Skarzewski, J. *Tetrahedron* **1989**, *45*, 4593-4598.

(5) Molecular modeling was performed on Silicon Graphics Personal Iris workstations (4D25 or 4D30) using MacroModel 3.5X. Mohamadi, F.; Richards, N. G.; Guida, W. C.; Liskamp, R.; Lipton, M.; Caufield, C.; Chang, G.; Hendrickson, T.; Still, W. C. *J. Comput. Chem.* **1990**, *11*, 440-467.

(6) Internal distances were estimated by directly measuring center to center atom distances from the molecular modeling generated structures.

(7) Buchner, E. *Chem. Ber.* **1888**, *21*, 2637-2647.

(8) Maier, G. *Chem. Ber.* **1962**, *95*, 611-615.

(9) Maria Tymoschenko, unpublished results.

(10) Griffin, G. W.; Peterson, L. I. *J. Org. Chem.* **1963**, *28*, 3219-3220.

(11) Hartman, A.; Hirshfeld, F. L. *Acta Cryst.* **1966**, *20*, 80-82.

(12) Simard, M.; Su, D.; Wuest, J. D. *J. Am. Chem. Soc.* **1991**, *113*, 4696-4698.

(13) Newman, H. *J. Heterocycl. Chem.* **1974**, *11*, 449-451.

(14) Kemp, D. S.; Sun, E. T. *Tetrahedron Lett.* **1982**, *23*, 3759-3760.

Chapter Two. Self-Assembly of a More Rigid Hydrogen Bonding Subunit: Towards the Preparation of a Self-Assembled Trilactam

2.1 Introduction

The solid state structures of the molecules previously described (chapter 1) established the need for structural rigidity when designing self-assembling building blocks. The α-bridged cyclic triglycine **1** possesses a degree of concavity and positioning of self-complementary hydrogen bond donors and acceptors between that of methane- and *cis*-cyclopropanetricarboxamide. However, molecule **1** has the advantage over the previously mentioned species in that it has a more structurally rigid skeleton, provided by the covalently linked cyclic backbone. This rigidity eliminates some of the possible structural variants discussed in the last section. Consequently, the trilactam does not have to rely solely on the existence of energetically favourable intramolecular hydrogen bonds to restrict the rotation and direction of hydrogen bonding groups. Instead, the directionality is provided by the chiral positioning of the lactam functions (enantiomers **1a** and **1b**).

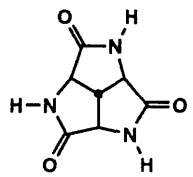

1a

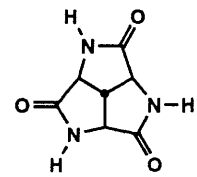

1b

The self-complementary binding of **1** can be expressed in two modes. One involves a lactam-lactam hydrogen bonding pair and the other, a glycine-glycine pair. Calculations by Jorgenson[1] indicated that the latter arrangement is favoured. For example, when six subunits occupy the corners of a cyclohexane-like chair structure (described previously for *cis*-cyclopropanetricarboxamide) the glycine-glycine pattern is more stable by 1.6 kcal/mole per hydrogen bond (Figure 1). This suggestion would be more valid in

the solid state, due to the need for a low energy lattice packing. However, in solution one would expect the entropy price to be too great to bring together so many subunits. The resulting chair β-lattice is therefore expected in the crystal but not in solution.

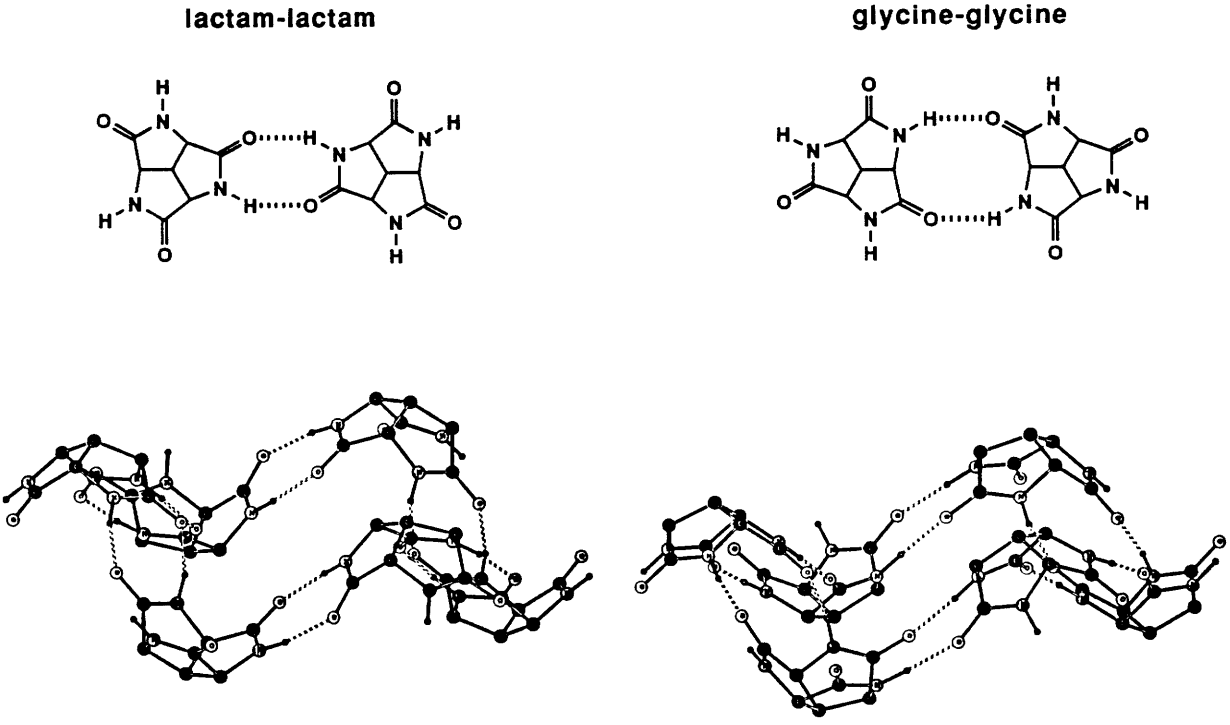

Figure 1. *Assemblies of trilactam **1** through both lactam-lactam and glycine-glycine hydrogen bond patterns. The latter is favoured by 1.6 kcal/mole per hydrogen bond.*

Molecular modeling predicted the existence of three-dimensional closed shell assemblies analogous to those described for methane- and *cis*-cyclopropanetricarboxamide (chapter 1). A tetrahedral tetramer (~7.5 Å cross section), a cubic octamer (with sides of ~8 Å) and a twenty-subunit sphere (~22 Å diameter) were suggested (Figure 2). In all three modeled structures, subunits are held together by strong hydrogen bonds. NH-O distances are, on average, 2.81 Å and display adequate linearity (N-H-O angles were estimated to be ~160-165 degrees).

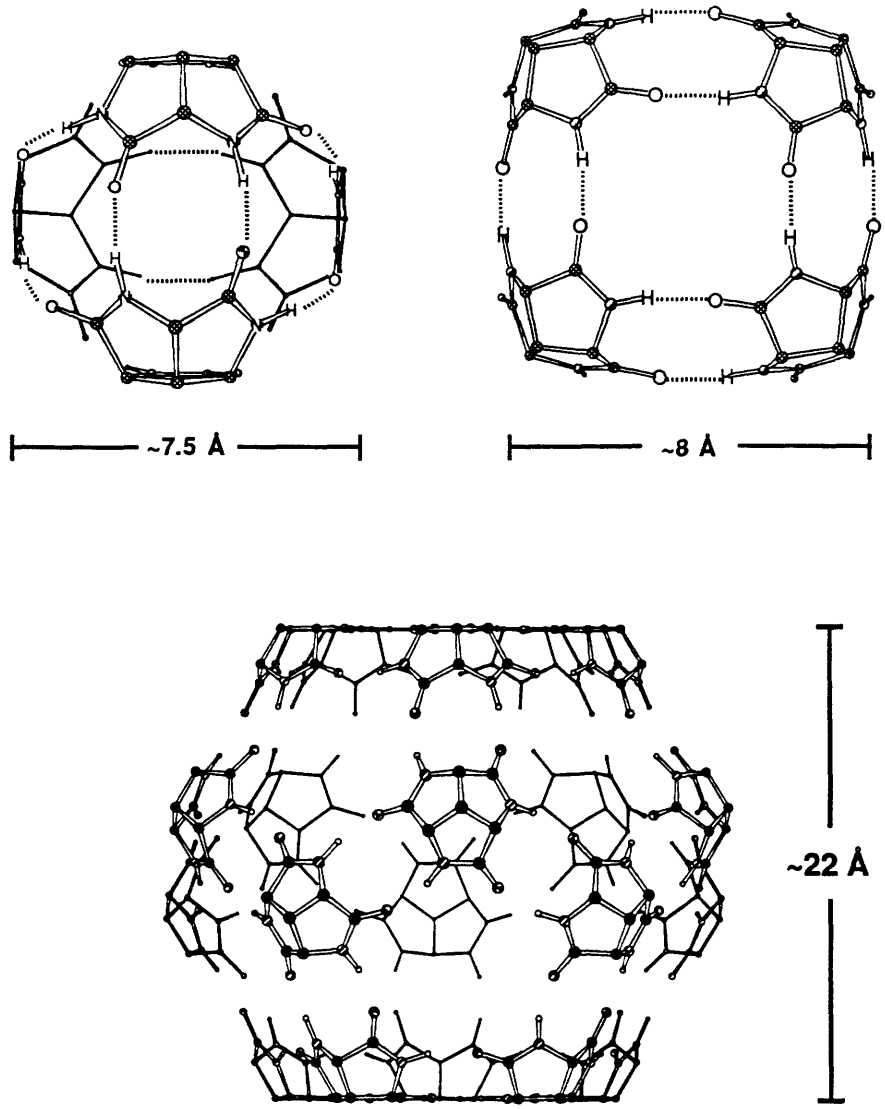

Figure 2. *Predicted assemblies of trilactam* ***1****. A tetramer, octamer and 20-mer form a closed-shell tetrahedron, a cube and a sphere. For clarity, only one half of the cubic assembly is shown.*

2.2 Synthetic Strategies

Two general retrosynthetic approaches to **1** are outlined below. The first route takes advantage of the preorganized trigonally-symmetric methanetriacetic acid skeleton. Introduction of nitrogen functions at all three α-positions would generate methane-

triglycine, which upon intramolecular cyclization would afford a racemic mixture of the trilactam.

Retrosynthesis 1.

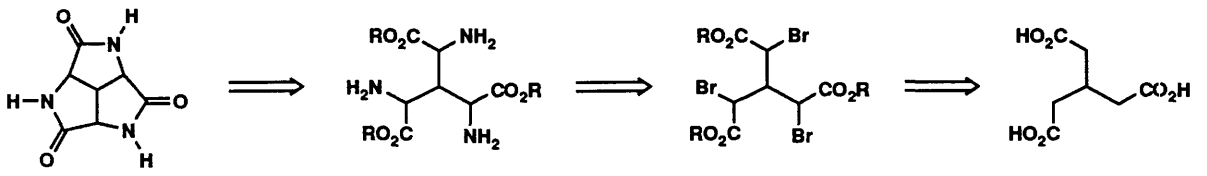

1 2 3

The second approach involves a [3+2] cycloaddition of diazoacetate on a 2-oxo-pyrroline precursor **4**, where 'X' is any functionality that can be converted to a carboxy function. Reductive cleavage of the nitrogen-nitrogen bond and cyclization would yield **1**.

Retrosynthesis 2.

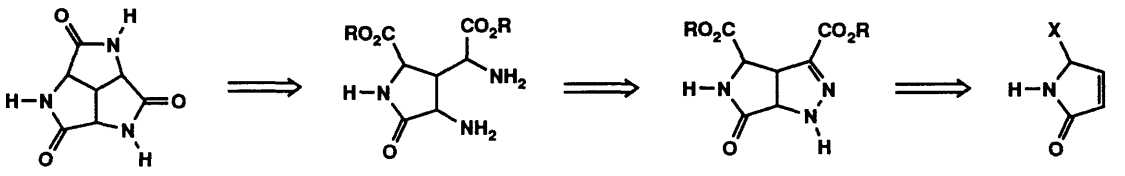

1 4

2.3 Retroanalysis 1

Methanetriacetic acid **3** was prepared by two literature routes (Scheme 1): a) the Michael addition of diethyl malonate to glutaconate followed by hydrolytic decarboxylation,[2,3] b) the reaction of an ylide with acetone dicarboxylate followed by hydrogenation and hydrolysis.[4] Both methods afforded triacid **3** in a straightforward manner, but the latter was more manageable and provided the triacid with greater purity.

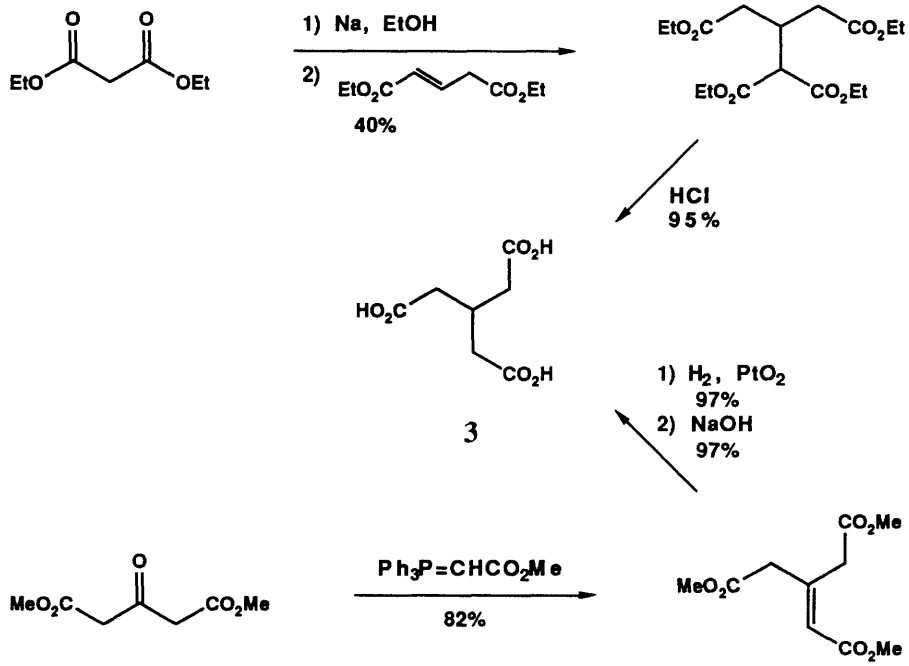

Scheme 1. *Synthesis of methanetriacetic acid 3.*

Methanetriacetic acid was α-brominated under Hell-Volhard-Zelinskii conditions[5] and quenched with methanol or ethanol to give a mixture of the two isomers **2a**, **2b** (Scheme 2). When thionyl chloride was used for the preparation of the triacid chloride a mixture of the triacid chloride and cyclic anhydride was obtained. The use of phosphorous pentachloride eliminated this problem by opening any of the anhydride that was initially formed.

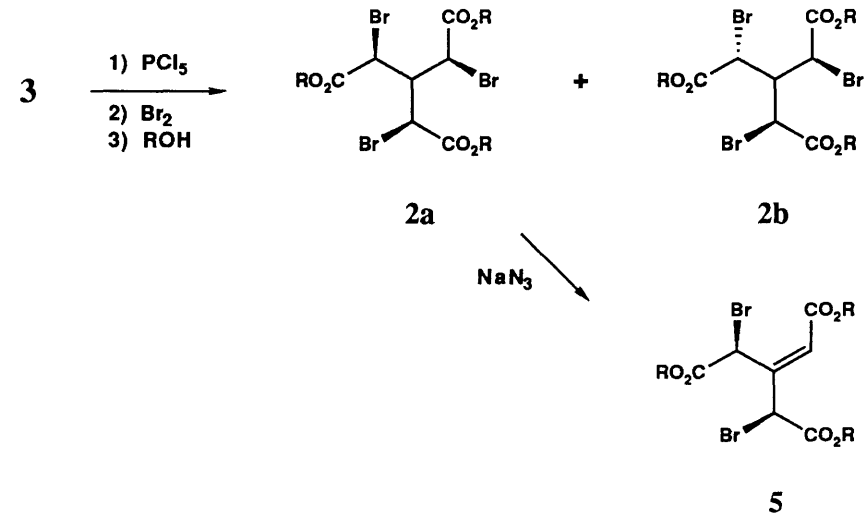

Scheme 2. *Hell-Volhard-Zelinskii bromination of methanetriacetic acid.*

The *C-3* symmetric isomer **2a** was isolated from the crude reaction mixture by fractional crystallization from methylcyclohexane. All attempts to displace the bromines by azides in varying solvents were unsuccessful. Sodium azide afforded the elimination product **5** while tetramethylguanidinium azide (TMGA) resulted in either recovery of starting material or isolation of an unidentifiable product mixture. This decomposition has been previously reported upon reacting **2** with mild bases.[5]

Ethanetriacetic acid **6** was examined as a solution to the elimination problem described above by replacing the central proton with a methyl group. Compound **6** was prepared from diethyl β-methylglutaconate[6] and was brominated and esterified as described for the methane derivative, but the two stereoisomers **7a** and **7b** (Scheme 3) could not be separated by either fractional crystallization or column chromatography. Treatment of **7** with sodium azide or TMGA in various solvents in the presence of catalytic amounts of crown ether resulted in complete recovery of starting material. This unreactivity can easily be rationalized by the steric constraints around the neopentyl reaction center.

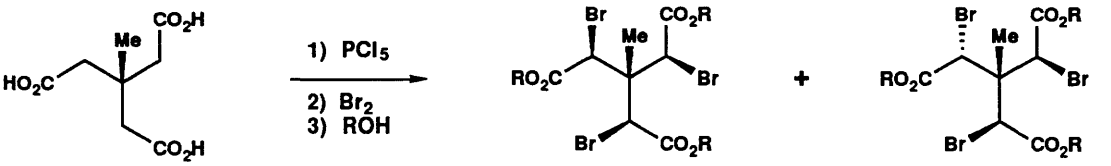

6 **7a** **7b**

Scheme 3. *Bromination of ethanetriacetic acid.*

The α,α',α"-tribromoethanetriacetic acid and amide (Figure 3) were examined because, unlike esters **2** and **7**, all subsequent bromide substitutions reactions would be intramolecular. Tricyclization of the amide would produce compound **1** while the acid would afford the trilactone which might be converted to **1** through an intramolecular Mitsinobu reaction. However, quenching the α-bromotriacid chlorides with water,

ammonia or alkyl amines, as well as acid- or base-assisted hydrolysis of triester **2a** did not yield the desired products, but instead resulted in unidentifiable tars.

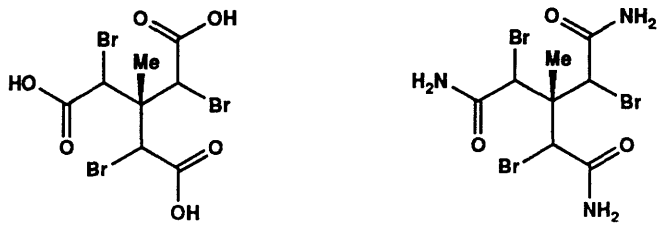

Figure 3. *α,α',α''-Tribromoethanetriacetic acid or amide. All reactions at the α-carbon center will be intramolecular.*

2.4 Retroanalysis 2

The key reaction step in the second retrosynthesis is the [3+2] cycloaddition of a diazoacetate and a 2-oxo-pyrroline **4**. The possible synthons possessing functionality that can lead to the desired pyrazoline-lactam can be grouped into four basic classes (Table 1).

In all cases, the reductive cleavage of the nitrogen-nitrogen double bond is essential to form the desired diamine (**B**).[7,8] Only then can the second and third lactam rings be formed by intramolecular displacement of the ester by the resulting amines (**C**).

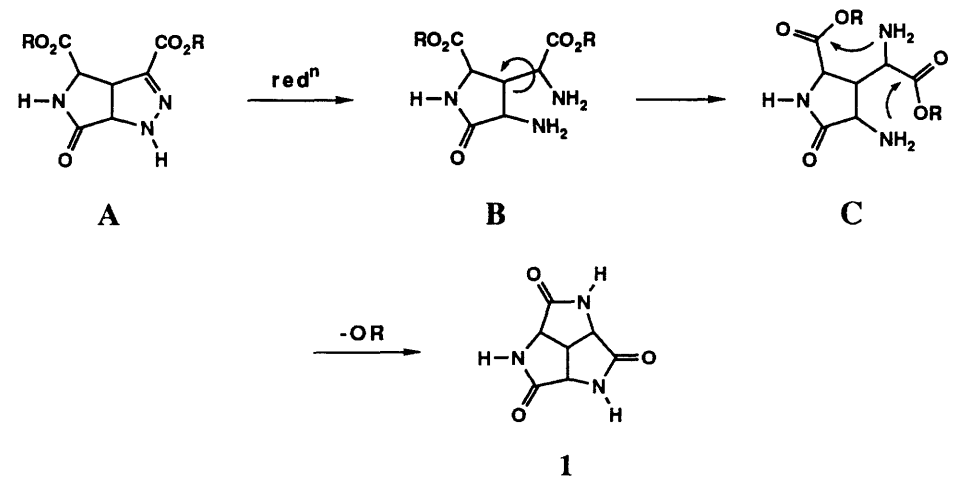

A **B** **C**

1

Table 1. Types of functionalities of **4** that can be transformed into direct precursors of trilactam **1**.

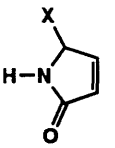	
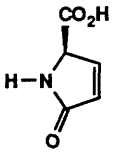	*Class 1*. Direct cycloaddition of an unsaturated pyroglutamic acid precursor.
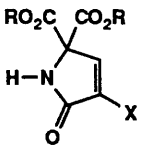 X = H, CO_2R	*Class 2*. Decarboxylation of polycarboxylate pyroglutamic acid derivatives.
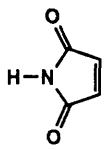	*Class 3*. Selective reduction of one imide carbonyl of a maleimide derivative followed by substitution of the hydroxyl of the resulting hydroxylactam by cyanide ion.
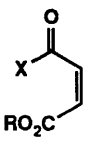 X = H, CN	*Class 4*. Reductive-amination of an acyl cyanide derived from a carboxylic acid or a Strecker-type amino acid synthesis from an aldehyde.
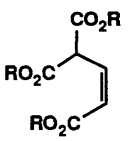	*Class 5*. Nitration or nitrosation of the acidic methine of a malonate derivative.

All attempts to prepare the unsaturated pyroglutamic acid derivative (*Class 1*) by selenium[9] or titanium-assisted[10] addition-elimination reactions met with little success. This can be attributed to the molecule's tendency to aromatize to an α-hydroxypyrrole because of the presence of an acidic proton adjacent to the carboxylic acid functional group. Masking the carboxyl of pyroglutamic acid as an *O,N*-acetal eliminated this problem

(Scheme 4).[11] Reduction of either methyl or benzyl *N*-carbobenzyloxypyroglutamates[12-14] followed by cyclization of the resulting hydroxy-pyrolidinone **8** yielded compound **9** which was converted to the olefin **10** by oxidative elimination of phenylseleninic acid.[15] This 2-oxo-pyrroline did not undergo cycloaddition with ethyl diazoacetate under a range of conditions such as various solvents, neat in a sealed tube, or at ambient or elevated temperatures.

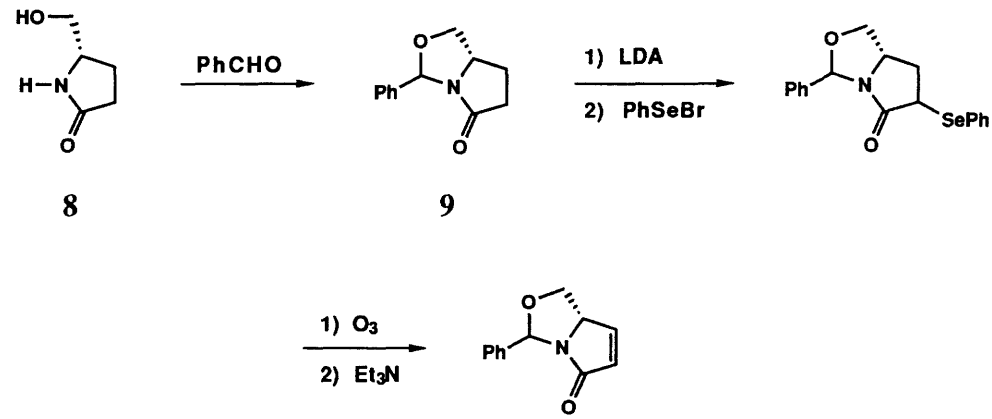

8 **9** **10**

Scheme 4. *Preparation of a masked unsaturated pyroglutamic acid derivative.*

The [3+2] cycloaddition, in a manner analogous to the Diels-Alder reaction, is LUMO controlled. Therefore additional electron withdrawing groups on the olefin should aid the reaction of olefins and diazo compounds. The electron deficient diester **11** (a *Class 2* molecule) was readily prepared by a cyclization of ethyl *cis*-bromoacrylate and diethyl acetamidomalonate.[16] This compound can be considered a masked pyroglutamate; mono-decarboxylation of the malonic acid substructure should lead to the desired product. The presence of the second carboxylate group not only provides a more electron poor system, but it also prevents aromatization to the hydroxypyrrole as described for the pyroglutamic acid derivatives. This olefin was completely unreactive towards cycloaddition of ethyl diazoacetate, perhaps due to the steric interference of the esters towards the approaching diazo species. Starting material was fully recovered in all cases.

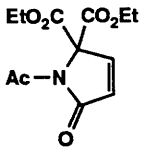

11

The more electron deficient 2-oxo-pyrroline **12** was prepared by cyclizing methyl 2-chloro-1-carbomethoxyacrylate and diethyl acetamidomalonate (Scheme 5). Pyrroline **12** was treated with ethyl diazoacetate to yield pyrazoline **13**. Initial attempts to hydrolyze the methyl ester under acidic conditions and to decarboxylate the resulting acid have been promising, although subsequent reductions of the pyrazoline nitrogen-nitrogen double bond met with limited success.

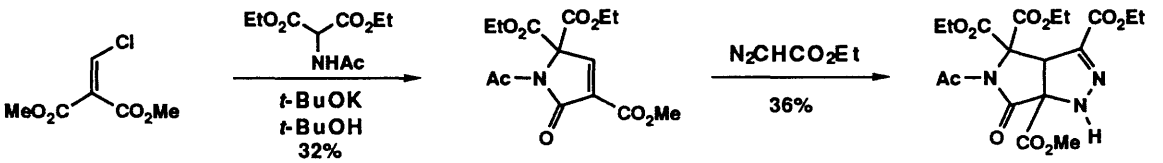

12 **13**

Scheme 5. *Synthesis of electron deficient dienophile 12 and its cycloaddition with ethyl diazoacetate.*

It was found that maleimide (a *Class 3* synthon) reacted violently with ethyl diazoacetate in an extremely exothermic reaction (Scheme 6). Yields were virtually quantitative and the pyrazoline was obtained in high purity by recrystallization from ethanol. Reduction of pyrazoline **14** with Raney nickel under high hydrogen pressures (2200 psi)[17] yielded the hydrazine **15** while reduction with palladium or platinum catalysts resulted in complete recovery of starting materials. The acidic imide proton prevented acylation in the presence of amine bases; however, acylation with acetic anhydride in actetic acid furnished the pyrazoline **16**. Reduction was then accomplished under mild conditions

using palladium in a water-acetic acid medium. Resubmitting the product (**17**) to the acylation conditions described above furnished diacetamide **18**.

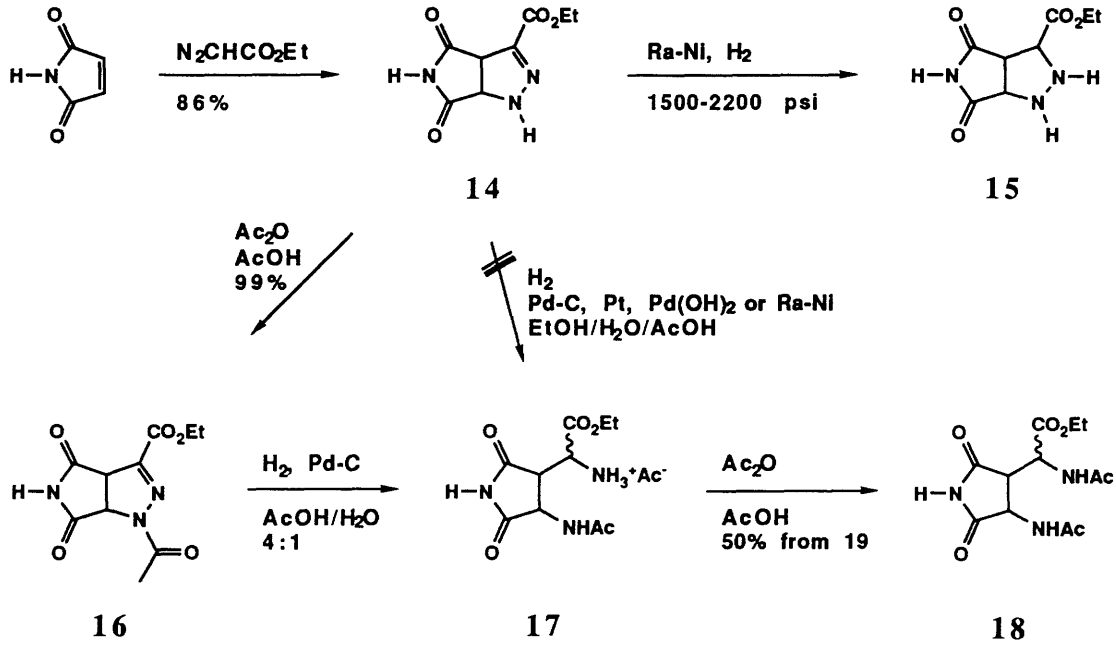

Scheme 6. *Cycloaddition of maleimide and reduction of the resulting pyrazoline.*

Selective reduction of the 4-carbonyl of imide **18** to the hydroxylactam with excess sodium borohydride resulted in an unidentifiable product mixture. This can be explained by the decomposition of the water soluble reduction product during the reaction workup. It has been reported that under these reaction conditions the products are often over-reduced unless they are stable to the excess $NaBH_4$.[18] An alternative is to remove the hydrophobic product without quenching the reaction from the aqueous solution. In the case of imide **18** the products of the reduction could not be extracted, thus a more organic soluble imide was desirable for this purpose.

N-Benzyl pyrazolinedicarboximide **19a** was prepared by Mitsinobu alkylation of imide **14** and in parallel by direct cycloaddition of *N*-benzyl maleimide[19] and ethyl diazoacetate. Reduction of **19a** with $NaBH_4$ was highly selective but afforded the

hydroxylactam **20** which had the undesired regiochemistry[20] (Scheme 7). This disfavoured regioreactivity may have resulted from the more sterically hindered "upper" carbonyl group (pyrazoline position *4*). In order to enhance the accessibility of the desired imide 4-carbonyl, acyl groups were introduced onto the nitrogen (position *1*). The lack of an acidic imide proton enabled smooth *N*-acylation of pyrazoline **19** under more traditional conditions (acyl chloride and triethylamine in methylene chloride). Carbamates **21** and acetamide **22** were prepared in this way. Reduction of these sterically hindered imides similarly afforded the undesired hydroxylactam with the more accessible 5-carbonyl position selectively reduced. It appears that the electronics, not the sterics, of the system is the major factor contributing to the reduction regiochemistry.

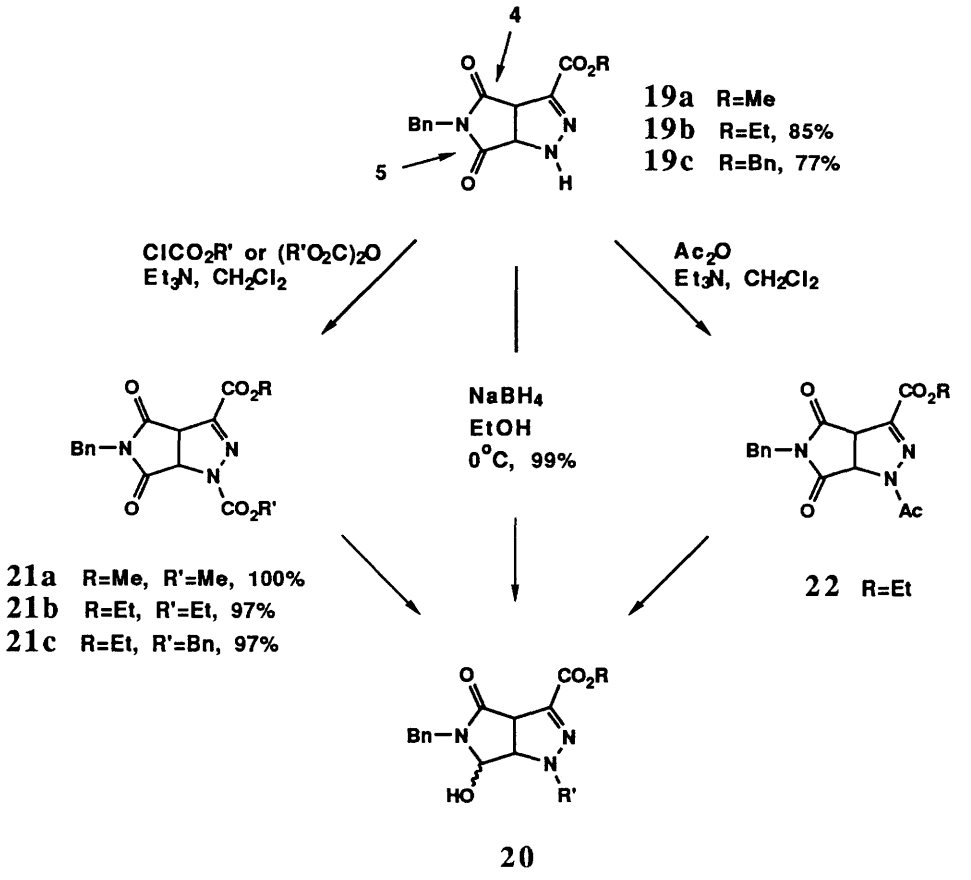

Scheme 7. *$NaBH_4$ reduction of imide pyrazoline derivatives.*

Scheme 8 describes the attempts to prepare **1** through a *Class 4* synthon. Ethyl diazoacetate underwent cycloaddition with maleic anhydride in a highly exothermic reaction to yield pyrazoline **23**. Acylation under both basic and acidic conditions resulted in insoluble polymer mixtures. Attempts to directly convert the anhydride to the 4-formyl-pyrazoline-5-carboxylic acid by opening with disodium tetracarbonylferrate(-II)[21] resulted in decomposition. Regioselective cleavage of the anhydride was accomplished when appropriate reaction conditions were found. Ratios of carboxylic acids **24a** to **24b** as high as a 9:1 were obtained when the cyclic anhydride was treated with methanol at 0°C. The regiochemistry of the products was determined by ^{1}H NMR NOE studies.[22] This preferred pathway for methanol supports the observation that the carbonyl adjacent to the pyrazoline nitrogen is more reactive. Esterification of acid **24** under numerous reaction conditions afforded either starting material or unidentifiable product mixtures. The presence of an acidic proton (carboxylic acid of **24**) not only prevented *N*-acylation under basic conditions, as previously described, but acidic conditions as well.

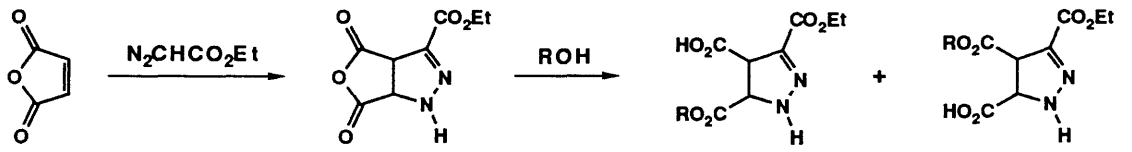

23

R	24a	24b
MeOH, RT	75	25
MeOH, -78-0°C	85-90	15-10
EtOH	77	23
i-PrOH	-	-
BnOH or PhOH	NR	

Scheme 8. *Selective opening of anhydride 23 in alcoholic solutions.*

When the reaction mixture of **24** was treated with a solution of phenyl-diazomethane,[23,24] the diethyl monobenzyl ester **25** was isolated after lengthy purification

(Scheme 9). After acylation and separation of isomers, compound **26** was debenzylated under reductive conditions to acetylpyrazolinecarboxylic acid **27**. Significant epimerization of the sp^3 pyrazoline ring carbon centers resulted from this treatment. Initial attempts to convert the carboxylic acid group of **27** to the acylcyanide through the acid chloride,[25] as well as direct reduction to the aldehyde, were not successful.

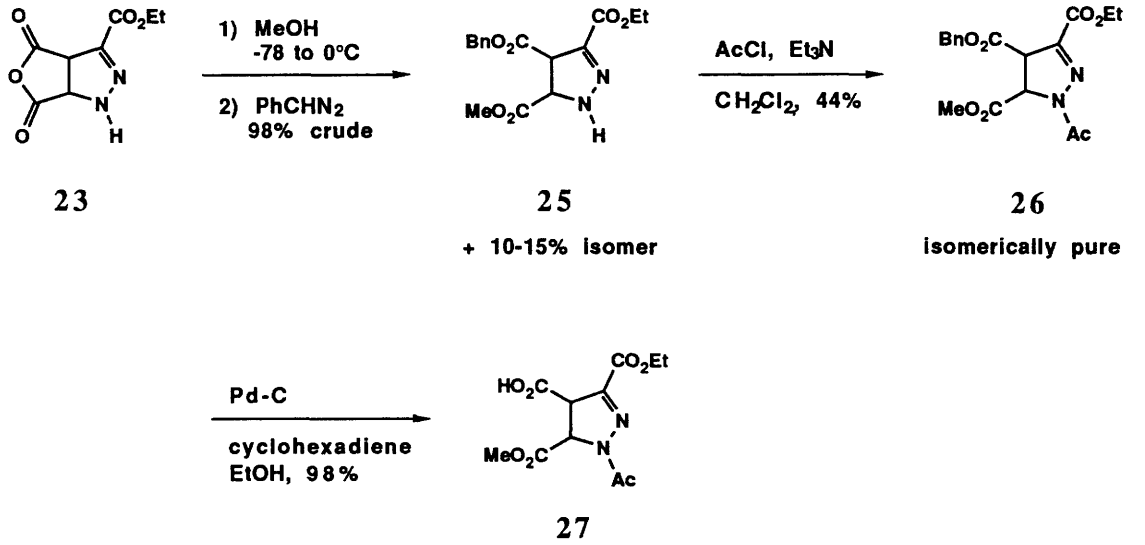

23 **25** + 10-15% isomer **26** isomerically pure **27**

Scheme 9. *Synthesis of pyrazoline carboxylic acid 27.*

Epimerization of the ring carbons of **25** prompted the synthesis of another *Class 4* carboxylic acid **29** (Scheme 10). Cycloaddition of ethyl diazoacetate on carbethoxyfumaric acid mono-*tert*-butyl monoethyl ester[26-28] readily afforded tetraester **28**, which could be smoothly de-*tert*-butylated to acid **29**. Attempts to convert the carboxylic acid functionality to acylcyanide or an aldehyde have been fruitless. Aldehyde **32** was prepared in parallel by cycloaddition of ethyl diazoacetate and diethylacetal **30**.[27,29] Deprotection of pyrazoline **31** furnished aldehyde **32** which upon subjection to Strecker-type amino acid synthesis conditions resulted in decomposition.

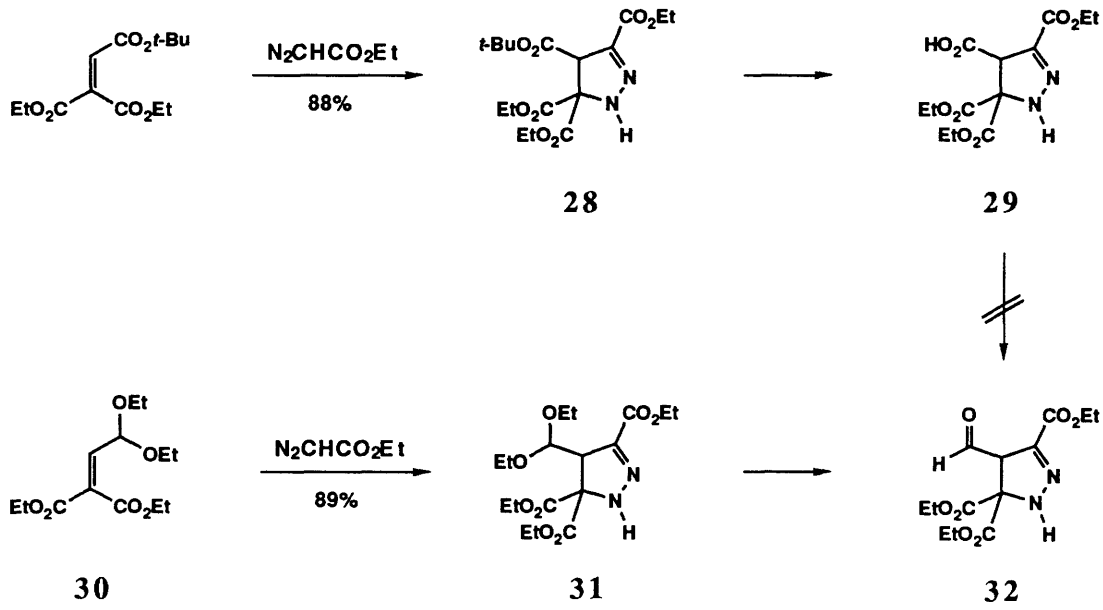

Scheme 10. *Synthesis of pyrazoline carboxylic acid and aldehyde.*

Cycloaddition of ethyl diazoactetate on tetraester **33**[30,31] yielded pyrazoline **34**, a *Class 5* synthon (Scheme 11). The attractive structural feature of this pyrazoline is the acidic malonate methine. Strategies to introduce nitrogen functional groups by nitration (HNO_3, H_2SO_4) or nitrosation ($NaNO_2$, AcOH, Zn) at the malonate carbon of **34** have met with no success.

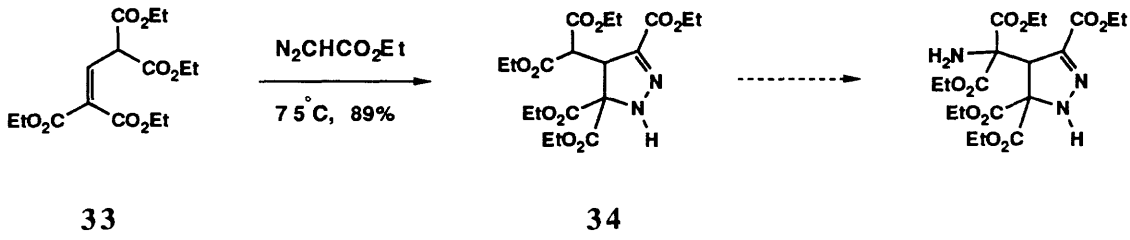

Scheme 11. *Synthesis of pentaester **34** bearing an acidic methine center.*

2.5 Discussion and Conclusions

The attempts to prepare trilactam **1**, although fruitless, afforded insight into the limitations of the cycloaddition reaction (Table 2).

Table 2. Dienophiles for the [3+2] Cycloaddition with Ethyl Diazoacetate

1) 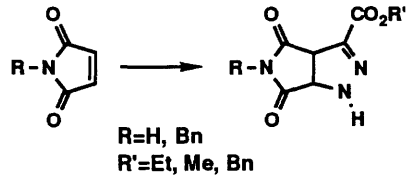	2) 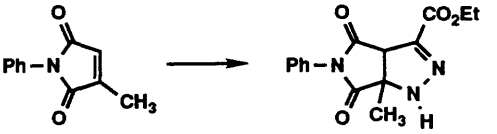
3) 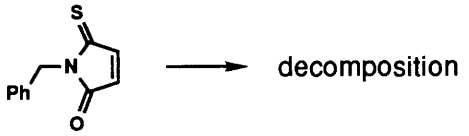	4) 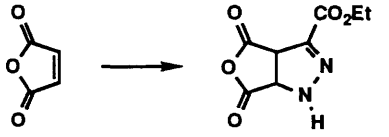
5)[32] 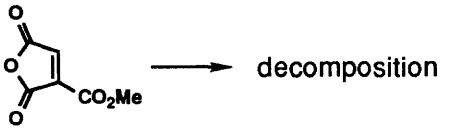	6)[33] 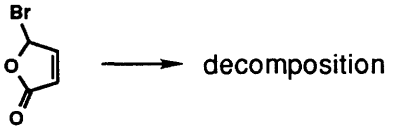
7)[34] 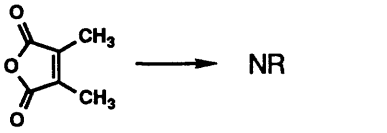	8) 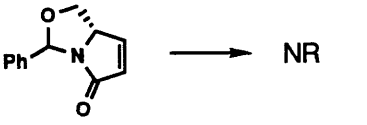
9) 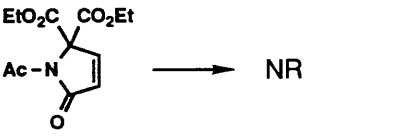	10) 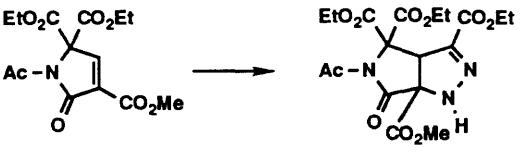
11) 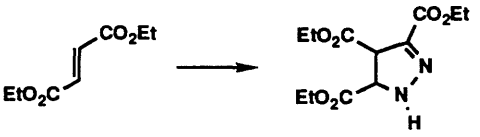	12)[35-37] 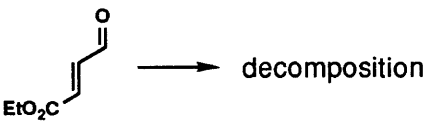

13) 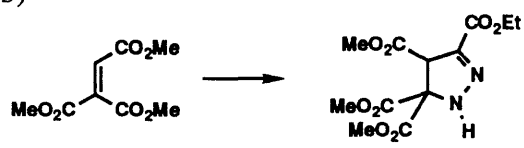	14) 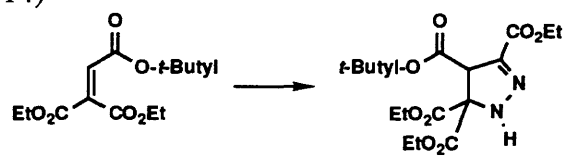
15) 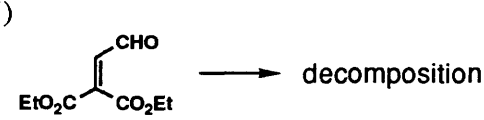 decomposition	16) 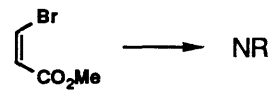 NR
17)[38] 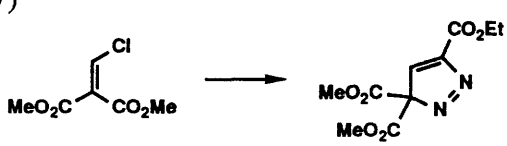	18) 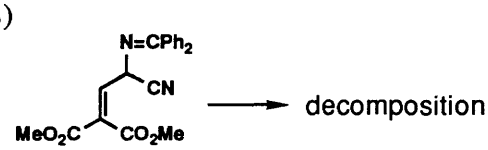 decomposition
19) 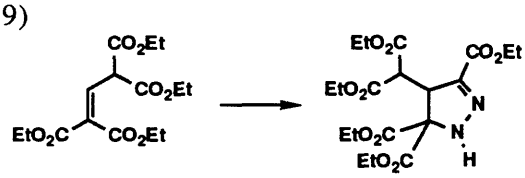	20) 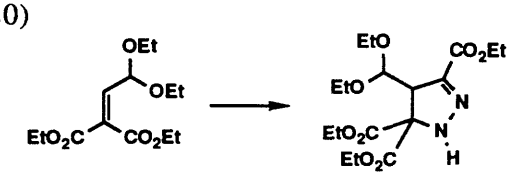

The trends can be summarized as follows: 1) At least two carbonyls adjacent to the olefin are required for cycloaddition. Maleic and fumaric acid derivatives (entries 1, 2, 4, 11), and carboxylacrylates (entries 13, 14, 17, 19, 20) all react with diazoacetates. On the other hand, simple acrylates (entries 6, 16) and unsubstituted 2-oxo-pyrrolines (entries 8 and 9) are completely unreactive. 2) The cycloaddition is sentitive to the electron withdrawing capability of the adjacent carbonyls. Maximizing the pi-electron overlap by cyclization enhanced induction is optimal. The order of reactivity is anhydride > imide > fumarate (entries 1, 4, 11). 3) A third carbonyl group is advantageous (entry 10 as compared to 9), although in some cases this additional carbonyl results in reactivity that cannot be controlled (the maleic anhydride derivative, entry 5, decomposes in an explosive reaction when treated with diazo compounds). 4) The minimization of steric interactions is favourable (entries 2 and 4 as compared to 7), and bulky groups are positioned on the same

side of the pyrazoline as the nitrogens (entry 2). 5) Certain functional groups are not compatable with the cycloaddition conditions. Sulfur compounds (entry 3), aldehydes (entries 12 and 15), and imines (entry 18) resulted in unidentifiable reaction mixtures. The β-chloroacrylate (entry 8) resulted in addition, elimination, and aromatization.

2.6 Experimental

Apparatus

^{1}H NMR measurements were performed on Bruker AC-250 and Varian XL-300, UN-300, and VXR-500 MHz spectrometers in the solvents indicated. Chemical shifts are reported as parts per million (δ) relative to either tetramethylsilane or to residual solvent peak. Melting points were obtained on an Electrothermal IA9100 digital melting point aparatus. IR spectra were recorded on a Mattson Cygnus 100 FT-IR spectrometer. High-resolution mass spectra were ontained on a Finnegan MAT 8200 mass spectrometer. GC studies were performed on a Hewlett Packard 5890A Gas Chromatograph (Methyl Silicone Gum Column).

Materials and Methods

All commercially available compounds (Aldrich, Sigma, Fluka) were used without further purification unless otherwise indicated. CD_3OH (99.8% D, Cambridge Isotope Labs), CD_2Cl_2 (99.6% D, Aldrich Chemical Co.), DMSO-d_6 (99.9% D, MSD Isotopes), DMF-d_7 (99.5% D, Cambridge Isotope Labs), and $CDCl_3$ (99.8% D, MSD Isotopes) were used from freshly opened ampoules or stored over molecular seives. Anhydrous tetrahydrofuran and ether were obtained by distilling from sodium-benzophenone ketyl. Column chromatography was performed on Merck Silica Gel 60 (230-400 mesh).

Methyl 1-Acetyl-2-oxo-5,5-dicarbethoxy-3-pyrroline-2-carboxylate (12)

Diethyl acetamidomalonate (10.86 g, 0.05 mol) was added to *t*-BuOK (prepared from 2.0 g, 0.05 mol potassium in 100 mL *t*-BuOH in an argon flushed 3-neck round bottom flask fitted with an addition funnel). After stirring for 15 minutes, a solution of methyl 2-chloro-1-carbomethoxyacrylate (8.93 g, 0.05 mol) in *t*-BuOH (20 mL) was added dropwise over 15 minutes. The reaction was stirred under argon for 24 h, then evaporated under reduced pressure. The sticky residue was treated with Et_2O, any solids were filtered, and the filtrate was evaporated. Purification by column chromatography through silica gel (50% EtOAc/hexanes) afforded 4.92 g (30%) of **12** as a colourless oil:

^{1}H NMR ($CDCl_3$, 300 MHz) δ 7.88 (s, 1H), 4.29 (q, *J*=7.0 Hz, 4H), 3.91 (s, 3H), 2.61 (s, 3H), 1.29 (t, *J*=7.2 Hz, 6H);

^{13}C NMR ($CDCl_3$) δ 169.1, 163.5, 162.0, 159.8, 150.7, 130.4, 72.7, 63.4, 52.5, 24.3, 13.6;

HRMS (EI) Calcd for $C_{14}H_{17}NO_8$ $[M+H]^+$: 328.1032 Found: 328.1035.

2-Pyrazolinepentaester *N*-Acetyl-lactam (13).

Pyrroline **12** (1.8 g, 5.50 mmol) and ethyl diazoacetate (1.26 g, 11.0 mmol) were stirred at 70 °C for 24 h resulting in a viscous yellow oil. Purification by column chromatography through silica gel (50% ethyl acetate/hexanes) afforded 882 mg (36%) of **13** as a colourless oil:

IR (KBr) 3346 (m), 2999 (m), 1769 (s), 1744 (s), 1716 (s), 1690 (s), 1564 (m) cm^{-1};

^{1}H NMR ($CDCl_3$, 300 MHz) δ 7.24 (s, 1H), 4.82 (d, *J*=0.6 Hz, 1H), 4.42-4.13 (m, 6H), 3.85 (s, 3H), 2.56 (s, 3H), 1.36 & 1.35 (2 triplets, *J*=7.0 Hz, 6H), 1.27 (t, *J*=7.0 Hz, 3H);

^{13}C NMR ($CDCl_3$) δ 170.2, 168.2, 166.0, 165.7, 164.1, 160.8, 140.1, 116.3, 77.7, 63.1, 61.6, 54.0, 53.4, 24.9, 13.9, 13.8, 13.4;

HRMS (EI) Calcd for $C_{18}H_{23}N_3O_{10}$: 441.1384 Found: 441.1369, (FAB, 3NBA) $[M+H]^+$ Calcd: 442.1462 Found: 442.1404.

3-Carbethoxy-2-pyrazoline-4,5-dicarboximide (14).

Maleimide (7.5 g, 0.077 mol) and ethyl diazoacetate (8.82 g, 0.077 mol) were mixed with occasional cooling to control the violently exothermic reaction (the temperature was maintained below 50 °C). When a solid mass was obtained the reaction was allowed to stand at room temperature for 1 h. Recrystallization from EtOH afforded 14.0 g, (86%) of **14** as a white solid:

mp 167-167.5 °C;

IR (KBr) 3328 (s), 3171 (m), 3090 (m), 2993 (w), 2769 (w), 1784 (s), 1728 (s), 1711 (s) cm^{-1};

^1H NMR ($CDCl_3$, 300 MHz) δ 7.80 (br s, 1H), 6.90 (br s, 1H), 4.93 (dd, *J*=10.8, 1.8 Hz, 1H), 4.60 (d, *J*=10.6 Hz, 1H), 4.37 (q, *J*=7.2 Hz, 2H), 1.38 (t, *J*=7.2 Hz, 3H);

^1H NMR (DMSO-d_6, 250 MHz) δ 11.54 (s, 1H), 9.50 (d, *J*=1.9 Hz, 1H), 4.85 (dd, *J*=11.1, 2.0 Hz, 1H), 4.43 (d, *J*=11.1 Hz, 1H), 4.16 (q, *J*=7.1 Hz, 2H), 1.21 (t, *J*=7.1 Hz, 3H);

^{13}C NMR ($CDCl_3$) δ 176.0, 174.5, 161.0, 133.8, 66.2, 60.2, 52.7, 14.1;

HRMS (EI) Calcd for $C_8H_9N_3O_4$: 211.0593 Found: 211.0592.

1-Acetyl-3-carbethoxy-2-pyrazoline-4,5-dicarboximide (16).

3-Carbethoxy-2-pyrazoline-4,5-dicarboximide **14** (12.5 g, 59.0 mmol) was stirred in a 1:1 mixture of acetic anhydride:acetic acid at room temperature for 16-24 h. The solvents were removed under reduced pressure affording 14.8 g (99%) of **16** as a white solid which was of high purity and was carried on without further purification. The product could also be recrystallized as a white solid (82%) from EtOH:

mp 182.5-183°C;

IR (KBr) 3147 (w), 2993 (m), 2773 (m), 1788 (m), 1731 (s), 1659 (m), 1594 (m) cm^{-1}; ^1H NMR (DMSO-d_6, 300 MHz) δ 11.73 (s, 1H), 5.44 (d, *J*=10.2 Hz, 1H), 4.60 (d, *J*=10.5 Hz, 1H), 4.28 (q, *J*=7.1 Hz, 2H), 2.25 (s, 3H), 1.27 (t, *J*=6.9 Hz, 3H); ^{13}C NMR ($CDCl_3$) δ 172.7, 171.7, 169.0, 159.8, 142.5, 62.6, 61.6, 54.7, 21.5, 13.9; HRMS (EI) Calcd for $C_{10}H_{11}N_3O_5$: 253.0699 Found: 253.0695.

2-Acetamido-3-(ethyl glycinato)maleimide acetate salt (17).

A solution of 1-acetyl-3-carbethoxy-2-pyrazoline-4,5-dicarboximide **16** (14.8 g, crude) in 4:1 acetic acid:water (200 mL) was treated with 10% Pd-C and reduced under balloon pressure with H_2 over 3 days. The catalyst was filtered off through Celite and the filtrate evaporated under reduced pressure affording **17** as a white solid which was carried on without further purification:

^1H NMR (DMSO-d_6, 250 MHz) δ 11.72 (s, 1H), 8.84 (br s, 3H, ammonium), 8.59 (d, *J*=7.1 Hz, 1H), 8.50 (d, *J*=7.1 Hz, 1H), 4.54-4.39 (m, 2H), 4.27-4.14 (m, 3H), 3.65-3.54 (m, 1H), 1.90 (s, 3H), 1.86 (s, 3H), 1.20 (dt, *J*=7.1, 1.4 Hz, 3H).

2-Acetamido-3-(ethyl *N*-acetylglycinato)maleimide (18).

The above 2-acetamido-3-glycinatomaleimide acetate salt was stirred in 1:1 acetic anhydride:acetic acid (150 mL) at room temperature for 24 h. Evaporation under reduced pressure and purification by column chromatography through silica gel (10% MeOH/CH_2Cl_2) afforded **18** as a colourless semi-solid:

^1H NMR (DMSO-d_6, 300 MHz) diastereomer 1: δ 11.42 (s, 1H), 8.54 (d, *J*=7.3 Hz, 1H), 8.33 (d, *J*=8.4 Hz, 1H), 4.70 (dd, *J*=8.4, 4.4 Hz, 1H), 4.16-4.00 (m, 3H), 3.43 (dd, *J*=7.0, 4.4 Hz, 1H), 1.88 (s, 3H), 1.85 (s, 3H), 1.17 (t, *J*=7.1 Hz, 3H) diastereomer 2: δ 11.47 (s, 1H), 8.52 (d, *J*=6.6 Hz, 1H), 8.33 (d, *J*=8.4 Hz, 1H), 4.77 (dd, *J*=8.0, 4.4 Hz, 1H), 4.31 (t, *J*=7.1 Hz, 1H), 4.15-4.05 (m, 2H), 1.88 (s, 6H), 1.74 (s, 6H), 1.16 (t, *J*=7.1 Hz, 3H);

^{13}C NMR (DMSO-d_6) (both diastereomers) δ 175.5, 175.3, 174.8, 174.6, 170.2, 170.1, 169.8, 169.5, 61.1, 61.0, 52.3, 51.8, 49.6, 49.5, 48.3, 47.9, 22.1, 22.0, 13.8.

***N*-Benzyl-3-carbethoxy-2-pyrazoline-4,5-dicarboximide (19b).**

1) Diethyl azidodicarboxylate (1.65 g, 9.47 mmol) was added dropwise over 10 minutes to a solution of 3-carbethoxy-2-pyrazoline-4,5-dicarboximide (2.00 g, 9.47 mmol), benzyl alcohol (1.03 g, 9.47 mmol) and triphenylphosphine (2.49 g, 9.47 mmol) in dry THF (30 mL) under argon. The reaction was stirred at room temperature for 18 h and evaporated under reduced pressure. Purification by column chromatography through silica gel (50% EtOAc/hexanes) yielded a mixture of **19b** and diethyl hydrazine-dicarboxylate. Pure **19b** was obtained by trituration with hot Et_2O (1.65 g, 58%).

2) N-Benzylmaleimide[19] (5.0 g, 26.7 mmol) and ethyl diazoacetate (3.05 g, 26.7 mmol) were stirred at room temperature until a solid mass formed. Recrystallization from EtOH afforded 6.86 g (85%) of **19b** as a white solid which was identical in all respects with the compound prepared in method 1:

mp 148-148.5 °C;

IR (KBr) 3278 (m), 2995 (w), 1724 (s), 1679 (s), 1525 (m) cm^{-1};

^1H NMR ($CDCl_3$, 300 MHz) δ 7.35-7.29 (m, 5H), 6.87 (br s, 1H), 4.89 (dd, *J*=10.8, 1.8 Hz, 1H), 4.65 (s, 2H), 4.55 (d, *J*=10.8 Hz, 1H), 4.36 (q, *J*=7.1 Hz, 2H), 1.37 (t, *J*=7.2 Hz, 3H);

^1H NMR (DMSO-d_6, 300 MHz) δ 9.61 (d, *J*=2.1 Hz, 1H), 7.34-7.16 (m, 5H), 5.01 (dd, *J*=11.1, 2.4 Hz, 1H), 4.57 (d, *J*=12.0 Hz, 1H), 4.55 (s, 2H), 4.20-4.14 (m, 2H), 1.22 (t, *J*=7.2 Hz, 3H);

^{13}C NMR (DMSO-d_6) δ 174.3, 172.8, 160.9, 135.7, 133.6, 128.6, 127.6, 127.3, 65.1, 60.4, 51.6, 41.7, 14.1;

HRMS (EI) Calcd for $C_{15}H_{15}N_3O_4$: 301.1063 Found: 301.1065.

_N_-Benzyl-3-carbomethoxy-2-pyrazoline-4,5-dicarboximide (19a).

The compound was prepared in 50% yield as described for **19b** except methyl diazoacetate was substituted for ethyl diazoacetate:

mp 159-159.5 °C;

IR (KBr) 3293 (s), 2942 (w), 1789 (m), 1715 (s), 1681 (s) cm^{-1};

^1H NMR (DMSO-d_6) δ 9.65 (d, J=1.8 Hz, 1H), 7.31-7.25 (m, 5H), 5.01 (dd, J=11.2, 2.0 Hz, 1H), 4.58 (d, J=11.4 Hz, 1H), 4.55 (s, 2H), 3.70 (s, 3H);

^{13}C NMR (DMSO-d_6) δ 174.1, 172.7, 161.3, 135.6, 133.1, 128.5, 127.5, 127.4, 65.1, 51.6, 51.5, 41.7;

HRMS (EI) Calcd for $C_{14}H_{13}N_3O_4$: 287.0906 Found: 287.0904.

_N_-Benzyl-3-carbethoxy-2-pyrazoline Hydroxylactam (20)

A suspension of _N_-Benzyl-3-carbethoxy-2-pyrazoline-4,5-dicarboximide (500 mg, 1.66 mmol) in EtOH at 0°C was treated with $NaBH_4$ (627 mg, 16.6 mmol) and stirred at this temperature for 4 h. The reaction was poured into ice water (100 mL) and quickly extracted with $CHCl_3$ (3 x 50 mL), dried over Na_2SO_4 and evaporated under reduced pressure affording 500 mg (99%) of the product as a white solid. The correct regiochemistry of the product was determined by evaluating the ^1H NMR in $CDCl_3$/DMSO-d_6 at 300 MHz (only relevant signals are given): δ signal 'a', 5.24 (d, J = 9.0 Hz, 1H); signal 'b', 5.10 (dd, J=9.0, 4.5 Hz, 1H); signal 'c', 4.60 (ddd, J=10.0, 4.5, 2.0 Hz, 1H); signal 'd', 4.18 (d, J=10.0 Hz, 1H). Upon addition of D_2O: signal 'a' disappeared completely; signal 'b', 5.10 (d, J=4.5 Hz, 1H); signal 'c', 4.60 (dd, J=10.0, 2.0 Hz, 1H); signal 'd' is uneffected. The signals can be assigned as: 'a', alcohol OH; 'b', H α to OH; 'c', pyrazoline H5; 'd', pyrazoline H4. This assignment was confirmed by NOE experiments.

_N_-Benzyl-1,3-dicarbomethoxy-2-pyrazoline-4,5-dicarboximide (21a).

A solution of _N_-benzyl-3-carbomethoxy-2-pyrazoline-4,5-dicarboximide **19a** (250 mg, 0.87 mmol) and methyl chloroformate (80 mg, 0.87 mmol) in CH_2Cl_2 (5 mL) was treated with triethylamine (180 μL) at room temperature for 2 h. The solution was washed with 1N HCl (25 mL), extracted with CH_2Cl_2 (3x25 mL), dried over Na_2SO_4, and evaporated affording 300 mg (100%) of pure **21a** as a white solid:

mp 216.5-217 °C;

IR (KBr) 3436 (w), 3126 (w), 2985 (w), 1720 (s), 1577 (w) cm^{-1};

^1H NMR ($CDCl_3$, 300 MHz) δ 7.36-7.29 (m, 5H), 5.45 (d, J=10.8 Hz, 1H), 4.73 (d, J=10.6 Hz, 1H), 4.66 (s, 2H), 3.96 (s, 3H), 3.93 (s, 3H);

HRMS (EI) Calcd for $C_{16}H_{15}N_3O_6$: 345.0961 Found: 345.0958.

_N_-Benzyl-1,3-dicarbethoxy-2-pyrazoline-4,5-dicarboximide (21b).

A solution of _N_-benzyl-3-carbethoxy-2-pyrazoline-4,5-dicarboximide **19b** (500 mg, 1.66 mmol) and ethyl pyrocarbonate (336 mg, 2.07 mmol) in dry THF (10 mL) was treated with triethylamine (350 mg, 3.46 mmol) and heated until refluxing for 30 minutes. The solvent was evaporated under reduced pressure, the residue was taken up in CH_2Cl_2 (50 mL), washed with 1N HCl (50 mL), and then water. Drying over Na_2SO_4 and evaporation afforded 604 mg (97%) of pure **21b** as a white solid:

mp 189.5-190 °C;

IR (KBr) 3475 (w), 3412 (w), 2987 (m), 1786 (m), 1731 (s), 1574 (m) cm^{-1};

^1H NMR ($CDCl_3$, 300 MHz) δ 7.36-7.28 (m, 5H), 5.43 (d, J=10.8 Hz, 1H), 4.71 (d, J=10.6 Hz, 1H), 4.65 (s, 2H), 4.45-4.36 (m, 4H), 1.41-1.36 (m, 6H);

HRMS (EI) Calcd for $C_{18}H_{19}N_3O_6$: 373.1274 Found: 373.1276.

_N_-Benzyl-1-carbobenzyloxy-3-carbethoxy-2-pyrazoline-4,5-dicarboximide (21c).

A solution of _N_-benzyl-3-carbethoxy-2-pyrazoline-4,5-dicarboximide **19b** (500 mg, 1.66 mmol) and benzylchloroformate (261 mg, 1.66 mmol) in CH_2Cl_2 (20 mL) was treated with triethylamine (350 mg, 1.66 mmol) under a $CaCl_2$ drying tube for 12 h. The reaction was washed with 1N HCl (25 mL), extracted with CH_2Cl_2 (3x25 mL), dried over Na_2SO_4, and evaporated. Purification by column chromatography through silica gel (2% $MeOH/CH_2Cl_2$) afforded 702 mg (97%) of **21c** as a white solid:

mp 68-70 °C;

IR (KBr) 3033 (w), 2982 (m), 1791 (m), 1728 (s), 1583 (m) cm^{-1};

^1H NMR ($CDCl_3$, 300 MHz) δ 7.48-7.28 (m, 10H), 5.42 (d, _J_=10.6 Hz, 1H), 5.36 (s, 2H), 4.69 (d, _J_=10.6 Hz, 1H), 4.64 (s, 2H), 4.38 (q, _J_=7.0 Hz, 2H), 1.37 (t, _J_=7.0 Hz, 3H);

^{13}C NMR ($CDCl_3$) δ 170.4, 169.3, 159.7, 151.6, 141.7, 134.8, 134.4, 128.9, 128.63, 128.5, 128.4, 128.2, 69.1, 62.5, 62.2, 52.9, 43.2, 14.0;

HRMS (EI) Calcd for $C_{23}H_{21}N_3O_6$: 435.1430 Found: 435.1425.

_N_-Benzyl-1-acetyl-3-carbethoxy-2-pyrazoline-4,5-dicarboximide (22).

A solution of _N_-benzyl-3-carbomethoxy-2-pyrazoline-4,5-dicarboximide **19b** (300 mg, 1.0 mmol) in 1:1 Ac_2O:AcOH (10 mL) was stirred at room temperature for 24 h. Evaporation and drying in vacuo afforded the product in quantitative yield as a white solid:

^1H NMR ($CDCl_3$, 300 MHz) δ 7.33-7.25 (m, 5H), 5.63 (d, _J_=10.5 Hz, 1H), 4.70 (d, _J_=10.5 Hz, 1H), 4.60 (d, _J_=0.6 Hz, 2H), 4.39 (q, _J_=7.2 Hz, 2H), 2.39 (s, 3H), 1.38 (t, _J_=7.2 Hz, 3H).

3-Carbethoxy-2-pyrazoline-4,5-dicarboxanhydride (23).

Maleic anhydride (2.58 g, 26.3 mmol) and ethyl diazoacetate (3.0 g, 26.3 mmol) were heated to reflux in Et_2O (100 mL) for 3 h. The solid product was filtered, washed with

ether and dried in vacuo. The product was unstable and carried on immediately without further purification:

^{1}H NMR (DMSO-d_6, 300 MHz) δ 9.84 (d, J=2.0 Hz, 1H), 5.23 (dd, J=11.5, 2.3 Hz, 1H), 4.79 (d, J=11.4 Hz, 1H), 4.19 (dq, J=7.0, 1.9 Hz, 2H), 1.23 (t, J=7.0 Hz, 3H).

3-Carbethoxy-5-carbomethoxy-2-pyrazoline-4-carboxylic Acid (24a and 24b).

3-Carbethoxy-2-pyrazoline-4,5-dicarboxanhydride **23** was stirred in MeOH at -20 to -10°C. The temperature of the solution was slowly allowed to warm to room temperature and the solvent was evaporated under reduced pressure affording a mixture of regioisomers as a colourless glass. For subsequent reactions, the products were prepared *in situ*:

^{1}H NMR ($CDCl_3$, 300 MHz) **24a** (~80-85%): δ 8.00 (br s, 1H), 4.85 (d, J=12.7 Hz, 1H), 4.38 (d, J=12.9 Hz, 1H), 4.34-4.26 (m, 2H), 3.75 (s, 3H), 1.33 (t, J=7.1 Hz, 3H). **24b** (~10-20%) : δ 8.00 (br s, 1H), 5.03 (d, J=5.9 Hz, 1H), 4.52 (d, J=5.9 Hz, 1H), 4.34-4.26 (m, 2H), 3.73 (s, 3H), 1.33 (t, J=7.1 Hz, 3H).

Benzyl 3-Carbethoxy-5-carbomethoxy-2-pyrazoline-4-carboxylate (25).

3-Carbethoxy-2-pyrazoline-4,5-dicarboxanhydride **23** (1.0 g, 4.71 mmol) was stirred in MeOH (30 mL) at -10°C for 15 minutes, then treated with a solution of phenyldiazomethane in CH_2Cl_2 until no starting material was detected by TLC. The reaction was poured into CH_2Cl_2 (100 mL), washed with saturated $NaHCO_3$ (100 mL), dried over Na_2SO_4 and evaporated under reduced pressure. The yellow oil (1.54 g, 98%) was carried on without further purification:

^{1}H NMR (DMSO-d_6, 300 MHz) δ 8.93 (s, 1H), 7.39-7.29 (m, 5H), 5.06 (q, J=22.4, 12.1 Hz, 2H), 5.00 (d, J=13.8 Hz, 1H), 4.40 (d, J=13.8 Hz, 1H), 4.08 (q, J=7.0 Hz, 2H), 3.48 (s, 3H), 1.13 (t, J=7.0 Hz, 3H). Approximately 19% of the regioisomer (derived from **24b**) was detected by signals at 8.96 (s, 1H) and 3.43 (s, 3H).

Benzyl 1-Acetyl-3-carbethoxy-5-carbomethoxy-2-pyrazoline-4-carboxylate (26).

A solution of pyrazoline **25** (1.40 g, 4.19 mmol) and acetyl chloride (329 mg, 4.19 mmol) in CH_2Cl_2 (25 mL) was treated with Et_3N (424 mg, 4.19 mmol) at room temperature for 1 h. The reaction was poured into CH_2Cl_2 (100 mL), washed with 1N HCl (100 mL), saturated $NaHCO_3$ (100 mL), and then brine (50 mL), dried over Na_2SO_4 and evaporated under reduced pressure. Purification by column chromatography through silica gel (50% EtOAc/hexanes) afforded 800 mg (45% from **23**) of isomerically pure product as a colourless oil:

^{1}H NMR (DMSO-d_6, 300 MHz) δ 7.40-7.30 (m, 5H), 5.06 (d, J=10.0 Hz, 2H), 5.20 (d, J=13.8 Hz, 1H), 4.72 (d, J=13.8 Hz, 1H), 4.18 (q, J=7.0 Hz, 2H), 3.67 (s, 3H), 1.15 (t, J=7.0 Hz, 3H).

1-Acetyl-3-carbethoxy-5-carbomethoxy-2-pyrazoline-4-carboxylic acid (27).

A solution of ester **26** (720 mg, 1.91 mmol) and cyclohexadiene (1.5 g) in EtOH (10 mL) was treated with Pd-C (10%) and stirred at room temperature for 1 h. The reaction was filtered through Celite and evaporated under reduced pressure affording 537 mg (98%) of **27** as an oily white solid:

^{1}H NMR (DMSO-d_6, 300 MHz) δ 5.03 (d, J=4.9 Hz, 1H), 4.36 (d, J=4.9 Hz, 1H), 4.26 (dq, J=7.1, 1.7 Hz, 2H), 3.67 (s, 3H), 2.27 (s, 3H), 1.25 (t, J=7.1 Hz, 3H).

Carbethoxy Fumaric Acid Mono-*t*-butyl Monoethyl Ester.[28]

Diethyl ketomalonate (1.74 g, 0.01 mol) was added to a solution of (*tert*-butoxycarbonylmethylene)triphenylphosphorane (3.76 g, 0.01 mol) in benzene (25 mL) and the resulting exothermic reaction was stirred at room temperature for 3 h. After

evaporation of solvent under reduced pressure, the oily residue was treated with pentane and stored at -5 °C overnight. The resulting solid was filtered and washed with cold petroleum ether. Evaporation of the filtrate afforded 2.88 g (100%) of the product as a yellow oil which was carried on without further purification:

^{1}H NMR ($CDCl_3$, 300 MHz) δ 6.77 (s, 1H), 4.34 (q, *J*=7.1 Hz, 2H), 4.27 (q, *J*=7.2 Hz, 2H), 1.47 (s, 9H), 1.33 (t, *J*=7.2 Hz, 3H), 1.29 (t, *J*=7.2 Hz, 3H).

Tert-Butyl 3,5,5-Tricarbethoxy-2-pyrazoline-4-carboxylate (28).

A mixture of carbethoxy fumaric acid mono-*t*-butyl monoethyl ester (2.72 g, 0.01 mol) and ethyl diazoacetate (1.14 g, 0.01 mol) were allowed to stand at room temperature for 20 h. The resulting yellow oil was purified by column chromatography through silica gel (50% EtOAc/hexanes) yielding 3.38 g (88%) of **28** as a colourless oil:

IR ($CHCl_3$) 3370 (w), 2984 (m), 2938 (w), 1745 (s), 1587 (w) cm $^{-1}$;

^{1}H NMR ($CDCl_3$, 300 MHz) δ 6.89 (br s, 1H), 4.76 (s, 1H), 4.41-4.26 (m, 5H), 4.13-4.07 (m, 1H), 1.45 (s, 9H), 1.34 (t, *J*=7.0 Hz, 3H), 1.29 (t, *J*=7.2 Hz, 3H), 1.28 (t, *J*=7.2 Hz, 3H);

^{13}C NMR ($CDCl_3$) δ 166.5, 166.3, 160.7, 141.0, 82.7, 78.7, 63.2, 63.0, 61.6, 57.0, 27.0, 14.1, 13.9, 13.8;

HRMS (EI) Calcd for $[M-C_4H_9]^+$ $C_{13}H_{17}N_2O_8$: 329.0985 Found: 329.0988.

3,5,5-Tricarbethoxy-2-pyrazoline-4-carboxylic Acid (29).

A solution of *tert*-butyl 3,5,5-tricarbethoxy-2-pyrazoline-4-carboxylate (2.70 g, 7.0 mmol) in CH_2Cl_2 (50 mL) was treated with trifluoroacetic acid (1.59 g, 14.0 mmol) at room temperature. After 25 h, the reaction was poured into 1N HCl, extracted with CH_2Cl_2 (3 x 50 mL), dried over Na_2SO_4 and evaporated under reduced pressure affording the product as a yellow oil:

^{1}H NMR ($CDCl_3$, 300 MHz) δ 8.20 (br s, 2H), 4.91 (s, 1H), 4.40 (m, 6H), 1.35-1.20 (m, 9H).

Ethyl 2-Carbethoxy-3-formyl-2-propenoate Diethyl Acetal (30).

Piperidine (1.92 g, 22.5 mmol) was added to a solution of diethyl malonate (3.6 g, 22.5 mmol) and glyoxal 1,1-diethyl acetal (1.98 g, 15.0 mmol) in EtOH (20 mL). The reaction was stirred at room temperature for 48 h and evaporated under reduced pressure. Purification by column chromatography through silica gel (3% MeOH/CH_2Cl_2) afforded 1.38 g (34%) of **30** as a colourless liquid:

^{1}H NMR ($CDCl_3$, 300 MHz) δ 6.83 (d, *J*=5.4 Hz, 1H), 5.28 (d, *J*=5.4 Hz, 1H), 4.33-4.21 (m, 4H), 3.70-3.49 (m, 4H), 1.33 (t, *J*=7.0 Hz, 3H), 1.29 (t, *J*=7.0 Hz, 3H), 1.21 (t, *J*=6.9 Hz, 6H).

Triethyl 4-Diethoxymethyl-2-pyrazoline-3,5,5-tricarboxylate (31).

A mixture of ethyl 2-carbethoxy-3-formyl-2-propenoate diethyl acetal **30** (1.38 g, 5.0 mmol) and ethyl diazoacetate (1.14 g, 10.0 mmol) was allowed to stand at 75 °C for 4 h. Removal of the excess ethyl diazoacetate under reduced pressure and purification by column chromatography through silica gel (25% EtOAc/hexanes) afforded 1.73 g (89%) of **31** as a pale yellow oil:

^{1}H NMR ($CDCl_3$, 300 MHz) δ 6.88 (s, 1H), 4.85 (d, *J*=6.6 Hz, 1H), 4.42 (d, *J*=6.3 Hz, 1H), 4.37-4.09 (m, 6H), 3.71-3.43 (m, 4H), 1.34 (t, *J*=7.2 Hz, 3H), 1.28 (t, *J*=7.2 Hz, 3H), 1.27 (t, *J*=7.2 Hz, 3H), 1.13 (dt, *J*=7.2, 1.5 Hz, 6H);

^{13}C NMR ($CDCl_3$) δ 168.2, 166.4, 161.5, 143.5, 98.8, 63.3, 62.8, 62.3, 61.6, 61.2, 52.9, 14.8, 14.1, 13.9, 13.5, 12.5;

HRMS (EI) Calcd for $C_{17}H_{18}N_2O_8$: 388.1846 Found: 388.1841.

Triethyl 4-Bis(carboethoxy)methyl-2-pyrazoline-3,5,5-tricarboxylate (34). Tetraester **33**[30,31] (661 mg, 2.0 mmol) and ethyl diazoacetate (466 mg, 4.0 mmol) were stirred at room temperature for 18 hours and at 60°C for 18 hours. Purification by column chromatography through silica gel (2.5% MeOH/CH_2Cl_2) afforded 832 mg (94%) of the product as a pale yellow oil:

^{1}H NMR ($CDCl_3$, 300 MHz) δ 6.95 (d, *J*=1.2 Hz, 1H), 4.92 (d, *J*=3.6 Hz, 1H), 4.30-4.15 (m, 10H), 1.35-1.22 (m, 15H).

***N*-Phenyl-3-carbethoxy-5-methyl-2-pyrazoline-4,5-dicarboximide (Table 2, entry 2).** *N*-Phenyl-2-methylmaleimide[39] (940 mg, 5.02 mmol) and ethyl diazoacetate (600 g, 5.26 mmol) were heated under reflux until homogeneous. After 1 h a solid mass resulted. Purification by column chromatography through silica gel (5% MeOH/CH_2Cl_2) afforded 1.40 g (93%) of the product as a white solid:

^{1}H NMR ($CDCl_3$, 300 MHz) δ 7.50-7.41 (m, 3H), 7.29-7.26 (m, 2H), 6.85 (s, 1H), 4.37 (m, 3H), 1.72 (s, 3H), 1.38 (t, *J*=7.2 Hz, 3H);

^{1}H NMR (DMSO-d_6, 250 MHz) δ 9.60 (s, 1H), 7.53-7.39 (m, 3H), 7.28-7.24 (m, 2H), 4.42 (s, 1H), 4.24-4.13 (m, 2H), 1.53 (s, 3H), 1.24 (t, *J*=7.1 Hz, 3H).

Triethyl 2-Pyrazoline-3,4,5-tricarboxylate (Table 2, entry 11). Diethyl fumarate (17.2 g, 0.10 mol) and ethyl diazoacetate (11.5 g, 0.01 mol) were stirred at room temperature for 1 h until a solid mass resulted. Standing at room temperature for 16 h afforded the product as a white solid in quantitative yield:

^{1}H NMR ($CDCl_3$, 300 MHz) δ 6.79 (s, 1H), 4.75 (d, *J*=5.1 Hz, 1H), 4.42 (d, *J*=5.7 Hz, 1H), 4.33-4.21 (m, 6H), 1.39-1.26 (m, 9H).

Trimethyl 3-Carbethoxy-2-pyrazoline-4,5,5-tricarboxylate (Table 2, entry 13).

A mixture of dimethyl carbomethoxy fumarate[32] (5.00 g, 0.025 mol) and ethyl diazoacetate (2.82 g, 0.025 mol) was allowed to stand at room temperature for 2 h until homogeneous. A slightly exothermic reaction resulted in a yellow oil. Purification by column chromatography through silica gel (4% MeOH/CH_2Cl_2) afforded 7.16 g, (92%) of the product as a colourless oil which solidified on standing:

mp 72.5-73.5°C;

^{1}H NMR ($CDCl_3$, 300 MHz) δ 7.08 (br s, 1H), 4.86 (d, *J*=1.2 Hz, 1H), 4.33-4.21 (m, 2H), 3.83 (s, 3H), 3.75 (s, 3H), 3.73 (s, 3H), 1.30 (t, *J*=7.0 Hz, 3H);

^{13}C NMR ($CDCl_3$) δ 167.4, 166.6, 166.5, 160.5, 140.4, 78.7, 61.7, 56.0, 54.1, 53.8, 52.9, 14.0;

HRMS (EI) Calcd for $C_{12}H_{16}N_2O_8$: 316.0907 Found: 316.0905.

Dimethyl 4-Carbethoxy-pyrazole-2,2-dicarboxylate (Table 2, entry 17).

Methyl 2-chloro-1-carbomethoxyacrylate (179 mg, 1.0 mol) and ethyl diazoacetate (115 mg, 1.0 mmol) were mixed at 70 °C for 10 minutes and allowed to stand at room temperature for 6 days. Purification by column chromatography through silica gel (3% MeOH/CH_2Cl_2) afforded 56 mg (22%) of the product as a yellow solid:

mp 62-63.5 °C;

^{1}H NMR ($CDCl_3$, 300 MHz) δ 7.60 (s, 1H), 4.33 (q, *J*=7.1 Hz, 2H), 3.80 (s, 3H), 3.79 (s, 3H), 1.32 (t, *J*=7.1 Hz, 3H);

^{13}C NMR ($CDCl_3$) δ 165.0, 164.7, 162.8, 133.6, 114.2, 62.5, 52.4, 51.8, 14.3;

IR (KBr) 3002 (m), 2955 (m), 2142 (s), 1716 (s), 1694 (s), 1593 (s) cm $^{-1}$;

HRMS (EI) Calcd for $C_{10}H_{12}N_2O_6$: 256.0695 Found: 256.0697.

References and Notes

(1) Obtained from Professor W. L. Jorgenson, Yale University, New Haven.

(2) Kohler, E. P.; Reid, G. H. *J. Am. Chem. Soc.* **1925**, *47*, 2803-2811.

(3) Nasielski, J.; Chao, S.; Nasielski-Hinkens, R. *Bull. Soc. Chim. Belg.* **1989**, *98*, 375-386.

(4) Serratosa, F.; Lopez, F.; Font, J. *An. Quim.* **1974**, *70*, 893-898.

(5) Mock, W. L. *J. Org. Chem.* **1971**, *36*, 3613-3614.

(6) Quast, H.; Berneth, C. *Chem. Ber.* **1983**, *116*, 1345-1363.

(7) Newbold, B. T. In *The Chemistry of Hydrazo, Azo and Azoxy Groups*; Patai, S., Ed.; John Wiley and Sons: London, 1975; Part 1, Chapter 15, pp 599-642.

(8) Jarboe, C. H. In *Heterocyclic Compounds: Pyrazoles, Pyrazolines, Pyrazolidines, Indazoles and Condensed Rings*; Wiley, R. H., Ed.; John Wiley and Sons: New York, 1967; Chapters 6-8, pp 175-278.

(9) Back, T. G. *J. Org. Chem.* **1981**, *46*, 1442-1446.

(10) Evans, D. A.; Urpi, F.; Somers, T. C.; Clark, J. S.; Bilodeau, M. T. *J. Am. Chem. Soc.* **1990**, *112*, 8215-8216.

(11) Thottathil, J. K.; Moniot, J. L.; Mueller, R. H.; Wong, M. K. Y.; Kissik, T. P. *J. Org. Chem.* **1986**, *51*, 3140-3143.

(12) Danishefsky, S.; Berman, E.; Clizbe, L. A.; Hirama, M. *J. Am. Chem. Soc.* **1979**, *101*, 4385-4386.

(13) Ohfune, Y.; Tomita, M. *J. Am. Chem. Soc.* **1982**, *104*, 3511-3513.

(14) Valasinas, A.; Frydman, B. *J. Org. Chem.* **1992**, *57*, 2158-2160.

(15) Hamada, Y.; Hara, O.; Kawai, A.; Kohno, Y.; Shioiri, T. *Tetrahedron* **1991**, *47*, 8635-8652.

(16) Kishida, Y.; Terada, A. *Chem. Pharm. Bull.* **1969**, *17*, 2417-2423.

(17) Carter, H. E.; van Abeele, F. R.; Rothrock, J. W. *J. Biol. Chem.* **1949**, *178*, 325-334.

(18) Hubert, J. C.; Wijnberg, J. B. P. A.; Speckamp, W. N. *Tetrahedron* **1975**, *31*, 1437-1441.

(19) Arnold, D. P.; Nitschinski, L. S.; Kennard, C. H. L.; Smith, G. *Aust. J. Chem.* **1991**, *44*, 323-330.

(20) The determination of regioisomers was done by examining the ^{1}H NMR (see experimental section) and by NOE studies (see reference 22).

(21) Watanabe, Y.; Yamashita, M.; Mitsudo, T.; Igami, M.; Takegami, Y. *Bull. Chem. Soc. Jpn.* **1975**, *48*, 2490-2491.

(22) Nuclear Overhauser ^{1}H NMR studies of **24** were performed on a Varian VXR-500 MHz spectrometer in DMSO-d_6. Longitudinal relaxation times (T_1) were measured by using the inversion-recovery method as implemented in the Varian software (VNMR version 3.1).

(23) Overberger, C. G.; Anselme, J. *J. Org. Chem.* **1963**, *28*, 592-593.

(24) Creary, X. *Org. Syn.* **1985**, *64*, 207-216.

(25) Hünig, S.; Schaller, R. *Angew. Chem. Int. Ed. Engl.* **1982**, *21*, 39-49.

(26) Carpino, L. A. *J. Org. Chem.* **1964**, *29*, 2820-2824.

(27) Kelly, R. *Tetrahedron Lett.* **1973**, 437-440.

(28) Snider, B. B.; Roush, D. M.; Killinger, T. A. *J. Am. Chem. Soc.* **1979**, *101*, 6023-6027.

(29) Stetter, H.; Mohrmann, K. H. *Synthesis* **1981**, 129-130.

(30) Zincke, T. *Chem. Ber.* **1882**, *15*, 279-287.

(31) Coutelle, C. *J. Prakt. Chem.* **1906**, *73*, 49-100.

(32) Evans, S. B.; Abdelkader, M.; Padias, A. B.; Hall, H. K. J. *J. Org. Chem.* **1989**, *54*, 2848-2452.

(33) Wolff, S.; Hoffmann, H. M. R. *Synthesis* **1988**, 760-763.

(34) Baumann, M. E.; Bosshard, H. *Helv. Chim. Acta.* **1978**, *61*, 2751-2753.

(35) Stotter, P. L.; Eppner, J. B. *Tetrahedron Lett.* **1973**, 2417-2420.

(36) Stambouli, A.; Amouroux, R.; Chastrette, M. *Tetrahedron Lett.* **1987**, *28*, 5301-5302.

(37) Franz, R. G.; Weinstock, J. *Synth. Commun.* **1988**, *18*, 1913-1917.

(38) Rappoport, Z.; Topol, A. *J. Chem. Soc., Perkin II.* **1972**, 1823-1831.

(39) Purchased from Aldrich Chemical Co.

Chapter Three. A Self-Assembled Calixarene "Football"

3.1 Introduction

A more synthetically convenient approach to the development of potential self-assembling systems is to utilize the preorganized architecture provided by macrocycles as starting materials for the preparation of novel subunits. For example, calixarenes exhibit vase-shaped structures with readily modified aromatic "upper-rims".[1-4] Introduction of self-complementary hydrogen bond donor and acceptor sites onto these rims would generate species which have the potential to assemble into dimeric structures resembling footballs (Figure 1).

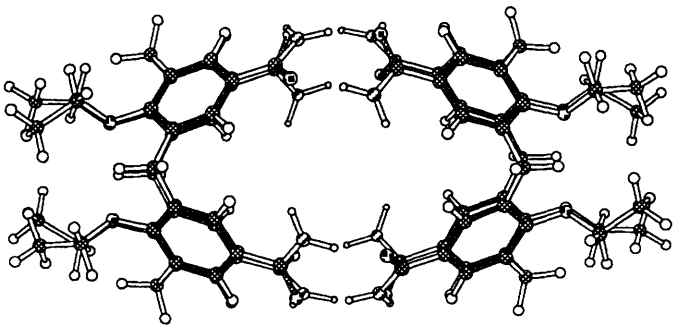

Figure 1. *Predicted dimeric assembly when two calix[4]arene subunits interact through hydrogen bonds. Amide groups are used as the example of "upper-rim" hydrogen bond donor and acceptor sites.*

The basket-like shape of the calixarenes has attracted much attention in the area of "cavity chemistry". The depth and openess of the basket is regulated by the size of the ring system as well as the presence of intramolecular phenolic hydrogen bonds. The angle formed by the planes of opposing benzenes (θ ~49°) of the cyclic tetramers is not sufficiently large to allow four subunits to adopt a tetrahedral geometry (60° angles are required for this type of structure). A dimer is therefore the more reasonable prediction

despite the poor intermolecular amide-amide angle (Ψ = 132-133°), as shown by molecular modeling (Figure 2).

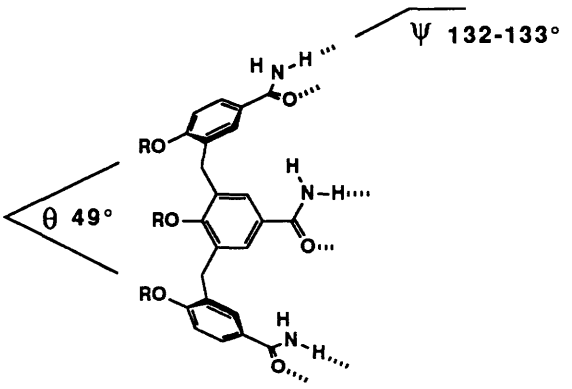

Figure 2. *Although the value of Ψ is not ideal, the value of θ is too small to allow for assembly of more than two subunits.*

In order to produce an optimal geometry for dimerization (decrease in angle θ), it is essential to alkylate the lower-rim hydroxyl groups. The lack of these alkyl groups introduces four intramolecular hydrogen bonds between adjacent hydroxyls resulting in a more open and shallow basket (an increase in angle θ). Phenolic alkylation also prevents the rapid interconversion between the four possible calix[4]arene conformations, defined as cone, partial cone, 1,2-alternate, and 1,3-alternate (Figure 3).[4] This restriction is necessary to adopt enforced cavities and limit their conformational mobility. The vase-shaped cone conformer predominates and can be readily isolated when the "locking" alkyl groups are present.

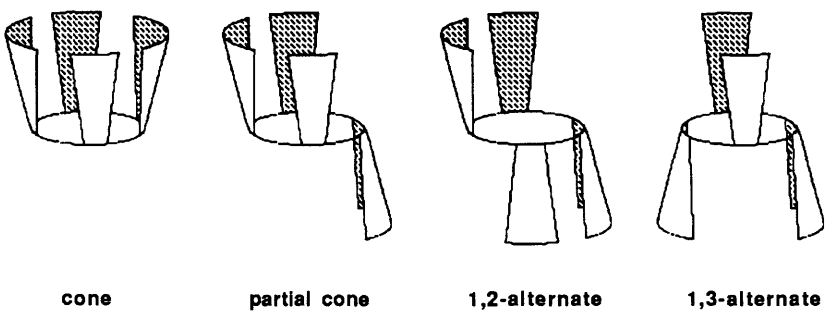

Figure 3. *Possible calix[4]arene conformations.*

Inclusion complexes of calixarenes have been realized, primarily in the solid state, where the macrocycles retain solvent from which they were crystallized.[5] Examples of guests trapped within the cyclic tetramer include acetonitrile,[6] chloroform,[7] dimethyl-sulfoxide,[8] methylammonium salts,[8,9] *tert*-butylamine[10] and toluene[7] (only the methyl group of toluene is located within the "basket"). There are few examples of similar *endo* calixarene-guest complexes in solution,[11-15] although recently, a solution complex between *tert*-butylcalix[8]arene and fullerenes has been reported along with its use as a means to purify C_{60}.[16]

A "capped" ditopic calixarene receptor would provide the means for more effective trapping of guests species within a larger, more enclosed cavity. "Double" calixarenes have been prepared through covalent linkages between the ether groups[17] as well as through upper rim (para-positions) functionality.[18] There are also examples of poly-macrocyclic systems composed of covalently linked calixarenes, crown ethers and cyclophanes.[10,19-23] There are few examples to date of "double" calixarenes held together completely through hydrogen bonds.[24]

3.2 Synthesis

The published preparation of calix[4]arenetetracarboxamide **1** makes it an attractive target molecule for preliminary self-assembling studies in solution.[25] De-*tert*-butylation of commercially available *tert*-butylcalix[4]arene **2** furnished tetrahydroxycalix[4]arene **3** which was octylated at the phenolic hydroxyl groups. The introduction of the octyl groups not only prevents the interconversion of conformers, but also provides organic solubility (unsubstituted calixarenes are sparingly soluble in organic solvents). Fractional recrystallization from acetone afforded the octylated calix[4]arene as its pure cone-conformer. The presence of a sharp pair of doublets for the Ar-CH_2-Ar methylene protons

in the ^{1}H NMR proves that only the cone conformer is present. Tetrabromination, cyanation and partial hydrolysis under mild conditions yielded tetraamide **1**.

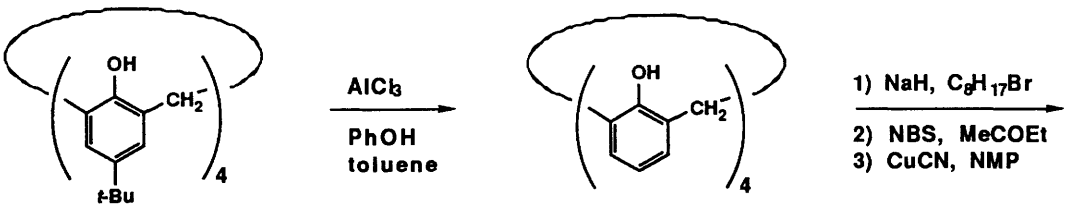

2 **3**

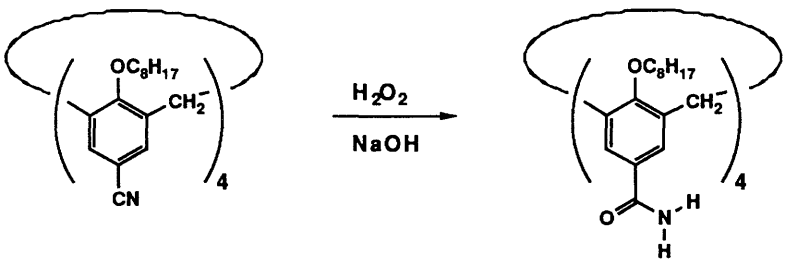

1

3.3 Assembly Studies

^{1}H NMR Methods

Tetraamide **1** was sparingly soluble in organic solvents, partially soluble in alcohols, but freely soluble in 5-20% mixtures of methanol/chloroform. The amphoteric behavior of **1** was evident from the formation of gels in solvents such as dimethylsulfoxide or chloroform. The assembling behaviour of **1** in methanol-chloroform was concentration dependent. An upfield shift of the amide N-H resonances in the ^{1}H NMR was observed as the solutions were diluted. Dilution titrations allowed for the evaluation of dimerization constants (K_{dim}) and were performed using 5-20% $CD_3OH/CDCl_3$ solutions. It was essential to use methanol-d_3 in order to observe the amide N-H proton signals (in methanol-d_4 these signals disappear due to rapid deuterium exchange). The upfield shift of the signals for the amide protons was followed during the course of the dilution, the change

in frequency was plotted as a function of concentration and values of K_{dim} were calculated using curve-fitting techniques.

In 20% $CD_3OH/CDCl_3$ the data deviated slightly from the simple dimerization program at high concentrations affording a K_{dim} value of 210 M^{-1} (Figure 4). The deviation implies to a first approximation (assuming a simple dimeric species) that at high concentrations, small amounts of assemblies other than the dimer are likely, despite molecular modeling showing them to be energetically disfavoured.

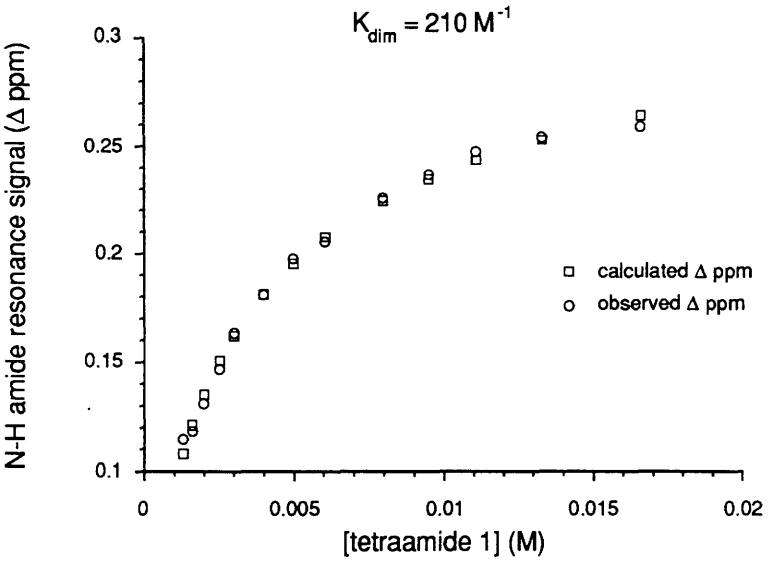

Figure 4. *Dilution titration of calixarene **1** in 20% methanol-d_3/chloroform-d. Calculated data points were obtained using curve-fitting programs. Deviation from the simple dimerization protocol is evident as solutions of **1** are concentrated.*

When the ratio of competitive to noncompetitive hydrogen bonding solvents was decreased to 5% methanol/chloroform, the deviation from the simple dimer protocol was enhanced, supporting the presence of higher-order aggregates (Figure 5). The amphoteric behaviour of **1** in pure organic solvents is described above and similar results can be expected as the solvent becomes more like chloroform. Although a K_{dim} of 446 M^{-1} was calculated in this solvent system, this value must be evaluated with caution as the solvent approaches one mole fraction.

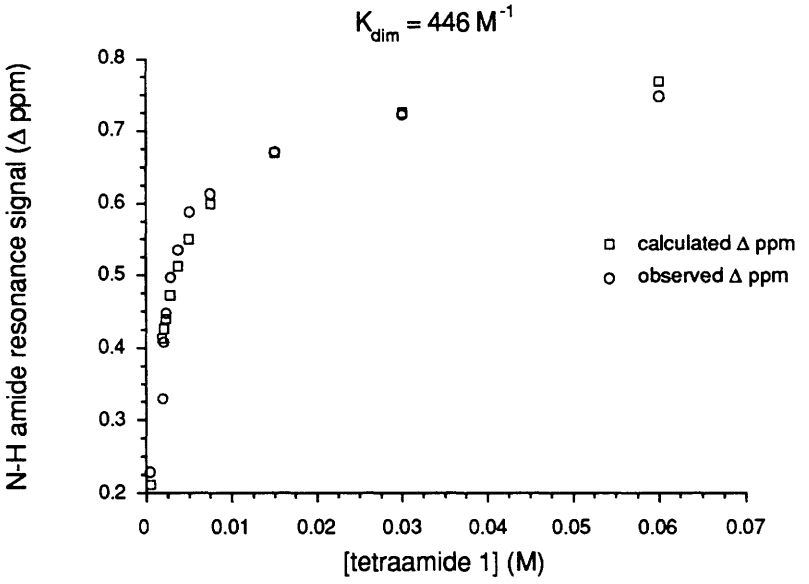

Figure 5. *Dilution titration of* ***1*** *in 5% methanol-d_3/chloroform-d. The observed data deviated significantly from the values calculated for only dimerization.*

The binding constant increased as lower methanol concentrations were used. This finding is consistent with assemblies held together by hydrogen bond interactions where increasing the methanol content enhances the hydrogen bonding competition of the solvent. It cannot be assumed that this is a genuine dimerization constant until the stoichiometry of the aggregate is determined and these binding constants must be regarded as K_{assoc}. Determining the make-up of the self-assembled system by mass spectrometry[26] and vapour-phase osmometry (VPO) could provide evidence into the composition of these aggregates.

Mass Spectrometry

Initial attmepts at crystallizing samples of **1** as well as VPO investigations have met with little success. The fast atom bombardment mass spectrum[27] indicated the presence of a dimeric species at 2091 atomic mass units (calculated for $C_{128}H_{184}N_8O_{16}$: 2091 amu)

(Figure 6). However, the predominance of such a species over higher-order aggregates cannot be assumed owing to the inability of this particular FAB spectrometer to measure accurate mass above 3000 amu. The plasma desorption mass spectrum can measure mass values in the thousands and biochemists use this technique to accurately measure molecular weights of proteins. The plasma desorption data[28] showed peaks corresponding to the dimer, but no peaks were observed at higher mass (up to 10 000 amu). It can, therefore, be concluded that the dimer is the only aggregate present under these conditions.

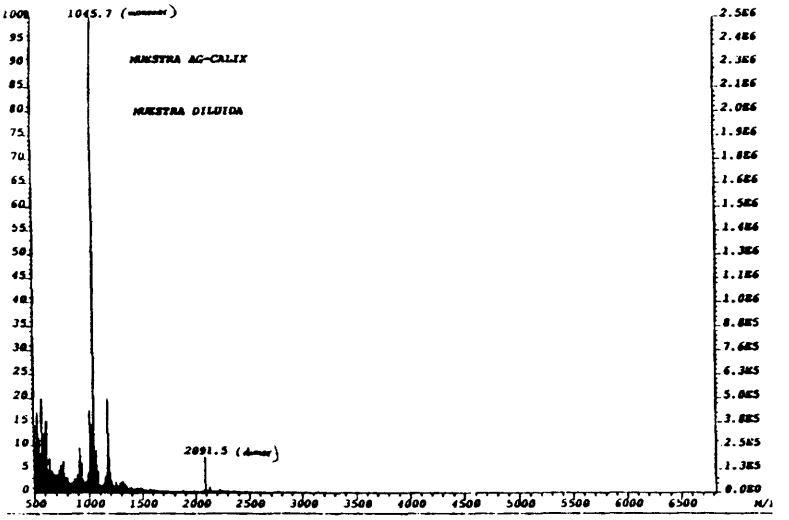

Figure 6. *FAB mass spectrum for calixarene 1 showing a signal for the dimer at 2091.5 amu (calculated: 2091.4). The monomer peak appears at 1045.7 amu (calculated: 1045.7).*

The mass spectra data of calixarenes must be evaluated with caution because there have been many reported peculiarities.[4] For example, the mass spectrum of 4-*tert*-butylcalix[8]arene shows a signal corresponding to the cyclic tetramer. Similarly, the spectrum of a trimethylsilylated cyclic tetramer showed a signal for the octamer.

Encapsulation

The acetonitrile and toluene-occupied calixarenes revealed that the methyl group of both guests is located within the basket provided by the aromatic calix[4]arene rings.

These results, which are supported by molecular modeling, suggest that 2-butyne is the appropriate size and shape to form inclusion complexes, if a dimeric species of **1** is assumed. However, the presence of 2-butyne resulted in no change in the dilution titrations of **1** in 5% methanol/chloroform. Although this observation does not completely exclude the possibility of forming an inclusion complex, only that the guest does not affect the assembling behaviour of **1**, it seems unlikely that 2-butyne is trapped within the dimer's cavity. This is not completely unexpected because, in order to ecapsulate 2-butyne, solvent must be expelled from the cavity (most likely two $CDCl_3$ molecules). The entropy gained from this expulsion will probably not be able to overcome the disfavoured enthalpy of desolvation (also, there is a great excess of solvent body over 2-butyne). Investigations using techniques such as X-ray crystallography, MS and VPO would clarify the inclusion properties of the dimer.

3.4 Conclusions

In order to promote the formation of distinct assemblies, the properties of the solvent system must be fine-tuned. This would prevent any amphoteric properties of the subunits, and the presence of any higher ordered aggregates would be minimized.

Larger baskets would allow for the formation of inclusion complexes with biorelevant species. The expansion to larger, more versatile calixarenes, the cyclic octamer and hexamer for example, introduces the disadvantage of conformational mobility. For instance, the cyclic octamer displays a "lower-rim" opening large enough for groups such as tosylates to pass through the plane defined by the aromatic rings. The hexamers are intermediate in behaviour; they are conformationally more mobile than the cyclic tetramer, but the conformations can be frozen out at low temperatures. These hexamers prefer the 1,3,5-alternate (three up and three down) or the "winged" 1,5-alternate. In most cases the cone is not preferred.

Another approach to encourage dimerization would be to introduce hydrogen bonding sites with stronger affinities for each other (the amide-amide interaction is one of the weaker hydrogen bond pairs). The positioning of these groups further from the periphery of the calix[4]arene ring system would result in dimers possessing larger internal cavities that would resemble the capacity of the cyclic hexamer or octamer.

3.5 Experimental

For a general description of apparatus, materials and methods, see chapter 2.

Dilution Titrations

All titrations were performed at ambient temperatures (~22°C) by diluting 600-700 μL solutions of the calix[4]arene (20-60 mM) with 5-20% methanol-d_3/chloroform-*d*. The changes in chemical shift of the substrate's amide N-H protons were recorded as a function of total concentration. Nonlinear least squares regression curve fitting was used to determine the dimerization constants, along with the estimated chemical shift of the monomer protons.

Calix[4]arene (2).[29]

A slurry of 4-*tert*-butylcalix[4]arene (24.0 g, 0.037 mol), phenol (16.28 g, 0.178 mol) and aluminum chloride (25.3 g, 0.194 mol) in toluene (225 mL) was stirred under argon for 1 h at room temperature. The reaction mixture was poured into 0.2 N HCl (450 mL), the organic layer was separated and concentrated under reduced pressure. Methanol was added to the residue, the solid was filtered, and washed with methanol yielding 15.52 g, (99%) of **2** as a white solid:

^{1}H NMR (DMSO-d_6, 300 MHz) δ 9.74 (br s, 4H), 7.10 (d, *J*=7.5 Hz, 8H), 6.64 (t, *J*=7.5 Hz, 4H), 3.87 (br s, 8H).

Calix[4]arene Tetraoctyl Ether (3, Cone Conformer).[25]

Calix[4]arene **2** (8.5 g, 0.02 mol) was added in one portion to a suspension of oil-free sodium hydride (6.8 g) in dry DMF (300 mL) under argon. After stirring at 70°C for 10 minutes, octyl bromide (42 g, 0.22 mol) was added dropwise and stirred at 70°C for 1 h. The reaction was cooled to room temperature and methanol (12 mL) was added dropwise to consume the excess sodium hydride. The solvent was removed under reduced pressure and water (400 mL) was added to the residue. After storing overnight at room temperature, the resulting solid was filtered and washed with cold methanol (3x200 mL) yielding 9.75 g (56%) of **3** as a white solid:

^{1}H NMR ($CDCl_3$, 300 MHz) δ 6.63-6.55 (m, 12H), 4.44 (d, *J*=12.9 Hz, 4H), 3.87 (t, *J*=7.8 Hz, 8H), 3.14 (d, *J*=13.2 Hz, 4H), 1.93-1.88 (m, 8H), 1.36-1.30 (m, 40H), 0.89 (t, *J*=7.2 Hz, 12H).

5,11,17,23-Tetrabromocalix[4]arene Tetraoctyl Ether.[25]

NBS (8.87 g, 0.05 mol) was added in one portion to a solution of the cone conformer of calix[4]arene tetraoctyl ether (6.55 g, 7.5 mmol) in ethyl methyl ketone (150 mL). The reaction mixture was stirred at room temperature for 48 h, treated with 10% $NaHCO_3$ (350 mL), and stirred for 15 minutes. Extraction with CH_2Cl_2 (3x200 mL), drying over Na_2SO_4 and evaporation of the solvent resulted in a yellow solid. Recrystallization from acetone-methanol afforded 8.0 g (90%) of the product as a white solid:

^{1}H NMR ($CDCl_3$, 250 MHz) δ 6.80 (br s, 8H), 4.33 (d, *J*=13.4 Hz, 4H), 3.83 (t, *J*=7.5 Hz, 8H), 3.07 (d, *J*=13.5 Hz, 4H), 1.85 (m, 8H), 1.33-1.29 (m, 40H), 0.89 (t, *J*=6.8 Hz, 12H).

5,11,17,23-Tetracyanocalix[4]arene Tetraoctyl Ether.[25]

5,11,17,23-Tetrabromocalix[4]arene (4.76 g, 4.0 mmol) and CuCN (5.0 g, 56.0 mmol) were heated in refluxing NMP (50 mL) under $CaCl_2$ drying tube for 4 h. The reaction

mixture was cooled to 100°C and $FeCl_3$ (15 g in 275 mL 2N HCl) was added. After stirring for 1 h at 100°C and overnight at room temperature, the precipitate was filtered off and washed with water. Purification by column chromatography through silica gel (5% $MeOH/CH_2Cl_2$) afforded 2.35 g (60%) of the product as a white solid:
^1H NMR ($CDCl_3$, 300 MHz) δ 6.99 (s, 8H), 4.43 (d, *J*=13.7 Hz, 4H), 3.92 (t, *J*=7.6 Hz, 8H), 3.24 (d, *J*=13.7 Hz, 4H), 1.87-1.84 (m, 8H), 1.39-1.29 (m, 40H), 0.89 (t, *J*=7.0 Hz, 12H).

5,11,17,23-Tetracarboxamidecalix[4]arene Tetraoctyl Ether (1).[25]

5,11,17,23-Tetracyanocalix[4]arene tetraoctyl ether (2.0 g, 2.05 mmol), Bu_4NHSO_4 (1.0 g, 30.0 mmol), aqueous H_2O_2 (7.8 mL of 30%), aqueous NaOH (7.8 mL of 20%) and CH_2Cl_2 (10 ML) were stirred vigorously at room temperature for 48 h. The solvent was evaporated and the residue resubmitted to the reaction conditions described above. After 16 h the reaction was quenched with 1N HCl (100 mL), extracted with $CHCl_3$ (5x100 mL), dried over Na_2SO_4 and the solvent evaporated. Purification by column chromatography through silica gel (20% $MeOH/CH_2Cl_2$) and recrystallization from methanol afforded 988 mg (46%) of **1** as a white solid:
^1H NMR (20% $CD_3OH/CDCl_3$, 300 MHz) δ 7.27 (br s, 4H, amide), 7.05 (s, 8H), 6.37 (br s, 4H, amide), 4.32 (d, *J*=13.5 Hz, 4H), 3.78 (t, *J*=7.3 Hz, 8H), 3.12 (d, *J*=13.5 Hz, 4H), 1.78-1.74 (m, 8H), 1.29-1.12 (m, 40H), 0.76 (t, *J*=6.8 Hz, 12H);
HRMS (FAB in 3-NBA) Cald for $C_{64}H_{92}N_4O_8$ $[M+H]^+$: 1045.6994 Found: 1045.7004.

References and Notes

(1) For comprehensive reviews on calixarenes, see: Gutsche, C. D. In *Host Guest Complex Chemistry-Macrocycles*; Vögtle, F.; Weber, E., Ed., Springer-Verlag: New York, 1985; pp 375-421. Also, references 2-5, 7.

(2) Atwood, J. L. *Inclusion Phenomena and Molecular Recognition*; Plenum Press: NY, 1990.

(3) Gutsche, C. D.; Rogers, J. S.; Stewart, D. *Pure Appl. Chem.* **1990**, *62*, 485-491.

(4) Gutsche, C. D. In *Calixarenes: A Versatile Class of Macrocyclic Compounds*; Vicens, J.; Böhmer, V., Ed.; Kluwer Academic Publishers: Boston, 1991; pp 3-37.

(5) Andretti, C. D., Ugozzoli, F. In *Calixarenes: A Versatile Class of Macrocyclic Compounds*; Vicens, J.; Böhmer, V., Ed., Kluwer Acedemic Publishers: Boston, 1991; pp 87-123.

(6) Beer, P. D.; Drew, M. G. B.; Hazelwood, C.; Hesek, D.; Hodakova, J.; Stokes, S. E. *J. Chem. Soc., Chem. Commun.* **1993**, 229-231.

(7) Gutsche, C. D. In *Inclusion Compounds*; Atwood, J. L.; Davies, J. E. D.; MacNicol., Ed.; Oxford University Press: Oxford, 1991; Vol. 4, pp 27-63.

(8) Atwood, J. L.; Orr, G. W.; Juneja, R. K.; Bott, S. G.; Hamada, F. *Pure Appl. Chem.* **1993**, *65*, 1471-1476.

(9) Shinkai, S. *J. Am. Chem. Soc.* **1990**, *112*, 9053-9058.

(10) Gutsche, C. D.; Iqbal, M.; Nam, K. S.; See, K.; Alan, I. *Pure Appl. Chem.* **1988**, *60*, 483-488.

(11) Shinkai, S.; Mori, S.; Tsubaki, T.; Sone, T.; Manabe, O. *Tetrahedron Lett.* **1984**, *25*, 5315-5318.

(12) Shinkai, S.; Koreishi, H.; Mori, S.; Sone, T.; Manabe, O. *Chem. Lett.* **1985**, 1033-1036.

(13) Shinkai, S. *Pure & Appl. Chem.* **1986**, *58*, 1523-1528.

(14) Shinkai, S.; Mori, S.; Koreishi, H.; Tsubaki, T.; Manabe, O. *J. Am. Chem. Soc.* **1986**, *108*, 2409-2416.

(15) Gutsche, C. D.; Bauer, L. J. *J. Am. Chem. Soc.* **1985**, *107*, 6052-6075.

(16) Atwood, J. L.; Koutsantonis, G. A.; Raston, C. L. *Nature* **1994**, *368*, 229-231.

(17) McKervey, M. A.; Owens, M.; Schulten, H.-R.; Vogt, W.; Böhmer, V. *Angew. Chem. Int. Ed. Engl.* **1990**, *29*, 280-282.

(18) Böhmer, V.; Goldmann, H.; Vogt, W.; Vicens, J.; Asfari, Z. *Tetrahedron Lett.* **1989**, *30*, 1391-1394.

(19) Canceill, J.; Collet, A.; Gabard, J.; Kotzyba-Hilbert, F.; Lehn, J.-M. *Helv. Chem. Acta.* **1982**, *65*, 1894-1897.

(20) Hamilton, A. D.; Kazanjian, P. *Tetrahedron Lett.* **1985**, *26*, 5735-5738.

(21) Saigo, K.; Lin, R.-J.; Kubo, M.; Youda, A.; Hasegawa, M. *Chem. Lett.* **1986**, 519-522.

(22) Gutsche, C. D.; See, K. *J. Org. Chem.* **1992**, *57*, 4527-4539.

(23) Wasikiewicz, W.; Rokicki, G.; Kielkiewicz, J.; Böhmer, V. *Angew. Chem. Int. Ed. Engl.* **1994**, *33*, 214-216.

(24) van Loon, J. **1992**, Dutch Thesis.

(25) Conner, M.; Janout, V.; Regen, S. L. *J. Org. Chem.* **1992**, *57*, 3744-3746.

(26) Ganem, B.; Henion, J. D. *Chemtracts-Organic* **1993**, 1-22.

(27) FAB mass spectra studies were obtained from Prof. Javier de Mendoza, Universidad Autonoma de Madrid.

(28) Plasma desorption mass spectra were run on BioIon spectrophotometer (Applied Biosystems) from a nitrocellulose target with 1,1,1,3,3,3-hexafluoropropanol as solvent. In general data aquisitions of 3 hours were used.

(29) Gutsche, C. D.; Lin, L. G. *Tetrahedron* **1986**, *42*, 1633-1640.

Chapter Four. Encapsulation of Small Organic Molecules Within a Self-Assembled Dimer

4.1 Introduction

Recent progress in molecular recognition has introduced a series of sophisticated compounds that sucessfully encapsulate ions and small molecules. Examples include cryptands,[1,2] cryptophanes,[3,4] and carcerands.[5-7] These structures consist of covalently fused macrocycles, possessing cavities of various sizes, and openings to permit entrance and exit of the guests. The free and bound guest species are related by energy barriers that depend on the ease of passage of the guests through the openings provided by the macrocycles.

In recent investigations Cram and coworkers reported the encapsulation of small organic molecules such as chloroform, methylene chloride and propylene oxide by organic soluble carcerand systems (**A**).[8] Slow exchange is evidenced by separate signals for free and bound guests ($\Delta\delta$ 3-4 ppm) in the ^{1}H NMR spectra. The entrance and exit of the guests are accompanied by a rotation of the "polar caps", resulting in an expansion of the cavity as well as an opening of the holes. In these cases, there is limited reversibility. An average of 100 hours at elevated temperatures is required to afford full decomplexation. Large guests (molecular weights above 200) were also encapsulated, but only at elevated temperatures (80-140°C).[7] Both of the above examples exhibit no complexation equilibria under ambient conditions.

Collet and coworkers have reported similar encapsulation properties of cryptophane systems (**B**). Signals for protons of small monocarbon species trapped within the cryptophane cage were observed at ambient temperatures.[4,9,10] The authors also have decribed solid state inclusion complexes of these encapsulators and methylene chloride. One molecule of solvent was found within the cavity.[3]

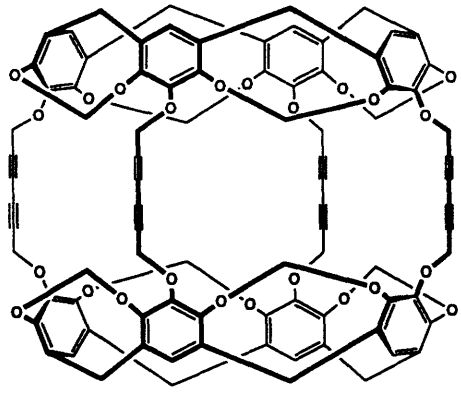

A

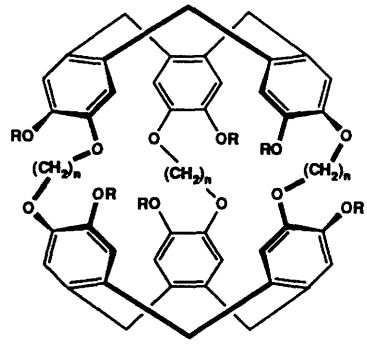

B

The covalent encapsulators described above have the distinct drawback that they are not lenient with regards to the morphology of the guests. The opening and closing of the holes, by twisting the "polar caps", is the rate determining step for entrance and exit of guests. This results in the need for definite host-guest shape complementarity. The complementarity is, however, with regard to that of the holes and not of the inner cavity. Guests of optimal volume will not be bound if they cannot squeeze through these holes. Thus, spherical guests of ideal volume are not bound. These entrance-exit problems can be solved by using an encapsulating assembly, held together by weak intermolecular forces.

Reversible guest binding is certainly not a new lesson, and is one which is frequently taught by biological systems. In nature, reversibility is provided by the complexation through weak intermolecular forces, viral capsids being one of the most elegant examples. The appeal of such a mode of superstructure formation is due primarily to the economics of using many copies of a single self-complementary subunit, as described previously.

4.2 Development of a Self-Assembled Tennis Ball

Recently, molecule **1** was introduced, and its dimerization in solution was described (Figure 1).[11] The structure features a series of hydrogen bonding donors and

acceptors and a skeletal curvature that positions these sites in a self-complementary manner. The outcome is a closed-shell hollow dimer held together by eight hydrogen bonds running along the seam of a roughly spherical structure resembling a tennis ball.

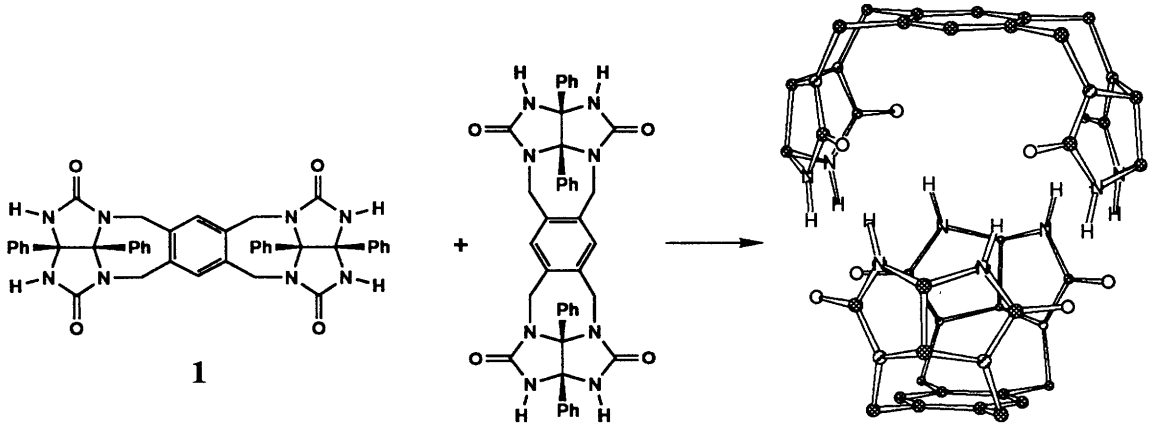

1

Figure 1. *Dimerization of molecule* **1** *into a "tennis ball" dimer. The phenyl groups and carbon-bound hydrogens have been removed from the computer generated structure for clarity.*

In the previous chapter, the idea of flexibility inducing structural ambiguity was described. In the case at hand, there is only one way for the hydrogen bonds to interact. Molecule **1** takes advantage of the attractive structural features of diphenylglycoluril (tetrahydro-3a,6a-diphenyl[4,5-*d*]imidazole-2,5(1H,3H)-dione), a system whose architecture was instrumental in building covergent molecular recognition systems.[12-20] The *syn* fusion of the glycolurils onto a durene spacer provides an enforced concavity, enhanced by the appending phenyl groups sterically shielding the structure's convex face. The glycoluril lactam functionality provides the self-complementary hydrogen bond donors and acceptors. The result is a hydrogen bond surface that limits the possibilities for assembling as a polymer in a "zig-zag" fashion. The structural preorganization restricts the assembly pattern into only a dimer.

4.3 Synthesis

Molecule **1** was readily prepared in two simple steps from commercially available starting materials. Treatment of benzil with urea under acidic conditions generated diphenylglycoluril as reported in the literature.[21,23] Fusion of two glycoluril units onto tetrabromodurene was accomplished under vigorous coupling conditions (Scheme 1).[11] It should be noted that a large excess of glycoluril was required to avoid other reaction products (including polymers). When only two equivalents of glycoluril were reacted, the tetraalkylated products of type **2** predominated. Isolation of **1** was accomplished by extracting the solid product (mainly unreacted glycoluril) with chlorinated solvents such as chloroform and methylene chloride. Evaporation of the extract and trituration of the solid residue with THF furnished pure **1**.

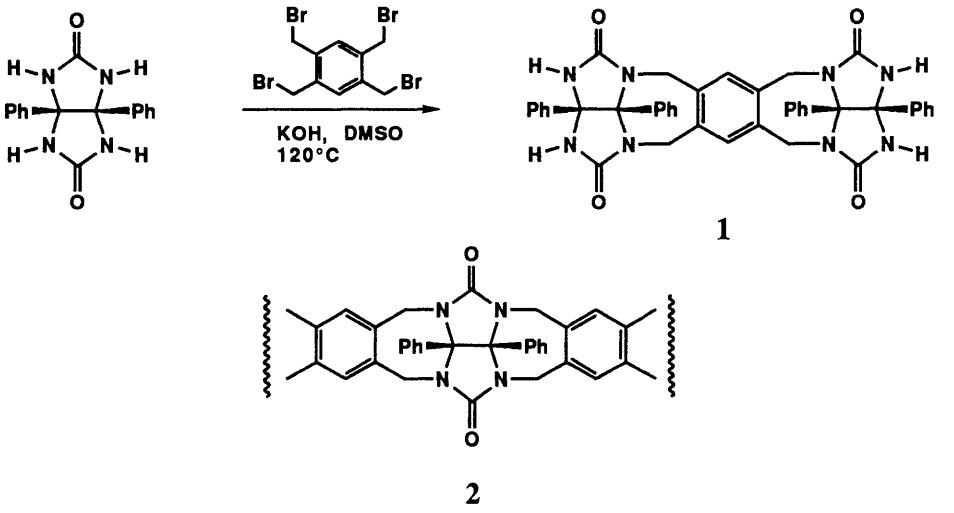

Scheme 1. *Synthesis of molecule **1** from glycoluril and tetrabromodurene. Excess glycoluril was required to avoid the formation of species of structure **2**.*

It is interesting to note that of the two possible conformational reaction products (Figure 2), only the desired *C*-shaped conformer could be isolated. This difference in lipophilicity can most likely be attributed to its high tendency to assemble into a dimer. The

result is a more organic soluble species (all hydrophilic functionality is involved in hydrogen bonding and is masked from the solvent body).

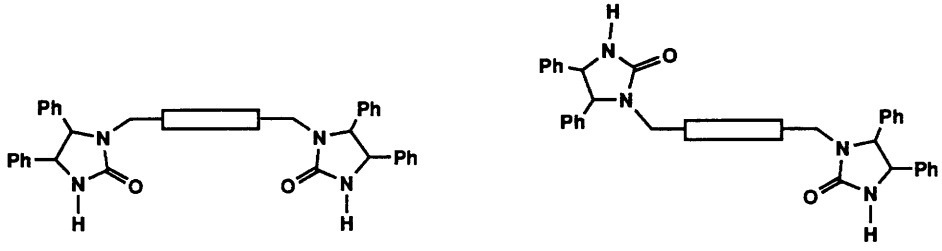

***C*-isomer** **S-isomer**

Figure 2. *Two possible synthetic geometric isomers of* ***1****. Only the C-shaped isomer was isolated from the extractions.*

The isolation of only the *C*-isomer was established by X-ray crystallographic analysis (Figure 3).[22] Crystals were grown from chloroform and were sealed in a capillary with mother liquor for analysis. More than one quarter of the contents of the crystal was occupied by solvent molecules, and because they were not tightly held, the crystals had the tendency to lose solvent and become powder when they were not enclosed with mother liquor. Structural refinement was impeded by the disorder within the crystal caused by these solvent molecules. These molecules were not in fixed positions within the unit cell, and large regions not occupied by **1** were evident. The structural picture shows that two *C*-shaped isomers of **1** are held together in a dimeric form by eight NH-O hydrogen bonds ranging in length from 2.80 to 2.95 Å. There were no solvent molecules observed within the dimer's cavity, despite the apparently available space.

Other species were detected in the ^{1}H NMR of the crude reaction mixture obtained from the durene coupling step. It seems likely that the undesired *S*-isomer was formed during the reaction and was eliminated during the extractive purification.

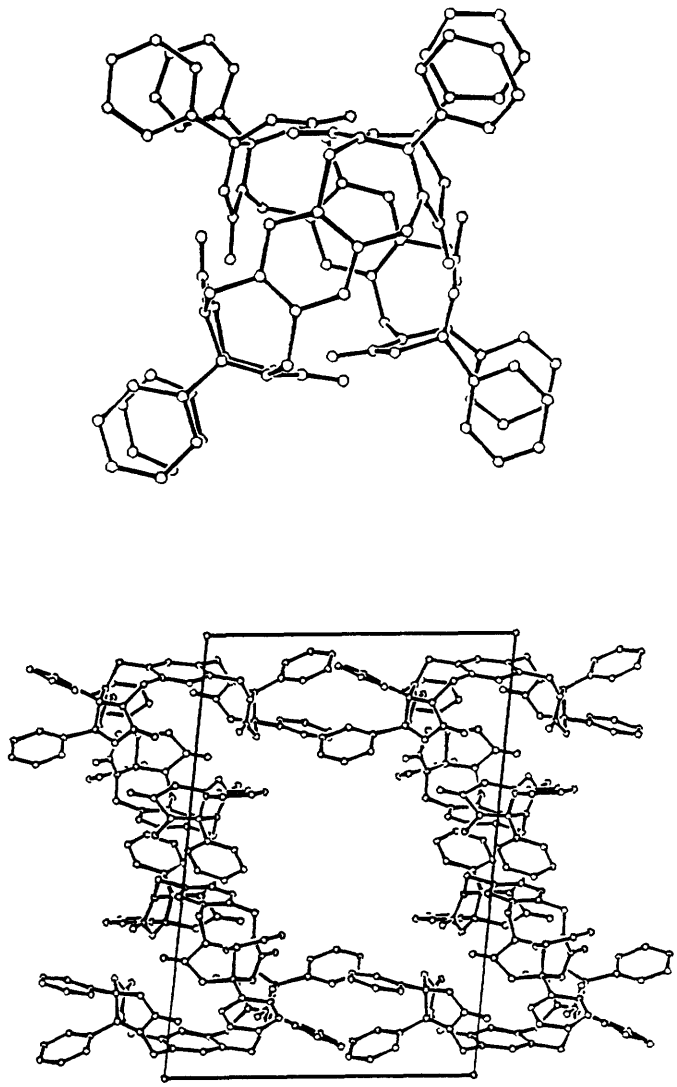

Figure 3. *X-ray crystal structure of **1**, showing a dimeric morphology. There are large gaps present in the unit cell (occupied by disordered solvent molecules).*

4.4 Structural Properties

Molecule **1** exhibits three additional torsional conformations. Each is created by inverting the two seven-membered ring systems generated by the fusion of the glycoluril to the benzene spacer. They can be assigned as *anti-anti* (**A**), *anti-syn* (**B**) and *syn-syn* (**C**), with regards to the orientation of the aromatic groups.

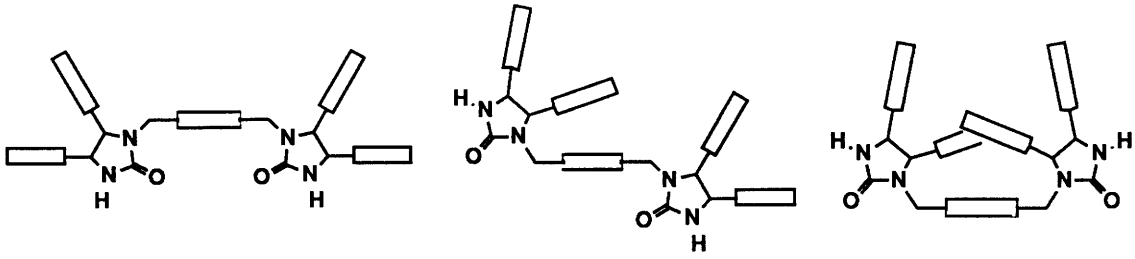

A B C

These assignments were initially described for similar glycoluril systems. Nolte and coworkers reported that in the solid state, only the *anti-anti* conformer is detected.[17,23-25] In solution, only one conformation exists, as visualized by the presence of only one pair of benzylic resonances in the ^{1}H NMR spectrum at temperatures from -95 to 150°C. This observation suggests that either one conformer predominates, or all three are rapidly interconverting. The ^{1}H NMR spectrum of an *anti-anti* locked macrocyclic system[17,18] was seen to be identical to that of the non-cyclized species, providing strong evidence that this is the major conformer in solution. One explanation for this dominance is that the *anti-anti* conformer increases the solvent accessible surfaces.

The *syn-syn* conformer can be eliminated due to the unfavourable overlap of the phenyl groups. Molecular modeling estimated a ±1-3 kcal/mole difference in energy between the *anti-anti* and *anti-syn* conformers, depending on the force field employed.[26] An energy barrier of ~4 kcal/mole for the interconversion between the possible torsionally unique species was estimated by restricting a series of ring torsional angles and minimizing under these restraints (Figure 4). This value was not large enough to confine the the molecule to one conformation, and an average of the conformations was expected on the NMR time-scale. The possible explanation of maximizing solvent accessible surfaces prompted the prediction that the *anti-anti* conformer will be favoured in solution. However, these arguments are not applicable because only the *anti-anti* conformer has the possibility to dimerize. As expected, only one species was observed in the ^{1}H NMR spectrum at 500 MHz due to this aggregation tendency.

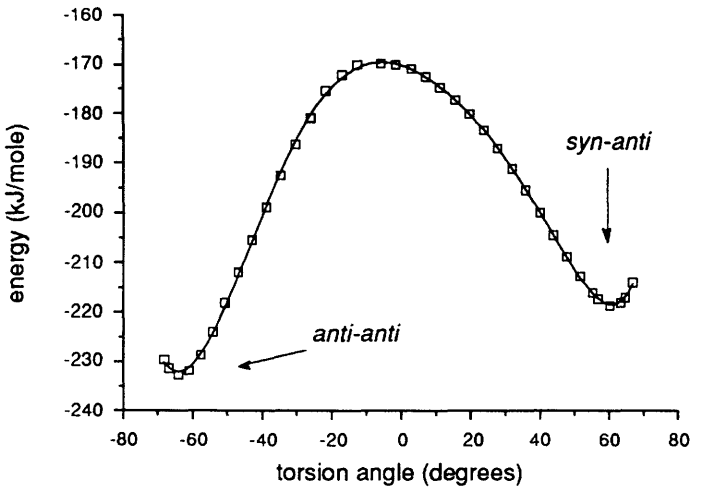

Figure 4. *Estimated energy barrier for seven-membered ring "flip". The force field employed was AMBER* with GB/SA chloroform solvation. Energies are in kJ/mole as read directly from the modeling simulations. A conversion factor of 4.184 was used to convert kJ to kcal.*

The dimerization of **1** was demonstrated by the following studies: 1) An average molecular weight of 1500-2000, corresponding to the dimer was calculated by vapour pressure osmometry.[11] 2) Electron impact (EI) and fast atom bombardment (FAB) mass spectrometry gave a peak at 1429 mass units (calulated for the dimer: 1429.6 amu).[11] 3) The ^{1}H NMR in chloroform-*d* revealed a downfield signal for the amide protons corresponding to a hydrogen bonded structure. This signal appeared at 9.28 ppm, as compared to 5.45 ppm for the "half"-tennis ball **3**, which cannot hydrogen bond as strongly. It is interesting to note that the resonances for the amides in DMSO-d_6, which destroys all intermolecular hydrogen bonds by strongly solvating all donors, appeared at 8.22 ppm (the amide resonances for the "half"-species appears at 8.14 ppm in this solvent).

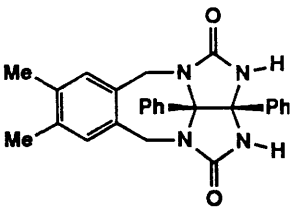

3

4.5 Encapsulation

The dimer of **1** exhibits a well-defined roughly spherical cavity with a volume of ~55 Å^3, as defined by molecular modeling. This value was estimated by measuring the corresponding van der Waal's diameters of the cavity. The diameters were calculated by subtracting the van der Waal's "half-thickness" of the aromatic surfaces (1.77 Å) from the values (atom center to center) obtained directly from the modeling. The cavity appears suitable for encapsulating small molecules of complementary size and shape. In solvents which compete weakly for hydrogen bonds, such as chloroform, there are two forms of the dimer observed in the ^{1}H NMR spectrum at 500 MHz. One form is assumed "empty", although the presence of dissolved gases cannot be excluded. The other form is most likely occupied by solvent. The exchange between these two forms on the NMR time scale was slow as evidenced by separate signals for the amide protons and the benzylic protons. As the temperature was lowered, the amount of the occupied form increased at the expense of the "empty" one, as visualized in the ^{1}H NMR spectrum of the benzyl region (Figure 5).

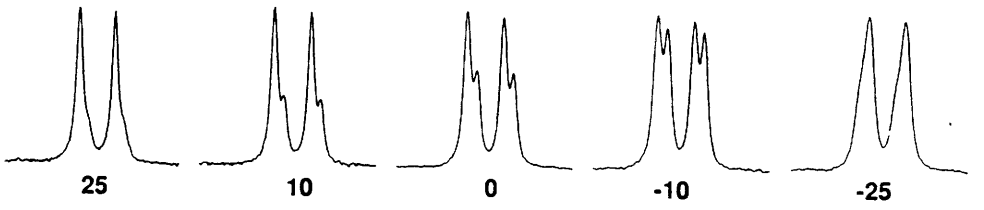

Figure 5. *Low temperature ^{1}H NMR at 500 MHz of one benzylic resonance of* **1** *in chloroform-d showing the appearance of a new solvent-occupied species (on the right).*

The inner dimensions of the cavity were probed by adding a series of small guest molecules to chloroform-*d* solutions of **1**. For example, the addition of trace amounts of methylene chloride to a $CDCl_3$ solution of the dimer at -10°C indicated the presence of a third species (Figure 6). In addition to the pair of signals assigned as "empty" and $CDCl_3$-occupied, a third doublet appeared, which was enhanced by further addition of CH_2Cl_2. These new signals correspond to those observed when the ^1H NMR of the dimer was analyzed using methylene chloride-d_2 (CD_2Cl_2) as solvent. There was also no change in the NMR spectrum when the CD_2Cl_2 solution was cooled. This observation implies that the dimer in CD_2Cl_2 was always occupied by the solvent, owing to the smaller size of CD_2Cl_2 as compared to $CDCl_3$.

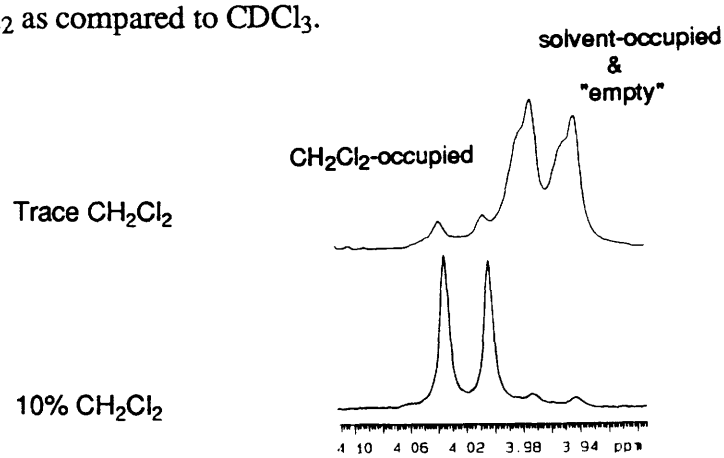

Figure 6. *^1H NMR at 500 MHz at -10°C of one benzyl resonance of **1** in chloroform-d with added CH_2Cl_2. A third species (CH_2Cl_2-occupied) appeared.*

In certain favourable cases, the slow-exchange on the NMR time scale allowed the direct visualization of signals for both solvated and encapsulated guests. Examples include methane, ethane, and ethylene. As previously seen, new signals for the amide and benzylic protons for the inclusion complex were observed. Sample NMR spectra are shown in figure 7, highlighting the signals for the encapsulated guests. The corresponding chemical shift differences between free and complexed guests were 1.13, 1.27 and 1.38 ppm for methane, ethane and ethylene respectively. The shielding effect of the aromatic rings that

make up the cavity walls resulted, in all cases, in an upfield shift of the guests' proton resonances.

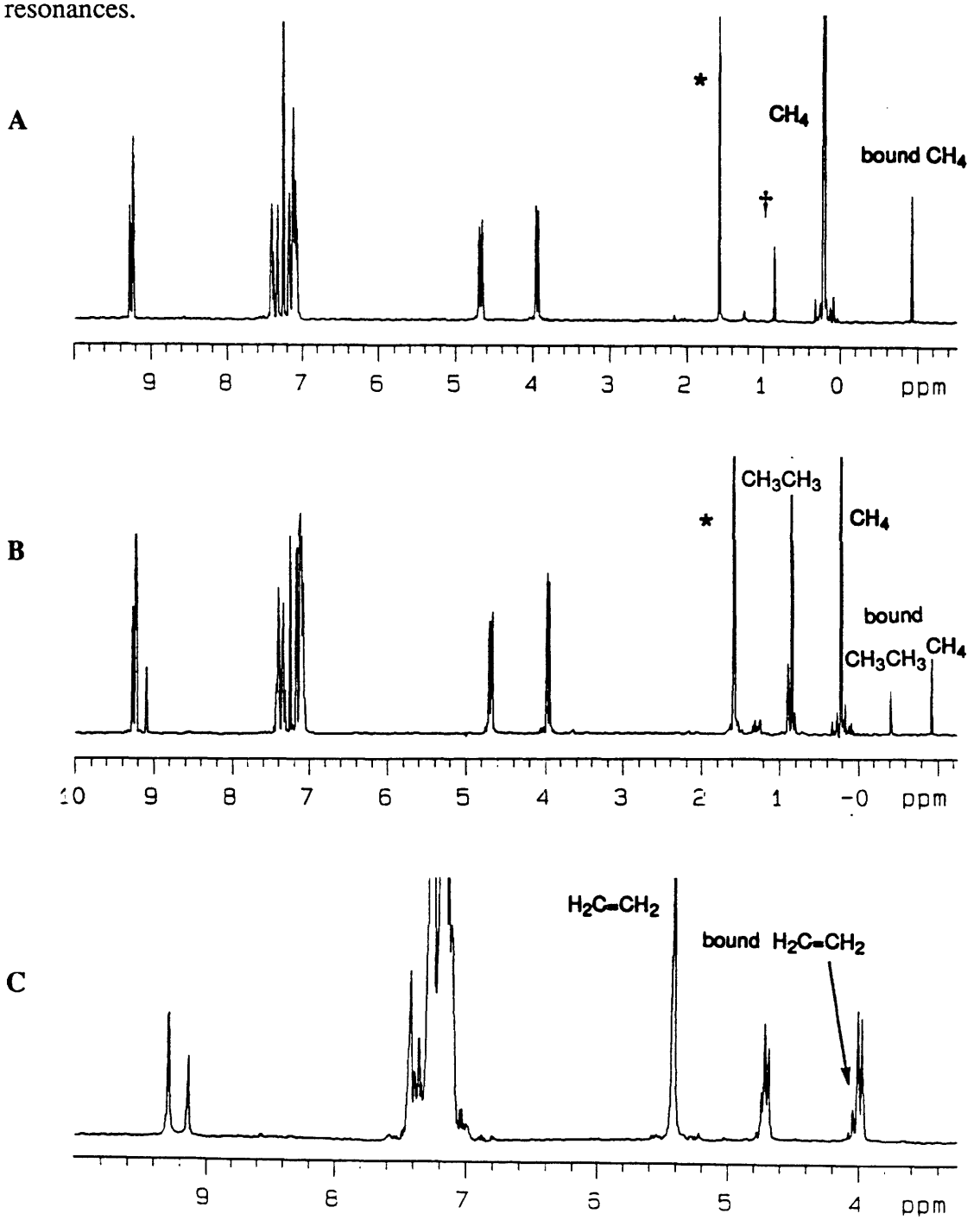

Figure 7. *Sample ^1H NMR spectra at 500 MHz of* ***1*** *in chloroform-d.* ***A****: in the presence of methane (CH_4),* ***B****: natural gas (CH_4 and CH_3CH_3), and* ***C****: ethylene ($H_2C{=}CH_2$). Free and encapsulated guests peaks are highlighted along with residual water *. The † symbol in spectrum* ***A*** *signifies residual ethane (a 7-11% contaminant in commercial grade methane).*

The inclusion constants (K_{inc}) for guests were calculated by integrating either the benzylic or the amide resonances of dimeric **1** in the ^1H NMR spectrum in $CDCl_3$. The ratio of the "empty" and variously occupied assemblies as a function of temperature (Arrhenius-type plot, Figure 8) allowed for the assessment of thermodynamic parameters. The results are listed in table 1.

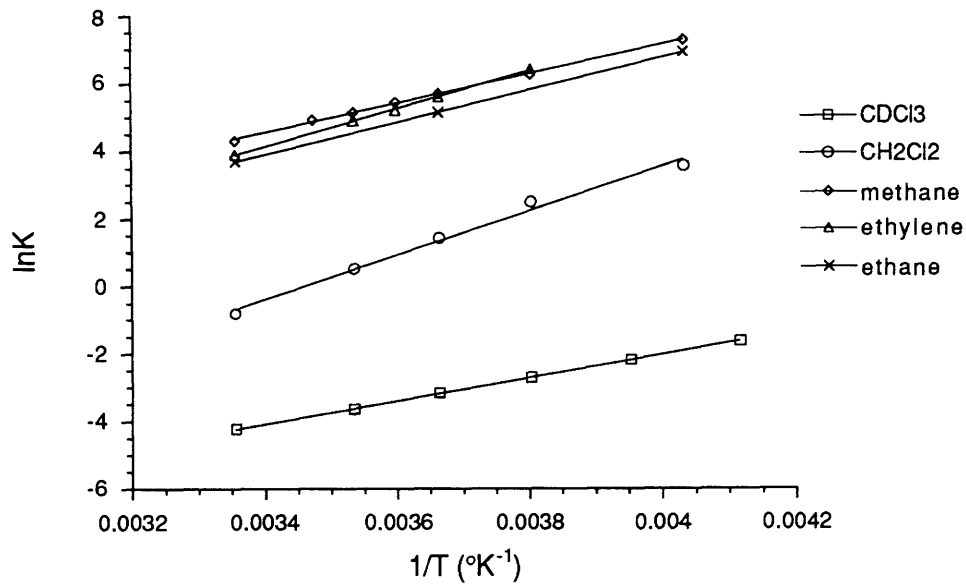

Figure 8. *Low temperature ^1H NMR studies of **1** in chloroform-d in the presence of small organic molecules.*

Table 1. Inclusion of guests in the cavity of dimeric **1**. All NMR spectra were run at 500 MHz in chloroform-*d* as solvent. Guest volumes were calculated using the protocol of Bondi.[27]

Guest	Guest volume (Å^3)	K_{inc} (M^{-1}) at 289°C	ΔH (kcal/mol)	ΔS (entropy unit)
$CHCl_3$	72	0.015	-6.8	-31.0
CH_2Cl_2	58	0.45	-14.7	-50.8
CH_3CH_3	45	41.2	-9.5	-24.2
$H_2C{=}CH_2$	40	50.7	-11.1	-29.6
CH_4	28	75.3	-8.6	-20.1

The following trends from these investigations can be described: 1) The inclusion of all guests involves a large entropic cost. Restricting the guests' translational freedom to that defined by the tennis ball's interior is compensated by enthalpic factors. The favourable enthalpy is due most likely to van der Waal's contacts with the interior lining of the cavity. 2) The exchange of all the guests in and out of the cavity is slow on the NMR time scale. Stochastic dynamics simulations[28] imply that the hydrogen bonds on one side of the tennis ball must be broken in order to facilitate entrance and exit of guest species. It can be assumed that this *clam-shell* opening is the rate limiting step involved in the decomplexation and is responsible for the slow exchange. 3) The correlations between guest volumes and the inclusion constant (K_{inc}) indicate that the internal volume enscribed by the dimer is, in fact, close to that predicted by modeling (~55 Å^3). It appears that approximately 50% of the cavity volume is unoccupied in the most stable inclusion complex (**1**-methane). However, the results correlate well with the suggestion that the van der Waal's radius of the ideal guest must be ~20% smaller than that expected to be optimum (the maximum radius of the cavity) as previously attested.[10]

The ^{1}H NMR investigations provided insight into some of the properties of the guest bound within the dimer's cavity. The integration of the signals for encapsulated guest resonances corresponds to a well-defined 1:1 complex. The relaxation times for these included guests were significantly shorter than those for the solvated molecules. For example, the T_1 value for the encapsulated methane (T_1 = 5.8 seconds) was measured to be more than double the value corresponding to the free species (T_1 = 14.2 seconds). This undeniably shows that the translational freedom of the methane molecule is indeed substantially reduced when trapped within the dimer, resulting in greater relaxation of the gaseous guest molecules by their impacting against the cavity walls.

Neutral organic guests which did not form inclusion complexes include propane and *iso*-butylene, presumably owing to their large van der Waal's volumes (62 and 74 Å^3

respectively). In the case of allene (51 $Å^3$ van der Waal's volume), encapsulation was observed when a large excess of allene was introduced at low temperatures. The high impurity content of commercial grade allene prevented the measurement of accurate binding parameters by masking relevant signals in the spectrum.

There were also some inexplicable behaviours of the dimer. For example, there was no evidence of trapped fluorocarbon guests. CH_3F, CF_4 and tetrabutylammonium tetrafluoroborate ($Bu_4N^+BF_4^-$) do not form inclusion complexes as evidenced by both proton and fluorine NMR, despite the expected good fit. This may be attributed to the much admired properties of Teflon, where it is anticipated that fluorine provide less van der Waals "stickiness" as compared to hydrogen. It was unexpected that the simple change from methane to monofluoromethane results in the complete lack of encapsulation.

Unexpectedly, the highly organic soluble tetrabutylammonium borohydride ($Bu_4N^+BH_4^-$) destroyed the dimer. Also, ammonium salts such as dimethylammonium and methylammonium 4-*tert*-butylbenzoate similarly showed no evidence of encapsulation.

In a recent study of the encapsulation of methane and other small one-carbon containing species, Collet used the principle of occupancy factor (ρ) as a macroscopic description of the state of the enclosed guests.[10] The occupancy factor (the ratio of guest to host volumes) is a crystallographic description used to relate the macroscopic states of matter. The trapping of methane by the tennis ball ($\rho \geq 0.5$) results in the description of methane as a supercritical fluid, while ethane ($\rho \geq 0.8$) and ethylene ($\rho \geq 0.7$) translate into densly packed crystals. The ρ values for encapsulated chloroform and methylene chloride are greater than 1, leading to the conclusion that the use of these descriptions for flexible cavities is not completely valid.

Stochastic dynamic simulations show that the encapsulation of large guests is accompanied by the lengthening and weakening of hydrogen bonds of the dimer, with an ultimate increase in cavity volume (Figure 9). Assemblies formed through weak

interactions will share this common feature of adjustable size and shape, making the use of the above descriptions unreliable.

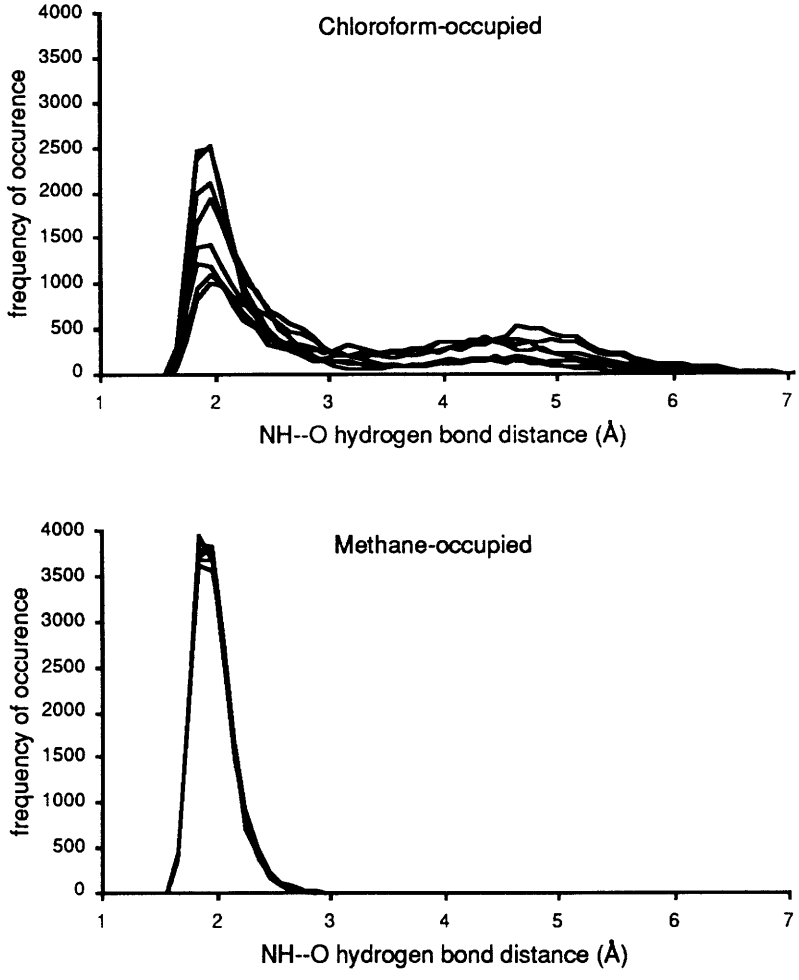

Figure 9. *Stochastic dynamic simulations for the $CHCl_3$- and CH_4-inclusion complexes of the dimer of* ***1****. The population of species possessing ideal hydrogen bond lengths (~2 Å) decreases when the dimer is occupied by chloroform as compared to methane.*

As expected, average NH-O intermolecular hydrogen bond distances of the dimer of **1** (measured directly from the stochastic dynamics simulation) were proportional to the van der Waal's volume of the guest encapsulated during the modeling (Figure 10). An inversly proportional trend was observed for these volumes and the association constants (K_{inc}).

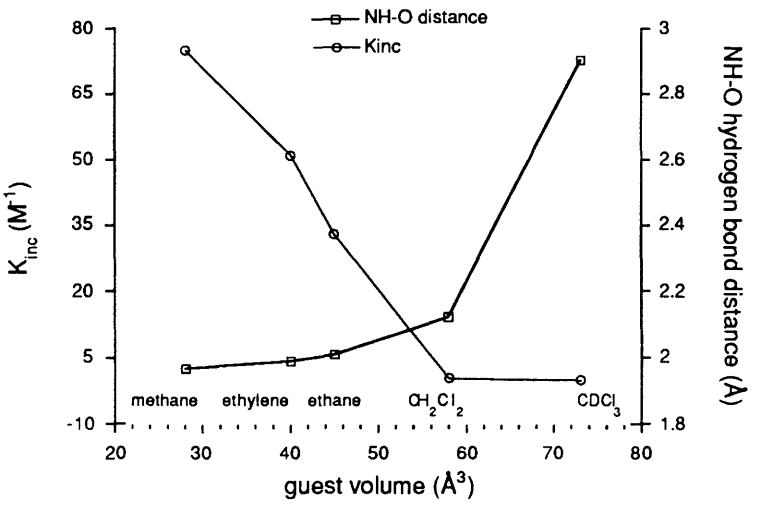

Figure 10. *Plots of guest volume as a function of K_{inc} and hydrogen bond length. Values of K_{inc} were calculated from the low temperature ^1H NMR studies. Values of NH-O length were estimated from stochastic dynamic simulations.*

The use of occupancy factor as a macroscopic descriptor requires more accurate measurements of cavity volumes. In the case of dimeric **1**, the dimensions of the cavity, after minimizing the inclusion complexes and removing the guest, must be used for the calculations instead of the minimized "empty" structure. The dimensions are directly dependent on the size and shape of the guest. The extreme cases are, on one hand, a sphere (CH_4, for example) and, on the other, an elongated ovoid ($H_2C{=}C{=}CH_2$). For example, the dimensions of the cavity when encapsulating methane are 5.2 Å and 4.9 Å for aromatic-aromatic distances and carbonyl-carbonyl distances respectively, resulting in a volume of ~65 Å^3. In contrast, when allene is encapsulated, the weakening and lengthening of the hydrogen bonds results in an elongation of the cavity, as shown by the increase of the aromatic-aromatic distance (5.4 Å). The flexibility provided by the seven-membered ring compensates for this elongation by compressing the width of the cavity (the carbonyl-carbonyl distance decreases to 4.7 Å). The balance of these two structural changes results in a similar overall volume as that for the smaller but more spherical guests.

These variable dimensions result in the flexible accomodation character of the tennis ball and compromise the use of occupancy factor as an appropriate descriptor.

The flexible cryptophane and carcerand encapsulators previously introduced are similarly prone to this problem. Rotation of the polar caps results in a great enhancement of the cavity size, so values of ρ must be evaluated with caution.

The calculation of more accurate cavity volumes is not a trivial task, and there are numerous computational strategies available to estimate these values. Unfortunately, none of the methods are completely universal. One of the most versatile methods calculates volume by measuring the solvent accessible surfaces exhibited by the cavity. A spherical probe of appropriate size (most commonly a water molecule of ~1.4 Å radius) is "rolled" around the interior of the cavity. In this way, the solvent accessible surfaces are measured, and the internal cavity volumes are calculated.

The technique fails when the probe encounters holes in the surface through which it can escape. To compensate for this, one program[29] adds a "fattening" factor (a constant value of the van der Waal's radii) to each atom, effectively shrinking the size of the cavity as well as the holes. This "fattening" is repeated until the probe no longer escapes the cavity. In this way, inner-vaginations (**A**) are converted to well-defined cavities (**C**). This method has found use primarily in the estimation of large inner-vaginations within protein structures, where a probe of radius 1.4 Å is adequate.

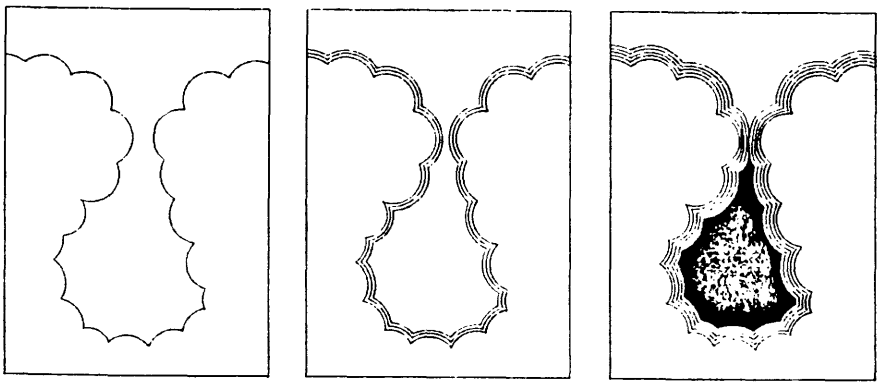

A **B** **C**

When the ratio of holes to surface becomes too great, the cavity must be "fattened" up to such an extent that the inner dimensions have limited meaning. The cavity defined by dimeric **1** is one of these cases. The values for the inner dimensions of the inclusion complexes were estimated using the VOIDOO program (Figure 11).[29]

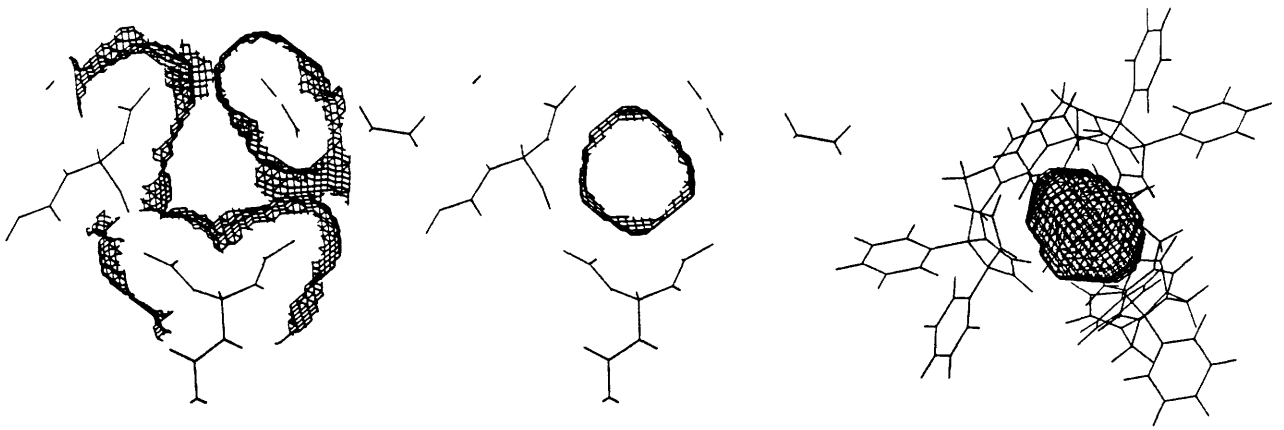

A **B** **C**

Figure 11. *The cavity of the dimer of **1** as mapped out by the VOIDOO Program. A "fattening" factor was added until the channels to the cavity were sealed (**A**). From the resulting solvent accessible surfaces the volume of the cavity was estimated (**B**). Plot **C** shows the complete cavity map.*

The volume of the cavity enscribed by the dimer **1** was measured after minimization of inclusion complexes and removal of the guests.[30] The results are: "empty", 40.3±1.6 Å; CH_4, 40.1±1.5 Å; $H_2C{=}CH_2$, 41.4±1.2 Å; CH_2Cl_2, 43.7±1.4 Å; $CHCl_3$, 51.0±1.1 Å; $H_2C{=}C{=}CH_2$, 36.5±1.6 Å. This results in the trend:

$$CHCl_3 > CH_2Cl_2 > H_2C{=}CH_2 \geq \text{"empty"} \sim CH_4 > H_2C{=}C{=}CH_2$$

which correlates well with the trend for guest volume (with the exception of allene):

$$CHCl_3 > CH_2Cl_2 > H_2C{=}C{=}CH_2 > H_2C{=}CH_2 > CH_4.$$

Smaller guest molecules such as molecular hydrogen (H_2) were also bound. Unlike the larger guests, there was no observation of multiple species present in the ^1H NMR. Instead, a temperature-dependent average signal was seen for the hydrogen resonance. As the temperature was lowered, the hydrogen signal shifted upfield to a lower ppm (Figure 12). To our knowledge, this is the first known example of reversible binding of molecular hydrogen by a synthetic encapsulating system.

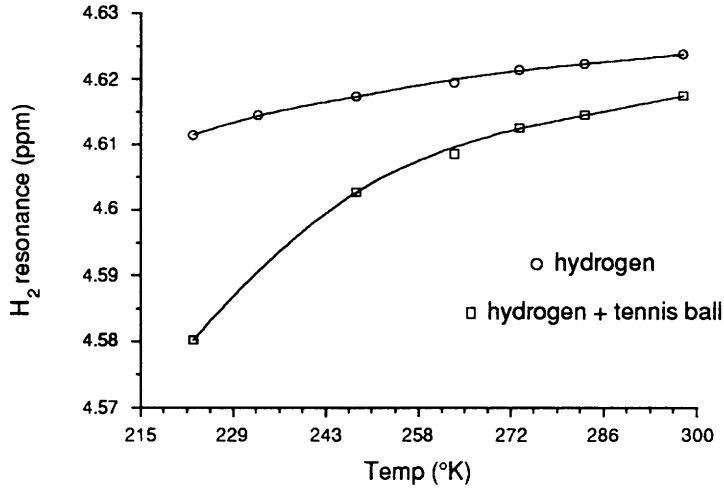

Figure 12. *Low temperature ^1H NMR plot of the shift of the H_2 resonance with and without added **1**.*

The presence of an average H_2 proton signal (rapid exchange) can be rationalized by considering two situations: 1) The holes exhibited by the dimer are roughly pentagonal in shape (Figure 13). A circle with a cross section area of 3.65 $Å^2$ is mapped out by these pentagons allowing for the passage of any guest having a radius of approximately 1-1.5 Å. This compares well with the H_2 van der Waal's radius of 1.20 Å. 2) The small volume of the hydrogen molecule permits a rapid tumbling motion when trapped within the

encapsulator. This tumbling would result in an averaging of ^1H NMR resonance signals as the protons pass through alternating shielding and deshielding regions of the aromatic cavity walls.

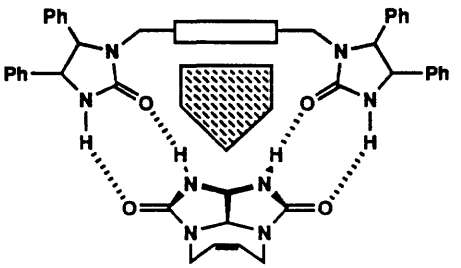

Figure 13. *The holes in the cavity enscribed by dimeric **1**.*

Bubbling hydrogen gas through a solution of tennis ball in $CDCl_3$ at -10 °C resulted in the full displacement of chloroform bound species as well as the species assumed "empty". A new benzylic doublet for H_2-bound **1** appeared at the expense of both doublets. This displacement method allows for the readily accessible determination of whether a guest is bound or not, although it provides limited evaluation of the strength of encapsulation (other than the K_{inc} is greater than that for chloroform, 0.015 M^{-1} at 298 °K). Other guests that were evaluated by this technique were helium, neon, argon and xenon. In all cases, a similar displacement as described above was observed (Figure 14).

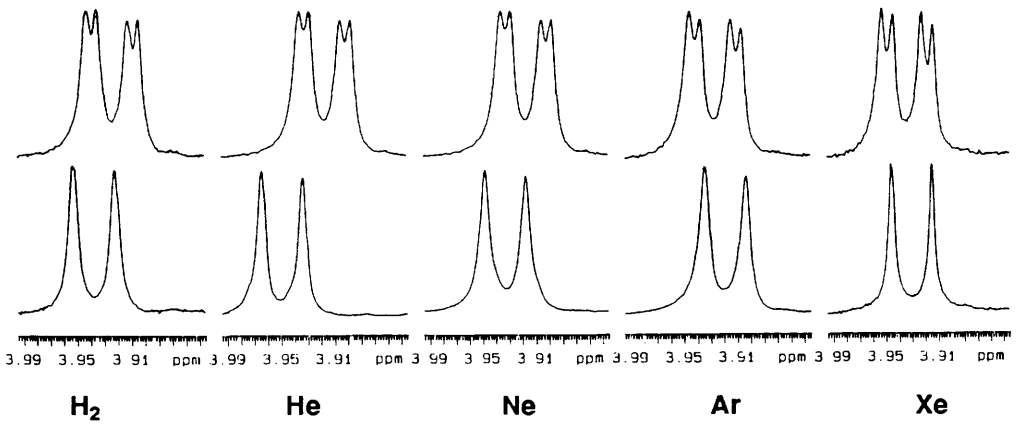

Figure 14. *^1H NMR at 500 MHz in chloroform-d of one of the benzylic resonances of **1** showing full displacement of included $CDCl_3$ by H_2, helium, neon, argon and xenon.*

Water Soluble Encapsulators

In an effort to obtain water-soluble derivatives of **1**, molecule **4** was prepared in an analogous fashion from the known bis(4-dimethylanilino)glycoluril.[31] This species behaved in an identical manner to the original derivative **1**. A solvent-occupied species was evident from low temperature NMR studies in $CDCl_3$. Also, methane and ethane-occupied complexes were formed when chloroform solutions were treated with natural gas.

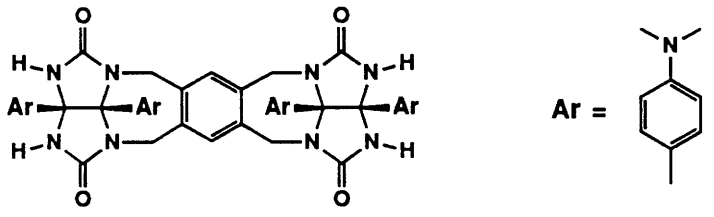

4

Compound **4** showed good solublility in more polar solvents. The ^1H NMR spectrum of this species in dimethylformamide-d_7 (DMF-d_7) revealed a fast dynamic exchange between monomer and dimer as evidenced by the characteristic broadened signal for the amide resonances (7.78 ppm) as well as for the resonances for half of the anilino aromatic and benzylic protons (Figure 15). The dynamics of this system can be assumed to be due to the rapid rate of decomplexation and complexation resulting from the effective weakening of the hydrogen bonds by the more competitive solvent.

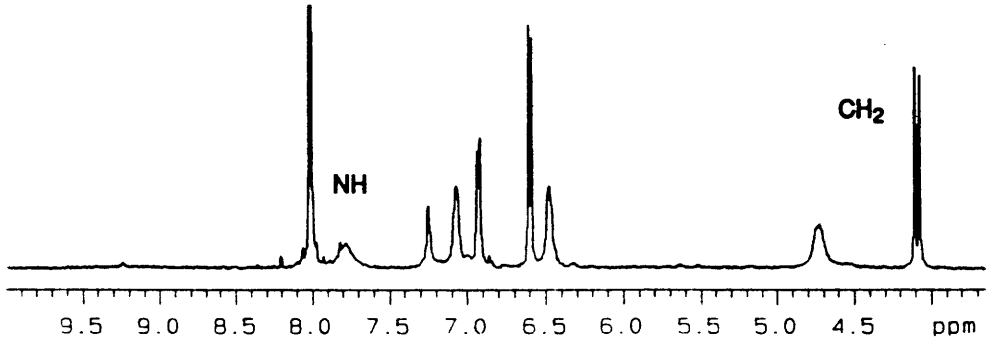

Figure 15. *^1H NMR spectrum of **4** in DMF-d_7. The broadened amide signal (NH) is highlighted, along with one of the benzyl resonances (CH_2).*

Modeling indicated that DMF cannot fit within the capsule and, once again, the dimer cannot be assumed to be "empty" (the occupation by dissolved gases cannot be ruled out). The dynamic exchange process can be perturbed, and the dimerization can be induced by the addition of small molecules or even atoms. For example, when DMF solutions of **4** are saturated with methane or ethylene, the appearance of the new dimer was monitored (Figure 16). The signals for the N-H amide (9.2 ppm) and one of the benzyl resonances (4.55 ppm) of the assembled capsid emerged. The signal for encapsulated methane was also observed at -0.92 ppm. The amount of tennis ball in the form of inclusion complexes is ~22% for methane and ~44% for ethylene.

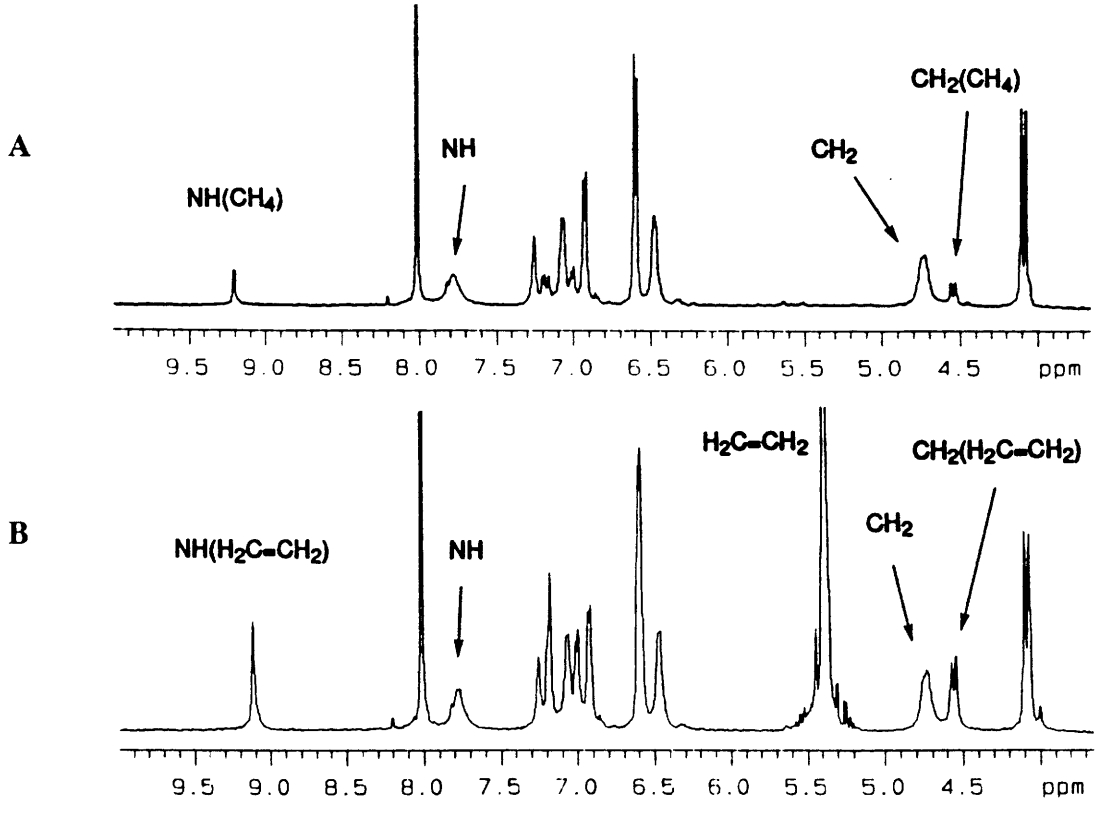

Figure 16. *^{1}H NMR spectra for dimer of **4** in DMF-d_7. **A**: treated with methane (CH_4) and **B**: ethylene ($H_2C=CH_2$). Signals for dynamic amides (NH) and one of the benzyl resonances (CH_2) of the inclusion complexes are highlighted.*

The observation of the characteristic ^{1}H NMR signals for the inclusion complexes permits the binding of other guests to be screened indirectly. For example, molecular

hydrogen, helium and neon failed to alter the ^{1}H NMR spectrum in DMF-d_7. However, xenon and argon induced the formation of the capsid (Figure 17). The experiments reveal a delicate balance between entropic cost of a termolecular complex and the enthalpic gains provided by the weak intermolecular forces in the assembly process. Even relatively competitive solvents for hydrogen bonds such as DMF are displaced by the satisfaction of the complementarity of size, shape and chemical linings.

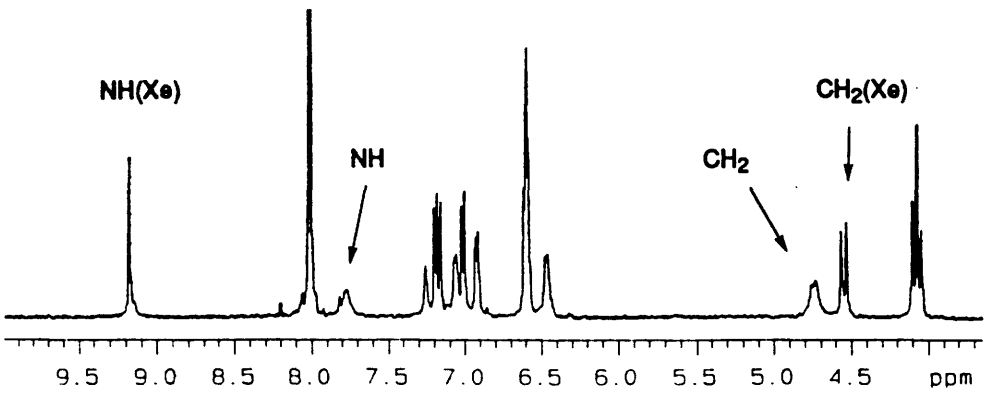

Figure 17. *^{1}H NMR spectra for dimer of **4** in DMF-d_7 treated with xenon. Signals for dynamic amides (NH) and one of the benzyl resonances (CH_2) are highlighted. Approximately 55% of the dimer is in the form of the inclusion complex.*

The presence of the basic dimethylamino groups on the periphery of **4** allow for regulation of the encapsulation phenomenon by changes in the acidity of the medium. As acid (*p*-toluenesulfonic acid) was added to DMF-d_7 solutions of **4**, the protonated monomer appeared (Figure 18). A large exces of acid (~80 equivalents) drove the equilibrium to the monomer. This dissociation can be attributed to the buildup of positive charge at the amino groups which forces apart the two subunits due to the sufficient buildup of electrostatic repulsions. When the medium is neutralized (with Na_2CO_3, for example) the neutral dimer containing xenon was regenerated. This type of reversibility as a function of the acidity of the medium is a phenomenon that has recently been reported for transferrin iron release.[32]

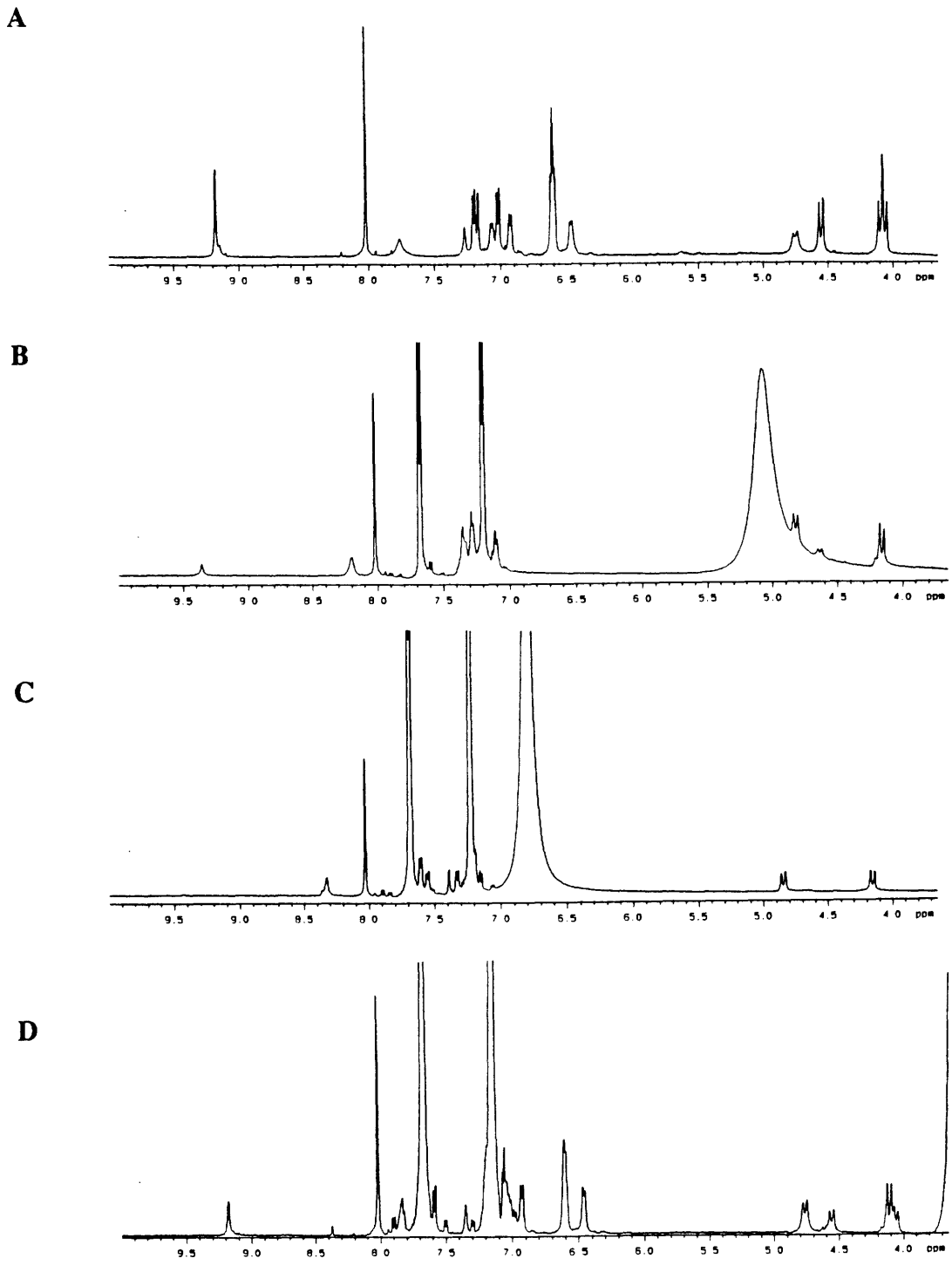

Figure 18. *Acidity regulated encapsulation of xenon by the dimer of* ***4****.* ***A****: the* ^1H *NMR in DMF-*d_7 *of the xenon-occupied capsule (~50% occupied).* ***B****: with addition of p-toluenesulfonic acid (~30 equivalents, ~25-30% Xe-occupied). Full dissociation results from an excess of acid (****C****, ~80 equivalents). Neutralization with* Na_2CO_3 *(****D****) affords the inclusion complex as apparent by the appearance of the amide NH resonance of the complex (~9.2 ppm).*

4.6 Conclusions and Outlook

The tennis ball has the advantage over already existing encapsulators in that it is held together by hydrogen bonds along its seam. This assembling through weak intermolecular forces allows for the reversible binding of guests. Decomplexation occurs rapidly, and in all cases the guests are released back into the solvent body. Other examples of encapsulation of organic guest molecules involve carcerand or cryptophane systems which irreversibly capture small molecules. In most cases, elevated temperatures are required to release the guests. The control of encapsulation by the tennis ball molecules described in this chapter comes from a delicate balance of the acidity of the medium and the formation of inclusion complexes is governed by a pH "switch".

Encapsulation of biologically interesting species will allow for transport across lipid membranes. Nitric oxide (NO), for example, has attracted attention because of its ability to pass freely through membranes to permeate the organism. This can be explained by the gaseous nature and small size of the NO molecule. The trapping of NO by the tennis ball described may allow for specific membrane transport. The size and shape of NO are appealing, making it a potential candidate for encapsulation within the tennis ball's cavity.

Expanding the size of the central aromatic spacer will result in the formation of encapsulators with larger cavity volumes. This increase in size will allow for the capture and transport of larger biologically relevant species (antibiotics such as penicillin, or antivirals such as AZT).

The assembly can also be envisioned as a reaction chamber. The probability of two reactive species encountering each other is greater when captured within the tennis ball than in bulk solution. Cycloaddition reactions are one example of possible reaction types.

4.7 Experimental

For a general description of apparatus, materials and methods, see chapter 2.

Stochastic Dynamics Simulations

Stochastic dynamics simulations[33] were run in the MacroModel version of the AMBER[34] force field at 300 K with GB/SA chloroform solvation,[35] extended nonbonded distance cutoffs and constrained bond lengths (SHAKE). After a 15-ps induction period, structures were sampled every 1.5-fs using the minimized conformation of the structure as the starting point. In general, each run was over a 240-ps time period.

X-ray Crystallography of Compound 1.

Crystal data: $C_{84}H_{68}N_{16}O_8$ (dimer), formula weight 1429.57, colourless triclinic hexagonal plate crystals, space group P1, a = 15.3211, b = 15.6086, c = 24.6124 Å, α = 80.698, β = 79.454, γ = 70.663 degrees, V = 5428 Å^3, Z = 2, T = ambient.

The crystals were unstable at room temperature when exposed to the atmosphere due to loss of chloroform solvent. The crystals were sealed in a capillary with mother liquor. Data were collected at ambient temperatures in the θ-2θ scan mode. Of the 8638 unique reflections were measured (I $>$ 2σ $>$ (I)) and used in the subsequent structure analysis. Data were corrected for Lorentz and polarization effects and for secondary extinction but not for decay and absorption. The structure was solved by modified versions of SHELX86 (Sheldrick) direct methods and refined with full-matrix least-squares methods. H on N were not located and were not included in the structure factor calculations. The final R factors were 20.8% and Rw = 22.5%. For atom coordinates, see Appendix 4.

Inclusion Constants (K_{inc})

The inclusion constants (K_{inc}) for guests were calculated by integrating either the benzylic or the amide resonances of dimeric **1** in the ^{1}H NMR spectrum in $CDCl_3$. The calculations relied on the assumption that the equilibria involved did not effect each other, that is, the

binding properties of the tennis ball with chloroform had no effect on the strength of binding to the other molecules. The binding constants for the equilibrium equations:

$$\mathbf{1} + CDCl_3 \overset{K_{CDCl_3}}{\rightleftharpoons} \mathbf{1}\cdot CDCl_3$$

$$\mathbf{1} + guest \overset{K_{guest}}{\rightleftharpoons} \mathbf{1}\cdot guest$$

can be expressed as:

$$K_{CDCl_3} = \frac{[\mathbf{1}\cdot CDCl_3]}{[\mathbf{1}][CDCl_3]} \quad \text{and} \quad K_{guest} = \frac{[\mathbf{1}\cdot guest]}{[\mathbf{1}][guest]}$$

The ratio of signals from the low temperature study is expressed in terms of the known value for the encapsulation of chloroform as:

$$\text{ratio of signals} = R = \frac{[\mathbf{1}\cdot guest]}{[\mathbf{1}] + [\mathbf{1}\cdot CDCl_3]}$$

$$= \frac{[\mathbf{1}\cdot guest]}{[\mathbf{1}] + K_{CDCl_3}[\mathbf{1}][CDCl_3]}$$

$$= \frac{[\mathbf{1}\cdot guest]}{[\mathbf{1}]} \frac{1}{(1 + K_{CDCl_3}[CDCl_3])}$$

$$= \frac{K_{guest}[guest]}{1 + K_{CDCl_3}[CDCl_3]}$$

Therefore the association constant for each guest can be calculated from the equation:

$$K_{guest} = \frac{R\,(1 + K_{CHCl_3}[CDCl_3])}{[guest]}$$

Natural gas (containing both ethane and methane) was used as the source of ethane. In this instance, both the binding equilibria of chloroform-*d* as well as methane must be considered in order to obtain accurate values for ethane K_{inc} and was calculated from the equation:

$$K_{ethane} = \frac{R\,(1 + K_{CDCl_3}[CDCl_3] + K_{methane}[methane])}{[ethane]}$$

where:

$$\text{ratio of signals} = R = \frac{[\mathbf{1}\cdot\text{ethane}]}{[\mathbf{1}] + [\mathbf{1}\cdot CDCl_3] + [\mathbf{1}\cdot\text{methane}][\text{methane}]}$$

References and Notes

(1) Dietrich, B.; Lehn, J.; Sauvage, J. *Tetrahedron Lett.* **1969**, 2885-2888.

(2) Lehn, J.-M. *Angew. Chem. Int. Ed. Engl.* **1988**, *27*, 89-112.

(3) Canceill, J.; Cesario, M.; Collet, A.; Guilhem, J.; Pascard, C. *J. Chem. Soc., Chem. Commun.* **1985**, 361-363.

(4) Collet, A. *Tetrahedron* **1987**, *43*, 5725-5759.

(5) Moran, J. R.; Karbach, S.; Cram, D. J. *J. Am. Chem. Soc.* **1982**, *104*, 5826-5828.

(6) Cram, D. J.; Stewart, K. D.; Goldberg, I.; Trueblood, K. N. *J. Am. Chem. Soc.* **1985**, *107*, 2574-2575.

(7) Cram, D. J.; Jaeger, R.; Deshayes, K. *J. Am. Chem. Soc.* **1993**, *115*, 10111-10116.

(8) Cram, D. J.; Tanner, M. E.; Keipert, S. J.; Knobler, C. B. *J. Am. Chem. Soc.* **1991**, *113*, 8909-8916.

(9) Canceill, J.; Lacombe, L.; Collet, A. *J. Am. Chem. Soc.* **1986**, *108*, 4230-4232.

(10) Garel, L.; Dutasta, J.; Collet, A. *Angew. Chem. Int. Ed. Engl.* **1993**, *32*, 1169-1171.

(11) Wyler, R.; de Mendoza, J.; Rebek, J., Jr. *Angew. Chem. Int. Ed. Engl.* **1993**, *32*, 1699-1701.

(12) Coolen, H. K. A. C.; van Leeuwen, P. W. N. M.; Nolte, R. J. M. *Angew. Chem. Int. Ed. Engl.* **1992**, *31*, 905-907.

(13) Niele, F. G. M.; Nolte, R. J. M. *J. Am. Chem. Soc.* **1988**, *110*, 172-177.

(14) Sijbesma, R. P.; Nolte, R. J. M. *J. Am. Chem. Soc.* **1991**, *113*, 6695-6696.

(15) Sijbesma, R. P.; Bosman, W. P.; Nolte, R. J. M. *J. Chem. Soc., Chem. Commun.* **1991**, 885-886.

(16) Sijbesma, R. P.; Nolte, R. J. M. *J. Org. Chem.* **1991**, *56*, 3122-3124.

(17) Smeets, J. H. W.; Sijbesma, R. P.; Niele, F. G. M.; Spek, A. L.; Smeets, W. J. J.; Nolte, R. J. M. *J. Am. Chem. Soc.* **1987**, *109*, 928-929.

(18) Smeets, J. W. H.; Sijbesma, R. P.; van Dalen, L.; Spek, A. L.; Smeets, W. J. J.; Nolte, R. J. M. *J. Org. Chem.* **1989**, *54*, 3710-3717.

(19) Flinn, A.; Hough, G. C.; Stoddart, J. F.; Williams, D. J. *Angew. Chem. Int. Ed. Engl.* **1992**, *31*, 1475-1477.

(20) Sijbesma, R. P.; van Dalen, L.; Spek, A. L.; Smeets, W. J. J.; Nolte, R. J. M. *J. Org. Chem.* **1989**, *54*, 3710-3717.

(21) Butler, A. R.; Leitch, E. *J. Chem. Soc., Perkin Trans. 2* **1980**, 103-109.

(22) Performed by William Davis, Massachusetts Institute of Technology, in collaboration with Carolyn Knobler, Berkeley University.

(23) For review on glycoluril preparation, see: Dunnavant, W. R.; James, F. L. *J. Am. Chem. Soc.* **1956**, *78*, 2740-2743. Nematollahi, J.; Ketcham, R. *J. Org. Chem.* **1963**, *28*, 2378-2380. Sijbesma, R. P.; Kentgens, A. P. M.; Nolte, R. J. M. *J. Org. Chem.* **1991**, *56*, 3199-3201.

(24) Bosman, W. P.; Beurskens, P. T.; Admiraal, G.; Sijbesma, R. P.; Nolte, R. J. M. *Z. Kristallogr.* **1991**, *197*, 305-308.

(25) Schouten, A.; Kanters, J. A. *Acta. Cryst.* **1990**, *C46*, 2484-2486.

(26) The AMBER* force field predicted the *anti-anti* isomer to be favoured by ~3.4 kcal/mole. Contrastly, the MM2 force field predicted the *anti-syn* isomer to be favoured by ~1.3 kcal/mole.

(27) Bondi, A. *J. Phys. Chem.* **1964**, *69*, 441-451.

(28) See experimental section.

(29) Kleyweht, G. J.; Jones, T. A. *Acta Cryst.* **1994**, *D50*, 178-185.

(30) VOIDOO calculations were performed by Gerard Kleywegt, Department of Molecular Biology, Uppsala University, Sweden.

(31) Synthesized by Robert Grotzfeld, Massachusetts Institute of Technology, unpublished results.

(32) Dewan, J. C.; Mikami, B.; Hirose, M.; Sacchettini, J. C. *Biochemistry* **1993**, *32*, 11963-11968.

(33) van Gunsteren, M. F.; Berendsen, H. J. C. *Mol. Simul.* **1988**, *1*, 173.

(34) Weiner, S. J.; Kollman, P. A.; Case, D.; Singh, U. C.; Alagona, G.; Profeta, S.; Weiner, P. *J. Am. Chem. Soc.* **1984**, *106*, 765-784.

(35) Still, W. C.; Tempczyk, A.; Hawley, R. C.; Hendrickson, T. *J. Am. Chem. Soc.* **1990**, *112*, 6127-6129.

Part II. Metal Ligation

Chapter Five. The Binding of Uranyl Ion by Convergent Polycarboxylates

5.1 Introduction

The extraction of uranium species from sea water has generated much attention because of the increasing popularity of environmental and energy issues. There is an estimated 4.5 x 10^{12} kg of uranium dissolved in sea water which is approximately 1000 times that available from terrestrial sources.[1] Virtually all of this uranium is in the form of U(VI) as the uranyl ion (UO_2^{2+}) due to the highly oxidizing marine environment, although total uranium only approaches 3.3 parts per billion. An effective uranyl binder, therefore, must possess appropriate structural features in order to exhibit high preference for UO_2^{2+} ion over other metal salts that are abundant in sea water. Certainly, selectivity is the most important concern when designing effective "uranophiles".[2]

The oxophilic nature of the uranyl ion is realized by the isolation of highly stable tris(carbonato) complexes.[3] The coordination numbers around the metal center are generally five or six with the two uranyl oxygens being collinear and chemically inert.[1,4,5] Consequently, the ligands must provide adequate depth to allow for induced-fit binding of the UO_2^{2+} "cylinder". This type of ligation has been provided extensively by macrocyclic ligands.

The preorganization of macrocyclic polydentates makes them some of the most widely used systems for the binding of metal ions and well suited for the pseudoplanar hexacoordinate uranyl ion. The high selectivity of macrocycles is governed mainly by the size of the cyclic interior and the nature of the heteroatom involved in complexation. Resulting complexes are highly stable owing to the "macrocyclic effect" (increased negative entropy involved in chelation). Examples of anionic macrocyclic ligands include enolates of poly-1,3-diketones (cyclic acetylacetones) **I**,[6-9] polycarboxylates **II**[10-13] and thiocarbamates,[14,15] Schiff bases **III**,[16-18] and calixarenes **IV** (R = CH_2CO_2H).[19-21] For

example, trienol **I** has effectively extracted 98% of uranyl ion from aqueous solutions. In macrocycle **II**, the six symmetrically positioned carboxyl groups satisfy UO_2^{2+} ion's preference for pseudoplanar hexacoordinate complexation, while the flexibility of the ring system allows for induced-fit binding.

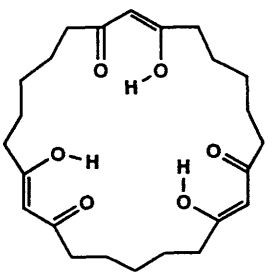

I

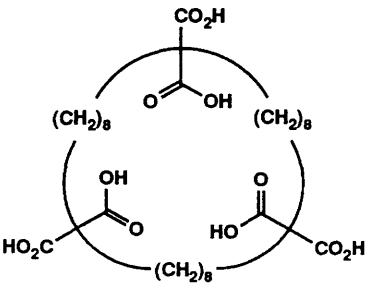

II

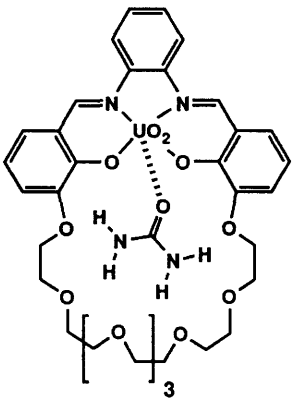

III

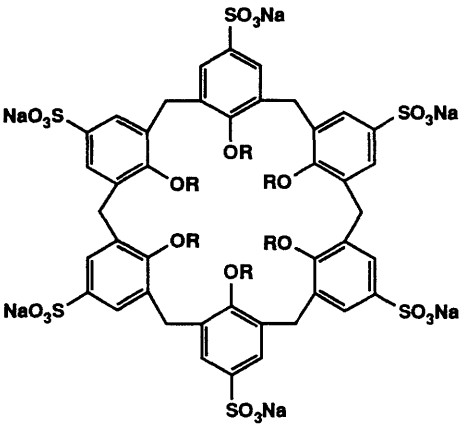

IV

The complexation of uranyl within the Schiff base-modified crown ether **III** introduces a system which can be considered to mimic an enzyme binding site. The salen-type site (salen = *N,N'*-ethylenebis(salicylideneaminato)) has a strong affinity for electrophilic transition-metals such as uranium while the crown ether portion complexes an additional molecule of urea. The urea carbonyl group is pointed towards the uranium core

and satisfies the fifth ligation site. The uranyl cation serves as a bridging electrophile, inducing a partial charge on the urea NH_2 functional groups. The result is stronger hydrogen bonding of the urea and the formation of a terniary complex. This simultaneous binding of a neutral guest species through hydrogen bonds and a metal center is a mode of complexation frequently seen in metalloenzymes.

The hexacarboxycalixarene complex **IV** exhibits high stability due largely to the preorganization of the ligand. Selectivity of UO_2^{2+} results from the architectural positioning of the carboxylates into a pseudoplanar conformation which is unable to accommodate square-planar or tetrahedral metals. The stability of the complex was taken advantage of by using macrocycle **IV** to transport uranyl ion across liquid-liquid as well as a polymer-liquid barriers.[21]

5.2 Design of Polycarboxylate Ligands

An alternative design approach towards metal ligands is the idea of convergency provided by the poly-Kemp's triacid derivatives which have been popularized by Rebek and coworkers.[22-27] The preference of uranyl ion for pseudoplanar tetra- and hexacoordinate carboxylate ligands suggests that hosts comprised of two or three convergent Kemp's triacids would be good candidates for binding studies. The architecture of the systems requires subtle tailoring in order to present a preorganized ligation cavity while retaining adequate flexibility to allow for facile uptake. The effects of rigidity and geometry on the binding of UO_2^{2+} was evaluated by screening a series of polycarboxylate ligands for their uranyl extracting abilities (Figure 1).

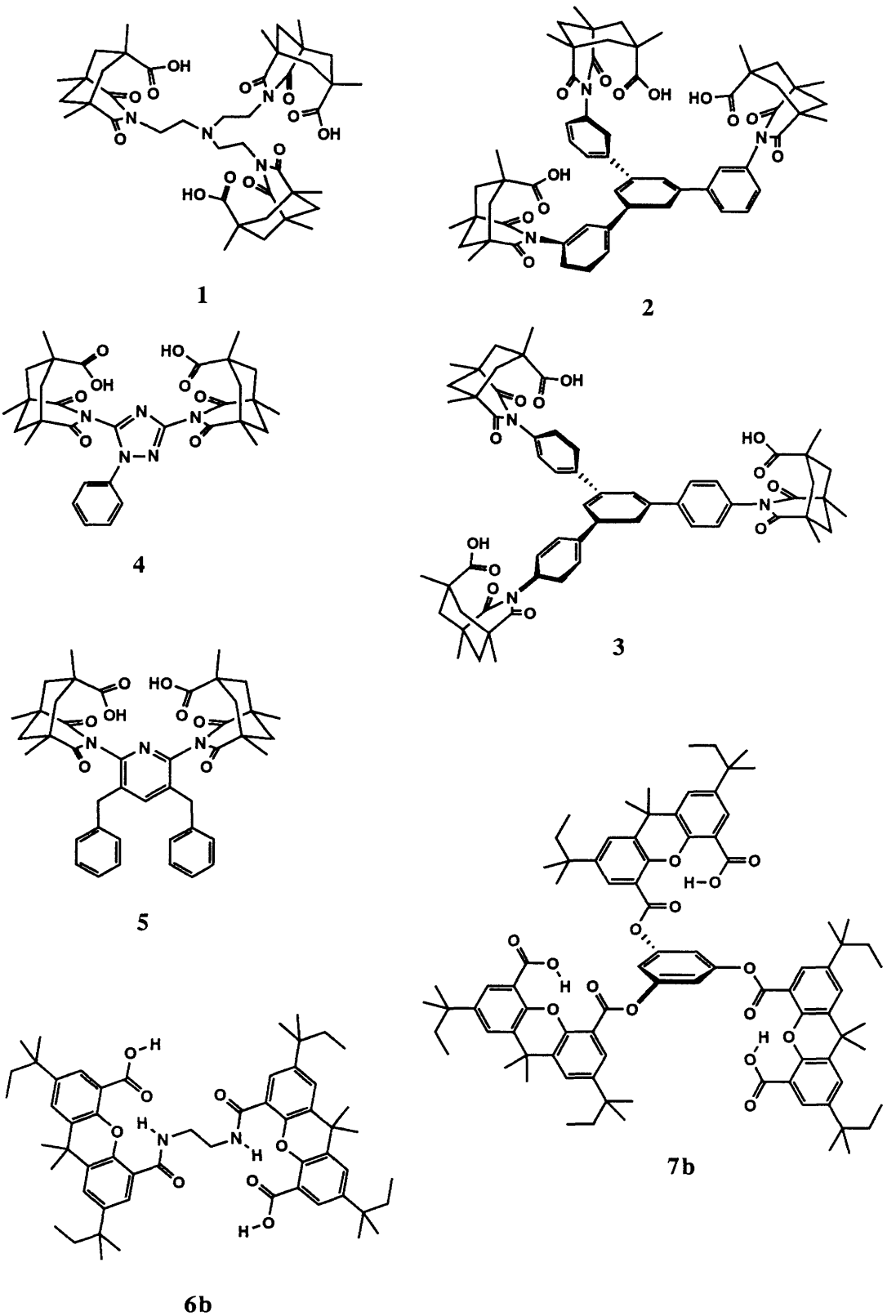

Figure 1. *Convergent Kemp's triacid- and xanthene-based carboxylate clefts for UO_2^{2+} extractions.*

5.3 Synthesis

Molecules **4** and **5** provide shallow dicarboxylate clefts, suitable for chelating relatively planar guests, and hosts of these types have been used successfully as adenine binders.[28-30] However, the cylindrical shape created by the axial UO_2^{2+} oxygens suggests that molecules presenting deeper clefts may be more effective binders. The recently introduced xanthene derivative **8**[31] increases the distance between the two carboxyl functions (~4.7 Å) as compared to that of the Kemp's triacid derivatives (~0.25 Å). The "U-turn" relationship necessary for building structures with convergent functional groups is retained by diacid **8**, and hosts prepared from this building block exhibit deeper clefts. The organic soluble xanthene-based di- and tricarboxylate ligands **6b**, **7b** and **9b** were designed and synthesized as outlined in schemes 1 and 2. The Kemp's carboxylic acid derivatives **1-5** were prepared following previously published methods.[32,33]

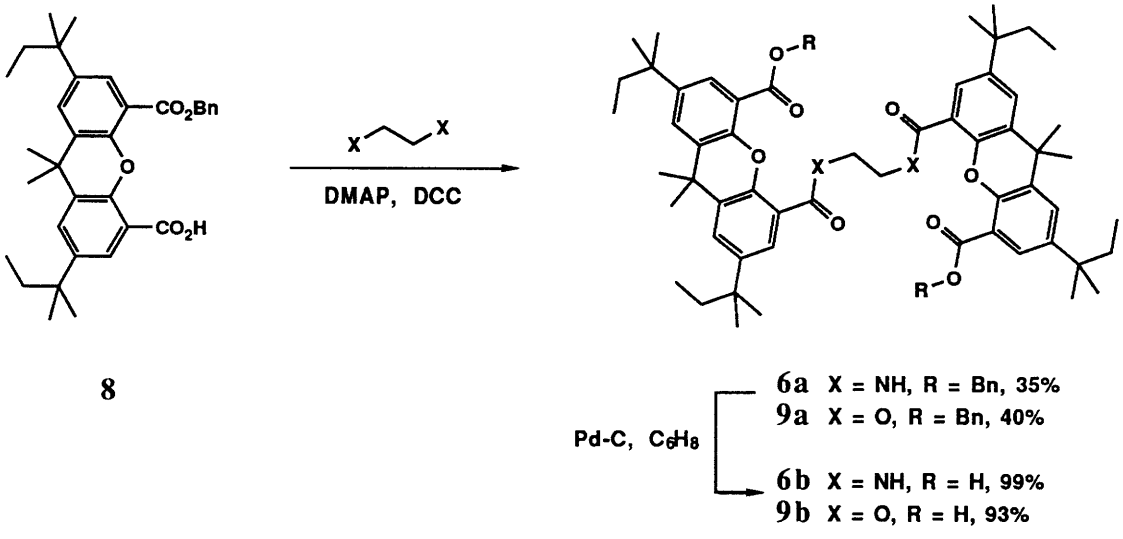

Scheme 1. *Synthesis of xanthene-based dicarboxylate clefts **6b** and **9b**.*

Xanthene dicarboxylic acid was synthesized as previously described.[31] It was reported that reacting **8** with 1 equivalent of benzyl alcohol and dicyclohexyldicarboximide

in the presence of catalytic *N,N*-dimethylaminopyridine, the monobenzyl ester can be obtained in yields as high as 85%. This procedure was extended to the synthesis of hosts **6b-9b**. When the crude reaction mixture was treated with 0.33 equivalents of phloroglucinol (1,3,5-trihydroxybenzene) and 1.0 equivalent DCC, the hexaester **7a** was isolated in 54% yield. Similarly 0.5 equivalents of ethylene glycol or ethylene diamine afforded the tetraester **9a** and the diester-diamide **6a** respectively. Cleavage of the benzyl esters was carried out by either trimethylsilyl iodide or hydrogenation with palladium on carbon. Both routes generated the free carboxylic acids in nearly quantitative yields. The ethylene glycol-based cleft **9b** was insufficiently stable to be used in the extraction studies.

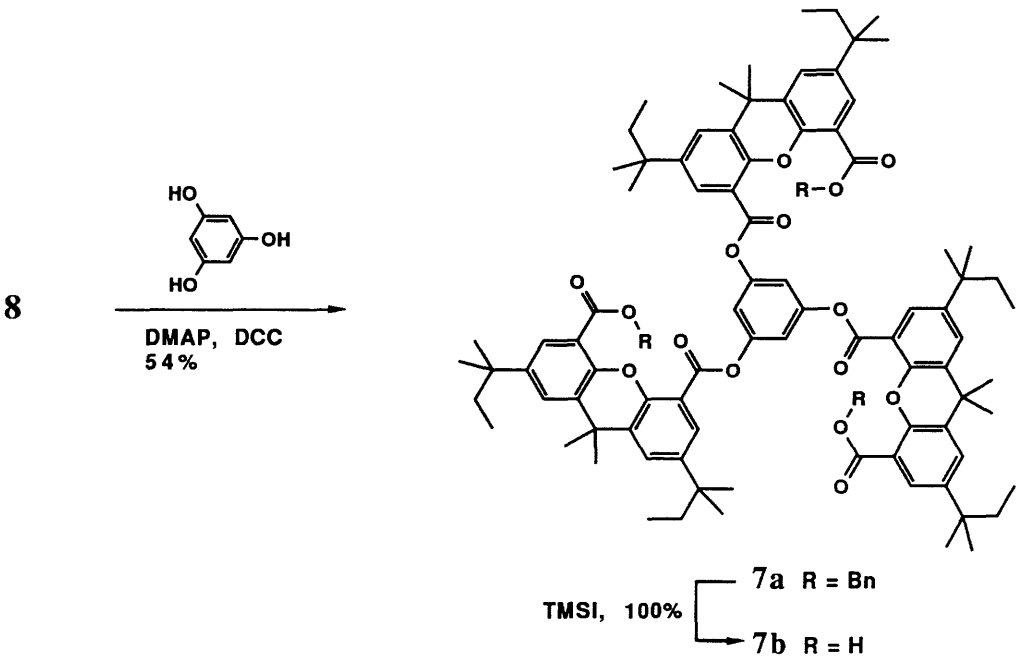

Scheme 2. *Synthesis of xanthene-based tricarboxylate cleft* ***7b***.

5.4 UO_2^{2+} Extractions with Clefts 1-7

The low-level radioactivity of the U^{238} atom provided a convenient method for assaying the amount of uranyl extracted from aqueous to organic solutions. Standards of UO_2^{2+} (uranyl acetate dihydrate) in the 0.05-2.0 mM concentration range were used.

Radioactivity was counted over a 2 minute period using the full scintillation window and produced activity readings of ~564 cpm/μmol UO_2^{2+}. Binding studies were performed by extracting aqueous solutions of uranyl diactetate with chloroform solutions of hosts **1-7**. The amount of UO_2^{2+} ion extracted was measured by analyzing the aqueous phase for decrease of uranyl. In cases where turbidity of the aqueous phase prevented clean separation, the amount of uranyl extracted into the chloroform solutions was measured. In all cases, plots of radioactivity as a function of ligand concentration were linear, and the most effective hosts extracted as much as one equivalent of UO_2^{2+} (Table 1).

Table 1. Equivalents of uranyl extracted from aqueous solutions of uranyl diacetate into $CHCl_3$ solutions. Extractions were performed at room temperature for 10 minutes.

Extractor	Equiv. UO_2^{2+} extracted	Extractor	Equiv. UO_2^{2+} extracted
1	0.59	**5**	0.04
2	0.75	**6b**	1.06
3	0	**7b**	0.71
4	0.01		

The trends that are evident from these studies are as follows: 1) The ligands are effective liquid-liquid extractors. 2) They are not successful at solubilizing solid samples of uranyl diactetate into chloroform. 3) There is no measurable uptake of uranyl ion into chloroform solutions when extractions are carried out for extended periods. A distinct precipitate was observed at the interfaces during these extended extractions (up to 13 hours). This precipitate is most likely due to a "soaping-out" effect of metal carboxylates in these two phase solvent systems, resulting in a settling out of the metal complexes. 4) It can be similarly noted that as the pH of the extraction solution is raised the soaping out effect increases. So much so, that in cases where the pH was brought above 7.5 (with

ammonium buffers, for example) the separation of the phases was impossible. 5) When the aqueous phase, after extracting for 10 minutes with solutions of triacid **1**, was evaporated and examined by ^{1}H NMR no trace of the acid was observed. It can, therefore, be concluded that UO_2^{2+} ion does not extract the host into water. 6) The extraction of UO_2^{2+} ion by the pyridine diacid **5** showed low extractability, while the extraction of the guanazole diacid **4** showed slightly improved results. This is most likely due to the "opening" effect the phenyl substituents have on host **4**, providing a larger cleft for the entry of the uranium coordination sphere. 7) Triphenylbenzenetricarboxylic acids **2** and **3** have opposite extracting abilities. The *para*-triacid **3** showed no UO_2^{2+} ion extraction into chloroform, as well as no decrease in the amount of uranyl in the aqueous phase. The *meta*-triacid **2** was observed to extract UO_2^{2+} ion into chloroform in a **2**/UO_2^{2+} ratio of 1.3:4. Both triacids exhibit clefts suitable for binding the cylindrical UO_2^{2+} ion, but the *meta*-triacid has convergent carboxyls which can form a pseudoplanar geometry around the metal. On the other hand, the carboxyl groups of the *para*-triacid are farther away from the metal center.

5.5 Conclusions

As much as one full equivalent of uranyl ion can be extracted from water when the host molecule is tailored appropriately. Ligands must exhibit clefts with adequate depth to accommodate the cylindrical shape of the UO_2^{2+} ion. In cases where the clefts are too shallow, low extractibility is observed.

Another strategy to increase the complexation of uranyl (over other metal salts) takes advantage of the uranium-oxo double bond in UO_2^{2+}. Historically, coordination chemistry and ligand design have regarded this metal-oxo group as an occupied metal coordination site. The oxo group has a partial negative charge, and the oxygen lone pair electrons are directed away from the metal core along the U=O axis.[4,5] Incorporating a

hydrogen bond donor site (N-H, for example) in the vicinity of this hydrogen bond acceptor would enhance the stability of the resulting metal-ligand complex. Raymond and coworkers have pursued this strategy through the incorporation of ammonium groups into their ligands.[34] The ammonium salt of the tren-based ligand **1** might further this endeavor.

5.6 Experimental

For a general description of apparatus, materials and methods, see chapter 2.

Scintillation counting was performed on a Pachard 1500 Tri-Carb Liquid Scintillation Analyzer.

General Coupling Procedure of Alcohols and Amines with Xanthene Dicarboxylic Acid.

Solutions of 2,7-di-*tert*-amyl-9,9-dimethylxanthene-4,5-diacid **8** in dry CH_2Cl_2 (10 mg/mL) were treated with dry benzyl alcohol (1 equiv) and catalytic DMAP. The solutions were cooled in ice to 0°C under argon and treated with DCC (1 equiv). The solution was stirred at 0°C for 5 minutes and at room temperature for 5 h. The alcohol or amine (0.5-0.33 equiv) was added followed by DCC (1.1 equiv). After stirring at room temperature for 14-20 h, the solid DCU was filtered and washed with CH_2Cl_2. The filtrate was evaporated under reduced pressure and the product was purified by column chromatography through silica gel:

Dibenzyl 2,2',7,7'-Tetrakis-*tert*-amyl-9,9,9',9'-tetramethyl-5,5'-[ethylenebis(aminocarbonyl)]-4,4'-xanthenedicarboxylate (6a).

Synthesized from 500 mg (1.14 mmol) **8** and 34.3 mg (0.5 equiv) ethylenediamine as a white solid in 35% yield after purification by column chromatography through silica gel (5-25% EtOAc/hexanes):

mp 210-212°C;

^{1}H NMR (250 MHz, $CDCl_3$) δ 9.76 (br s, 2H), 8.31 (d, *J*=2.3 Hz, 2H), 7.76 (d, *J*=2.2 Hz, 2H), 7.51 (d, *J*=2.0 Hz, 2H), 7.44 (d, *J*=2.3 Hz, 2H), 7.40-7.26 (m, 10H), 5.25 (s, 4H), 3.97-3.95 (m, 4H), 1.64-1.61 (m, 20H), 1.27-1.25 (m, 24H), 0.67-0.61 (m, 12H).

Tribenzyl 2,2',2",7,7',7"-Hexakis-*tert*-butyl-9,9,9',9',9",9"-hexamethyl-5,5',5"-[phenylenetris(oxocarbonyl)]-4,4',4"-xanthenetricarboxylate (7a).

Synthesized from 500 mg (1.14 mmol) **8** and 47.9 mg (0.333 equiv) phloroglucinol as a white solid in 54% yield after purification by column chromatography through silica gel (5-30% EtOAc/hexanes):

^{1}H NMR (300 MHz, $CDCl_3$) δ 7.86 (d, *J*=2.0 Hz, 3H), 7.61 (d, *J*=2.0 Hz, 3H), 7.56 (d, *J*=2.0 Hz, 3H), 7.51 (d, *J*=2.0 Hz, 3H), 7.34 (s, 3H), 7.27 (m, 6H), 7.09 (m, 9H), 5.23 (s, 6H), 1.67 (m, 30H), 1.34 (s, 18H), 1.28 (s, 18H), 0.73 (t, *J*=7.5 Hz, 9H), 0.68 (t, *J*=7.4 Hz, 9H).

^{13}C NMR ($CDCl_3$) δ 166.3, 163.4, 151.6, 147.8, 146.7, 143.8, 136.4, 130.7, 130.16, 128.1, 127.7, 127.4, 126.7, 126.3, 120.5, 118.4, 114.1, 66.8, 37.8, 36.8, 32.0, 31.4, 28.4, 9.1.

Dibenzyl 2,2',7,7'-Tetrakis-*tert*-amyl-9,9,9',9'-tetramethyl-5,5'-[ethylenebis(oxocarbonyl)]-4,4'-xanthenedicarboxylate (9a).

Synthesized from 500 mg (1.14 mmol) **8** and 35.4 mg (0.5 equiv) ethylene glycol as a white solid in 40% yield after purification by column chromatography through silica gel (5-25% EtOAc/hexanes):

mp 75-80°C;

IR (KBr) 3331 (w), 2965 (s), 2932 (s), 2875 (m), 2857 (m), 1732 (s), 1707 (s), 1656 (m), 1617 (w) cm^{-1};

^{1}H NMR (250 MHz, $CDCl_3$) δ 7.57 (d, *J*=2.3 Hz, 2H), 7.53 (d, *J*=2.3 Hz, 2H), 7.47 (d, *J*=2.7 Hz, 2H), 7.45 (d, *J*=2.5 Hz, 2H), 7.44-7.40 (m, 4H), 7.33-7.24 (m, 6H), 5.43 (s, 4H), 4.50 (s, 4H), 1.61 (m, 20H), 1.27 (s, 12H), 1.20 (s, 12H), 0.66 (t, *J*=7.6 Hz, 6H), 0.60 (t, *J*=7.6 Hz, 6H).

General Procedure for Cleaving Benzyl Esters (6a-9a).

Method A: Solutions of the benzyl esters in dry CH_2Cl_2 (10 mg/mL) were treated, under argon, with trimethylsilyl iodide (3 equiv). The reactions were stirred at room temperature for 2.5 h and quenched with HCl (1 M). The organic phase was removed, washed with sodium bisulfite (5%), water, brine, dried over $MgSO_4$, and evaporated under reduced pressure.

Method B: 10% Pd-C (1 equiv) and cyclohexadiene (5 equiv) were added to a suspension of the benzyl esters in absolute EtOH (~8 mM). The reactions were refluxed for 4-10 h and filtered. Evaporation of solvent and purification by recrystallization or column chromatography through silica gel afforded the free carboxylic acids:

2,2',7,7'-Tetrakis-*tert*-butyl-9,9,9',9'-tetramethyl-5,5'-[ethylenebis(aminocarbonyl)]-4,4'-xanthenedicarboxylic Acid (6b).

215 mg (0.20 mmol) ester **6a** was debenzylated by method B afforded the dicarboxylic acid as a white solid in 99% yield:

mp 185-190°C;

IR (KBr) 3373 (s), 3339 (m), 2963 (s), 2929 (s), 2918 (s), 2875 (m), 2852 (m), 1729 (s), 1646 (s), 1628 (s), 1607 (m), 1597 (m), 1575 (m) cm^{-1};

^{1}H NMR ($CDCl_3$, 300 MHz) δ 10.05 (br s, 2H), 8.25 (d, *J*=2.4 Hz, 2H), 7.98 (d, *J*=2.4 Hz, 2H), 7.59 (d, *J*=2.4 Hz, 2H), 7.52 (d, *J*=2.4 Hz, 2H), 3.84-3.77 (m, 4H), 1.69-1.62 (m, 20H), 1.37-1.29 (m, 24H), 0.73-0.64 (m, 12H).

2,2',2",7,7',7"-Hexakis-*tert*-butyl-9,9,9',9',9",9"-hexamethyl-5,5',5"-[phenylenetris(oxocarbonyl)]-4,4',4"-xanthenetricarboxylic acid (7b).

Treatment of the hexaester **7a** (340 mg, 0.21 mmol) with TMSI (263 uL) afforded the triacid **7b** as a colourless solid in quantitative yield:

IR (KBr) 3365 (m), 2966 (s), 1735 (s), 1609 (m), 1444 (s) cm^{-1};

^1H NMR (300 MHz, $CDCl_3$) δ 8.22 (d, *J*=2.5 Hz, 3H), 8.19 (d, *J*=2.5 Hz, 3H), 7.77 (d, *J*=2.5 Hz, 3H), 7.65 (d, *J*=2.5 Hz, 3H), 7.31 (s, 3H), 1.72 (m, 30H), 1.42 (s, 18H), 1.32 (s, 18H), 0.78 (t, *J*=7.5 Hz, 9H), 0.68 (t, *J*=7.5 Hz, 9H).

2,2',7,7'-Tetrakis-*tert*-butyl-9,9,9',9'-tetramethyl-5,5'-[ethylenebis(oxocarbonyl)]-4,4'-xanthenedicarboxylic Acid (9b).

Ester **9b** (217 mg, 0.20 mmol) was debenzylated by method B to afford the dicarboxylic acid as a white solid in 93% yield:

mp 130-135°C;

^1H NMR (250 MHz, $CDCl_3$) δ 7.55 (d, *J*=2.4 Hz, 2H), 7.51 (d, *J*=2.4 Hz, 2H), 7.45 (d, *J*=2.5 Hz, 2H), 7.35 (d, *J*=2.5 Hz, 2H), 4.30 (s, 4H), 1.65-1.60 (m, 20H), 1.25 (s, 12H), 1.20 (s, 12H), 0.65 (t, *J*=7.6 Hz, 6H), 0.60 (t, *J*=7.6 Hz, 6H).

^{13}C NMR ($CDCl_3$) δ 164.7, 164.1, 150.0, 147.8, 146.7, 145.3, 138.5, 130.8, 130.4, 129.9, 128.4, 122.2, 38.0, 36.8, 34.4, 32.6, 31.3, 28.4, 9.1.

References

(1) For a general review on the structure and reactions of uranyl, see: Cordfunke, E. H. P. *The Chemistry of Uranium, Including Its Applications in Nuclear Technology*; Elsevier Publishing Company: New York, 1969.

(2) Tabushi, I.; Kobuke, Y. *Isr. J. Chem.* **1985**, *25*, 217-227.

(3) Cinneide, S. O.; Scanlan, J. P.; Hynes, M. J. *J. Inorg. Nucl. Chem.* **1975**, *37*, 1013-1018.

(4) Tatsumi, K.; Hoffmann, R. *Inorg. Chem.* **1980**, *19*, 2656-2658.

(5) Wadt, W. R. *J. Am. Chem. Soc.* **1981**, *103*, 6053-6057.

(6) Alberts, A. H.; Cram, D. J. *J. Am. Chem. Soc.* **1977**, *99*, 3880-3882.

(7) Alberts, A. H.; Cram, D. J. *J. Am. Chem. Soc.* **1979**, *101*, 3545-3553.

(8) Ito, Y.; Sugaya, T.; Nakatsuka, M.; Saegusa, T. *J. Am. Chem. Soc.* **1977**, *99*, 8366-8367.

(9) Tabushi, I.; Kobuke, Y.; Nishiya, T. *Tetrahedron Lett.* **1979**, 3515-3518.

(10) Newcomb, M.; Cram, D. J. *J. Am. Chem. Soc.* **1975**, *97*, 1257-1259.

(11) Newcomb, M.; Moore, S. S.; Cram, D. J. *J. Am. Chem. Soc.* **1977**, *99*, 6405-6410.

(12) Cram, D. J.; Helgeson, R. C.; Koga, K.; Kyba, E. P.; Madan, K.; Sousa, L. R.; Siegel, M. G.; Moreau, P.; Gokel, G. W.; Timko, J. M.; Sogah, J. D. Y. *J. Org. Chem.* **1978**, *43*, 2758-2772.

(13) Grey, R. A.; Pez, G. P.; Wallo, A. *J. Org. Chem.* **1980**, *102*, 5947-5948.

(14) Tabushi, I.; Kobuke, Y.; Yoshizawa, A. *J. Am. Chem. Soc.* **1984**, *106*, 2481-2482.

(15) Tabushi, I.; Yoshizawa, A.; Mizuno, H. *J. Am. Chem. Soc.* **1985**, *107*, 4585-4586.

(16) Rajan, O. A.; Chakravorty, A. *Inorg. Chim. Acta* **1981**, *50*, 79-84.

(17) van Staveren, C. J.; Fenton, C. J.; Reinhoudt, D. N.; van Eerden, J.; Harkema, S. *J. Am. Chem. Soc.* **1987**, *109*, 3456-3458.

(18) van Staveren, C. J.; van Eerden, J.; van Veggel, F. C. J. M.; Harkema, S.; Reinhoudt, D. N. *J. Am. Chem. Soc.* **1988**, *110*, 4994-5008.

(19) Shinkai, S.; Koreishi, H.; Ueda, K.; Manabe, O. *J. Chem. Soc., Chem. Commun.* **1986**, 233-234.

(20) Shinkai, S.; Koreishi, H.; Ueda, K.; Arimura, T.; Manabe, O. *J. Am. Chem. Soc.* **1987**, *109*, 6371-6376.

(21) Araki, K.; Hashimoto, N.; Otsuka, H.; Nagasaki, T.; Shinkai, S. *Chem. Lett.* **1993**, 829-832.

(22) Rebek, J., Jr.; Askew, B.; Islam, N.; Killoran, M.; Nemeth, D.; Wolak, R. *J. Am. Chem. Soc.* **1985**, *107*, 6736-6738.

(23) Rebek, J., Jr.; Marshall, L.; Wolak, R.; Parris, K.; Killoran, M.; Askew, B.; Nemeth, B.; Islam, N. *J. Am. Chem. Soc.* **1985**, *107*, 7476-7481.

(24) Rebek, J., Jr.; Askew, B.; Killoran, M.; Nemeth, D.; Lin, F. *J. Am. Chem. Soc.* **1987**, *109*, 2426-2431.

(25) Lindsey, J. S.; Kearney, P. C.; Duff, R. J.; Tjivikua, P. T.; Rebek, J., Jr. *J. Am. Chem. Soc.* **1988**, *110*, 6575-6577.

(26) Rebek, J., Jr. *Pure Appl. Chem.* **1989**, *61*, 1517-1522.

(27) Rebek, J., Jr. *J. Heterocycl. Chem.* **1990**, *27*, 111-117.

(28) Benzing, T.; Tjivikua, T.; Wolfe, J.; Rebek, J., Jr. *Science* **1988**, *242*, 266-268.

(29) Jeong, K. S.; Tjivikua, T.; Muehldorf, A.; Deslongchamps, G.; Famulok, M.; Rebek, J., Jr. *J. Am. Chem. Soc.* **1991**, *113*, 201-209.

(30) Galan, A.; de Mendoza, J.; Toiron, C.; Bruix, M.; Deslongchamps, G.; Rebek, J., Jr. *J. Am. Chem. Soc.* **1991**, *113*, 9424-9425.

(31) Nowick, J. S.; Ballester, P.; Ebmeyer, F.; Rebek, J., Jr. *J. Am. Chem. Soc.* **1990**, *112*, 8902-8906.

(32) Marshall, L.; Parris, K.; Rebek, J., Jr. *J. Am. Chem. Soc.* **1988**, *110*, 5192-5193.

(33) U.S. Patent no. 4 698 425.

(34) Stack, T. D. P.; Hou, Z.; Raymond, K. N. *J. Am. Chem. Soc.* **1993**, *115*, 6466-6467.

Chapter Six. Neighbouring Group Participation in Kemp's Triacid Derivatives

6.1 Introduction

In the previous chapter, it was shown that derivatives of Kemp's triacid (*cis,cis*-1,3,5-trimethylcyclohexane-1,3,5-tricarboxylic acid) are useful scaffolds for building molecular recognition systems possessing "U-turn" convergent structures. This architectural feature is due to the enforcement of all three carboxylic acid groups into axial positions by the sterically bulkier methyl groups.[1,2] The triaxial positioning of the carbonyl groups (~0.25-nm separation) encourages neighbouring-group participation, making these derivatives useful probes for studying the stereoelectronic effects at the carbonyl oxygen.[3,4] This proximity effect results in highly enhanced rates of chemical reactions, for example hydrolyses, which can perhaps be attributed to the relief of strain factors. Initially this was demonstrated by the ease of dehydrating the parent tricarboxylic acid to the bicyclic anhydride, as well as by the inability to isolate the Kemp's tricarboxylic acid chloride upon treatment with thionyl chloride (instead the anhydride acid chloride is generated).

The strong neighbouring-group participation has also been demonstrated using the lactam of the bicyclic acid (**1**).[5] This derivative was readily prepared from Kemp's tricarboxylic acid and resolved into its optically active form.[6] Complete racemization of enantiomerically pure **1** resulted from the treatment with excess reagents ($SOCl_2$, oxalyl chloride or PCl_5) during the conversion to the acid chloride. This was realized, for instance, when the reaction was quenched with water and the racemic bicyclic lactam acid was obtained. The experimental evidence suggested the presence of a cyclic, *meso*-symmetric aza-adamantane intermediate **2**, similar in structure to other known Kemp's acid derivatives.[5,7,8] Approach of the chlorine ion towards the active intermediate structure **2** along the two paths outlined in scheme 1 (assigned *Re* and *Si*, based on the chiral

arrangment of the products) resulted in a 1:1 mixture of the two enantiomers. The amino-lactone **3** is another possible intermediate. This structure is formed by intramolecular attack of the acid oxygen on an α-cloroiminium ion. The *Si*-isomer of **1** can be generated from the *Re*-isomer (**1**-*Re*) by the attack of the nitrogen of structure **3** on the lactone function. Experimental support for this particular intermediate (**3**) came from the fact that upon addition of one equivalent of thionyl chloride to lactam **1**, an asymmetric species was generated.[9] The resulting product was not an acylating source and treatment with amines did not afford the amides.

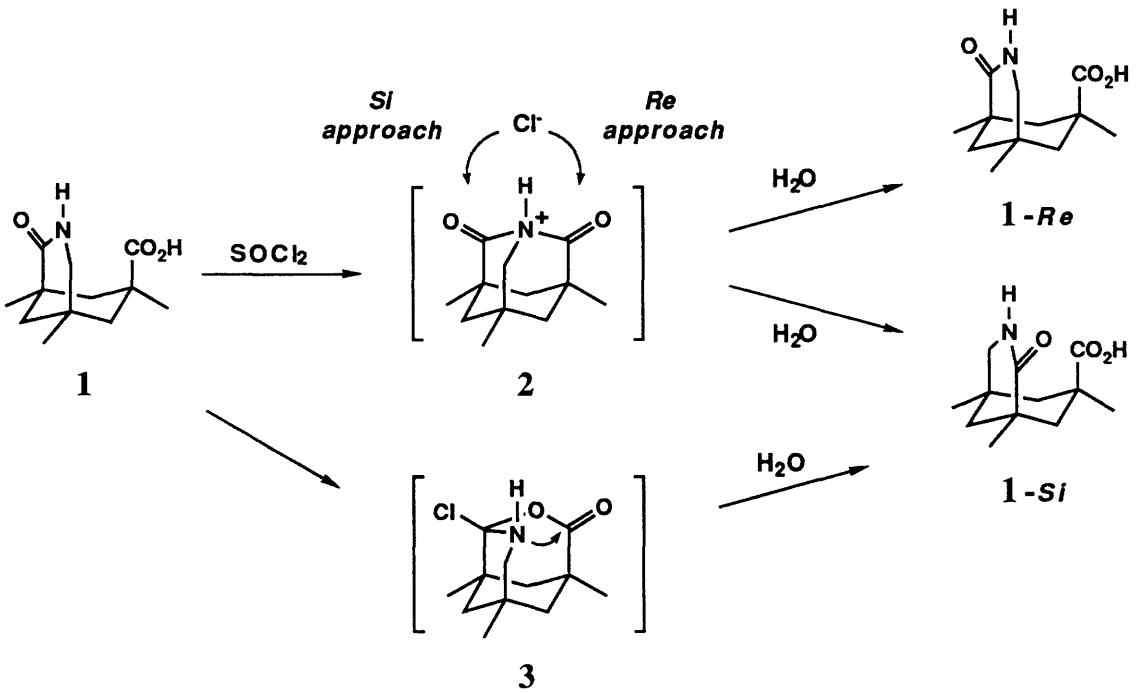

Scheme 1. *The approach of chloride ion towards 2 along two possible reaction paths results in a racemic mixture of the bicyclic lactam acid after quenching with water. Intramolecular attack of the amine on the lactone of 3 has the same effect.*

6.2 ^{18}O Labelling Study

The existence of the cyclic intermediates **2** and **3** was further supported by ^{18}O-labelling studies. After treating the lactam carboxylic acid with excess thionyl chloride, the

residue was quenched with $H_2{}^{18}O$ affording the bicyclic lactam labelled in the carboxylic acid. Resubmission of this compound to the thionyl chloride-water sequence regenerated the lactam carboxylic acid possessing ^{18}O in both the lactam and acid chloride oxygen functions. The presence of ^{18}O was determined by evaluating the change in signals in the ^{13}C NMR spectra of the bicycles. The effect of ^{18}O-labelling has been documented as a shift of the resonances directly attached to the labelled oxygen to positions of lower frequency (upfield).[10]

The bicyclic derivative **4** uses the same structural scaffold to position an imide in a similar environment as exhibited by the lactam of **1**. This derivative provides a means to study whether a less nucleophilic nitrogen can participate in similar in neighbouring-group effects. The involvment of the aza-adamantane intermediate **5** or the lactone **6** (Scheme 2) was examined by analogous ^{18}O-labelling ^{13}C NMR experiments.

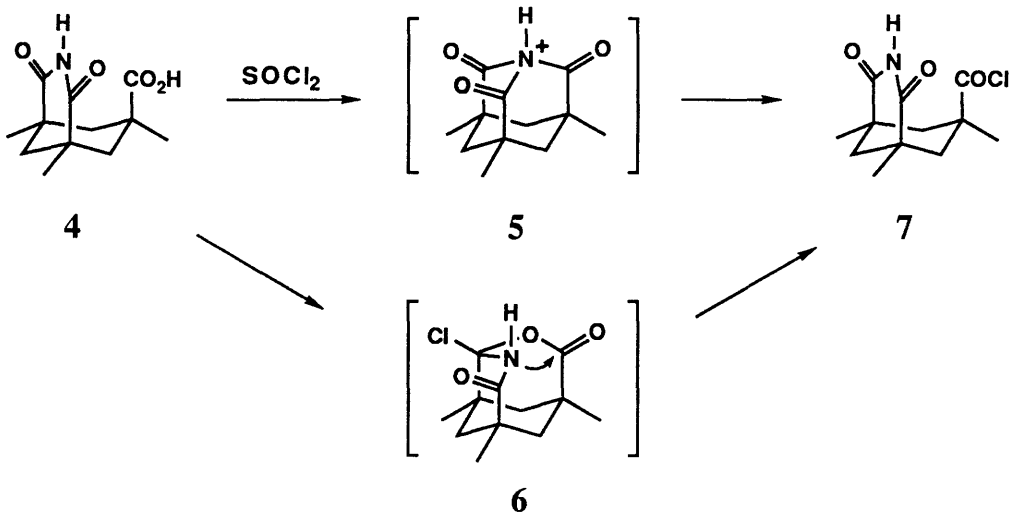

Scheme 2. *Proposed aza-adamantane and amino-lactone intermediates for the bicyclic imide **4** upon treatment with thionyl chloride.*

In order to ensure the reliability of the ^{13}C NMR study as an analytical tool for this application, authentic samples of ^{18}O-labelled imide acid **9** and acid chloride **10** were

prepared. Hydrolysis of the bicyclic anhydride acid chloride **8** with $H_2{}^{18}O$ followed by dehydrative ring closure generated the imide acid **9** with both acid and imide oxygens labelled (Scheme 3). Treatment with excess thionyl chloride afforded the labelled imide acid chloride **10**. A representative ^{13}C NMR spectrum of compound **9** in pyridine-d_5 is depicted in figure 1.

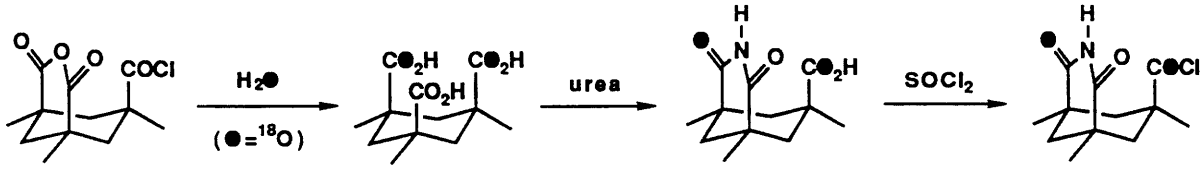

8 **9** **10**

Scheme 3. *Synthesis of authentic samples of ^{18}O-labeled imide derivatives **9** and **10**.*

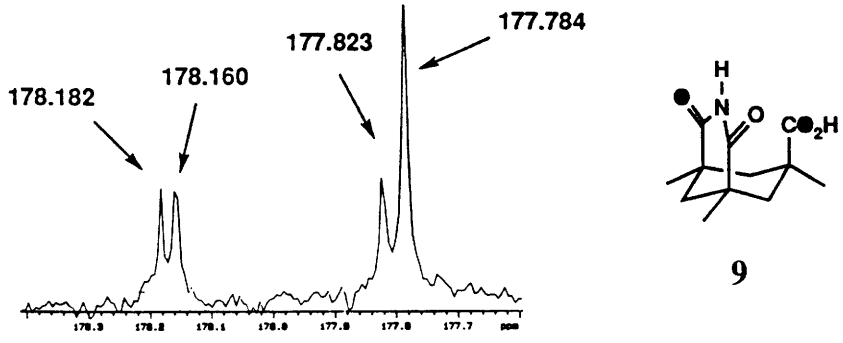

9

Figure 1. *^{13}C NMR at 500 MHz in pyridine-d_5 of the carbonyl region for imide acid **9**.*

Treating unlabelled Kemp's imide acid **4** with excess thionyl chloride followed by quenching with $H_2{}^{18}O$ afforded carboxylic acid **11** with ^{18}O incorporated solely into the carboxylic acid group (Figure 2). A second treatment with thionyl chloride and quenching with water regenerated the carboxylic acid **12** with no observed transfer of ^{18}O to the imide carbonyls.

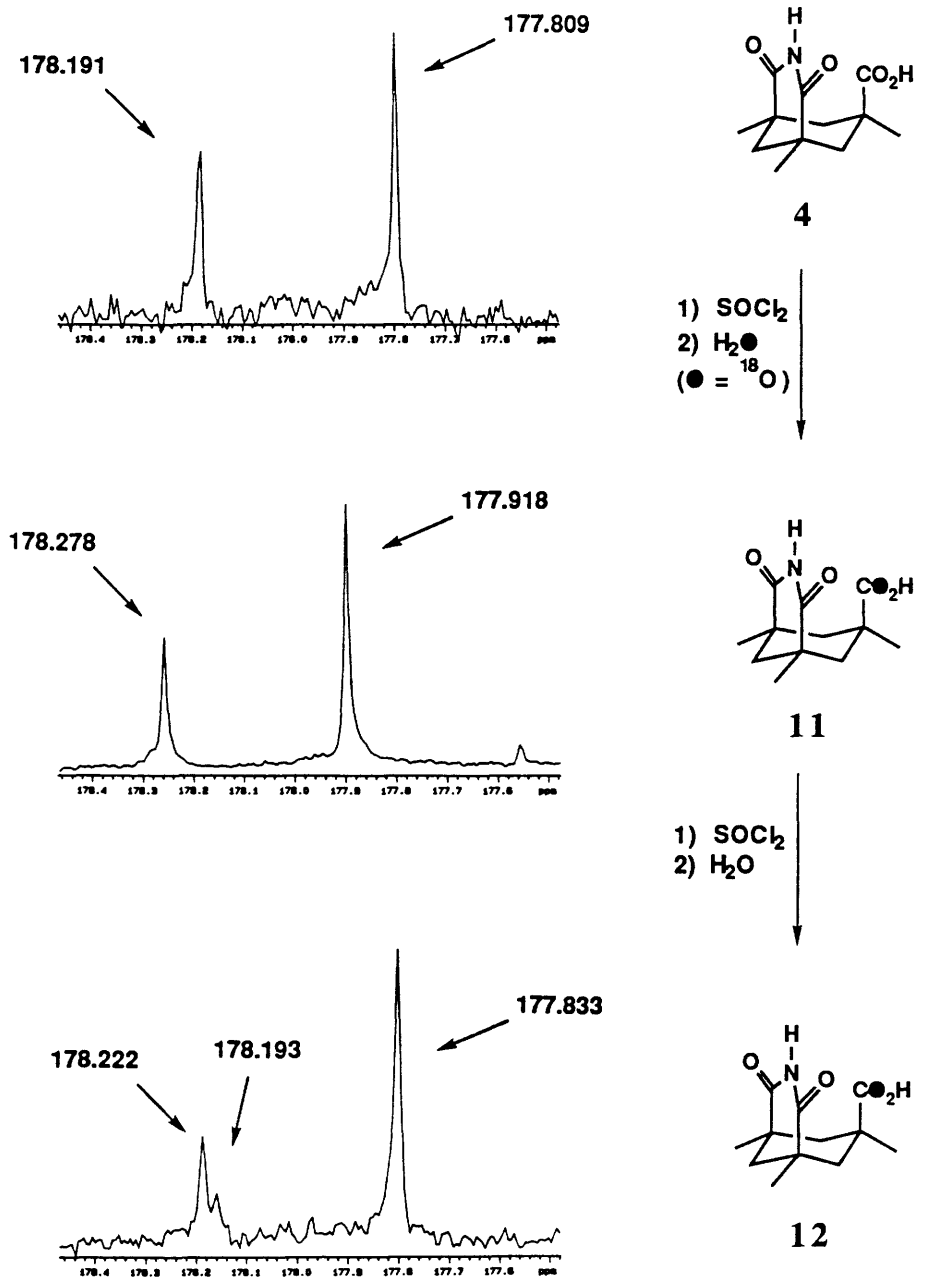

Figure 2. *500 MHz ^{13}C NMR of bicyclic imide acids. In all cases, ^{18}O-labelled carbonyls are shifted upfield. Non-correlations in resonance frequency are due to the strong concentration dependence of the carboxylic acids in the basic pyridine medium.*

The ^{13}C NMR spectra of the corresponding imide acid chlorides in chloroform-*d* produced identical results: there was ^{18}O incorporated into the acid chloride carbonyl, but there was no transfer of the label to the imide function.

The non-involvement of the aza-adamantane or lactone intermediates by the less-nucleophilic imide nitrogen of **4** differs from studies using other imide derivatives of Kemp's triacid.[5] For example, optically active bicyclic imide **13** racemizes upon treatment with $SOCl_2$ followed by quenching with water (Scheme 4). Structures **14** and **15** were proposed as intermediates.

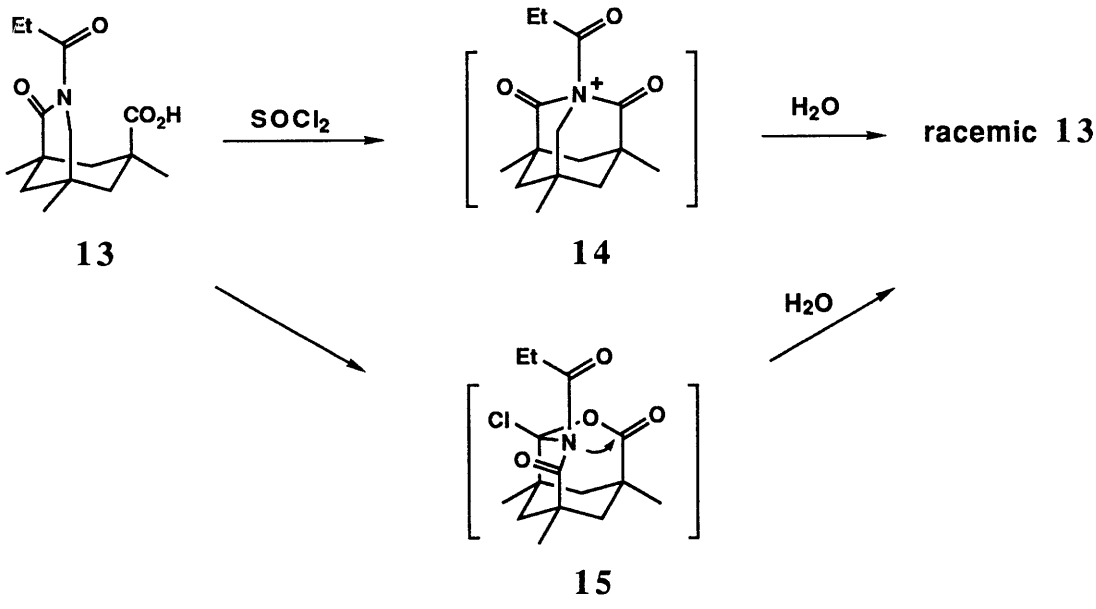

Scheme 4. *Racemization of optically active imide **13** through the aza-adamantane intermediate **14** or the amino-lactone **15**.*

An imide nitrogen is certainly capable of being involved in these neighbouring group effects as demonstrated with imide **13**. The lack of racemization for imide **4** could be due in part to the strain of the cyclic intermediate **5** or **6** as compared to that for structure **14** or **15**.

6.3 Experimental

For a general description of apparatus, materials and methods, see chapter 2.

^{18}O-Kemp's Imide Acid (preparation of an authentic sample, labelled at both acid and imide carbonyls) (9).

Kemp's anhydride acid chloride (100 mg, 0.39 mmol) and $H_2{}^{18}O$ (250 mg) in dry THF (1 mL) was heated at 150°C in sealed tube for 48 h. Evaporation of the solvent under reduced pressure afforded a white solid (77 mg). The solid was reacted with urea (31.5 mg, 0.52 mmol) in triglyme (3 mL) at 180°C for 4 h. The resulting solution was cooled to room temperature, poured over hexane, and the solid imide acid was collected by filtration:

^{13}C NMR (pyridine-d_5) δ 178.2, 178.2, 177.8, 177.8, 44.7, 44.3, 42.2, 40.2, 31.2, 25.1.

^{18}O-Kemps Imide Acid (11).

Kemp's imide acid chloride (100 mg, 0.39 mmol) was dissolved in dry THF (1 mL) under argon. $H_2{}^{18}O$ (250 mg) was added and the solution stirred at room temperature for 48 h. The solvent was evaporated and the residue was washed with $CHCl_3$ to afford the labelled imide acid as a white solid:

^{13}C NMR (pyridine-d_5) δ 178.3, 177.9, 44.6, 44.2, 42.1, 40.1, 31.08, 25.0.

^{18}O-Kemp's Imide Acid Chloride.

^{18}O-Labelled imide acid was heated in refluxing $SOCl_2$ (5 mL) for 2 h. Excess $SOCl_2$ was distilled under reduced pressure and the residue taken up in ethyl acetate. The labelled imide acid chloride was precipitated by the addition of hexane, filtered, washed with hexane and dried under reduced pressure:

^{13}C NMR (pyridine-d_5) δ 178.7, 178.7, 175.4, 52.2, 44.3, 44.1, 39.8, 30.2, 24.0.

Hydrolysis of ^{18}O-Kemp's Imide Acid Chloride.

^{18}O-labelled imide acid chloride was heated in refluxing H_2O for 4 h. The water was evaporated and the residue washed with $CHCl_3$ to afford the labelled imide acid **12** as a white solid:

^{13}C NMR (pyridine-d_5) δ 178.22, 178.19, 177.83, 44.69, 44.30, 42.19, 40.21, 31.19, 25.11.

References

(1) Kemp, D. S.; Petrakis, K. S. *J. Org. Chem.* **1981**, *46*, 5140-5143.

(2) Kemp's triacid is commercially available from Aldrich Chemical Co. For the synthesis of Kemp's triacid, see: Rebek, J., Jr.; Askew, B.; Killoran, M.; Nemeth, D.; Lin, F. *J. Am. Chem. Soc.* **1987**, *109*, 2426-2431.

(3) Rebek, J., Jr.; Duff, R. J.; Gordon, W. E.; Parris, K. *J. Am. Chem. Soc.* **1986**, *108*, 6068-6069.

(4) Tadayoni, B. M.; Huff, J.; Rebek, J., Jr. *J. Am. Chem. Soc.* **1991**, *113*, 2247-2253.

(5) Ballester, P.; Tadayoni, B. M.; Branda, N.; Rebek, J., Jr. *J. Am. Chem. Soc.* **1990**, *112*, 3686.

(6) Jeong, K.; Parris, K.; Ballester, P.; Rebek, J., Jr. *Angew. Chem.* **1990**, *102*, 550-551.

(7) Askew, B.; Ballester, P.; Buhr, C.; Jeong, K.; Jones, S.; Parris, K.; Williams, K.; Rebek, J., Jr. *J. Am. Chem. Soc.* **1989**, *111*, 1082-1090.

(8) For studies on bridgehead lactams and imides, see: Pracejus, H.; Kehlen, M.; Kehlen, H.; Matschiner, H. *Tetrahedron* **1965**, *21*, 2257-2270.

(9) Pablo Ballester, unpublished results.

(10) Vederdas, J. C. *J. Am. Chem. Soc.* **1980**, *102*, 374-376.

Chapter Seven. Catalytic Oxidations and Cyclopropanations

7.1 Introduction

The area of asymmetric synthesis seeks to combine the ideas of reaction mechanism, catalysis, and metal coordination with molecular recognition. Catalytic asymmetric induction is advantageous because it offers direct chemical amplification of the chiral catalyst. Some of the most significant developments in this area include the ruthenium-catalyzed chiral hydrogenation,[1,2] the copper- and ruthenium-catalyzed cyclopropanations,[3,4] and the osmium-catalyzed dihydroxylation,[5] and titanium-catalyzed epoxidations.[6]

One of the most heavily researched classes of naturally occurring metal ligands is the porphyrins because they are analogues of the prosthetic groups of the heme-containing enzymes.[7] Nature uses them for oxygen transport and oxidation of substrates: oxygenation of organic substrates by cytochrome P-450, oxidation by peroxidases, oxidative halogenation by chloroperoxidases, and hydrogen peroxide dismutation by catalase.[8] The porphyrin macrocyclic ring system provides an ideal geometry for the efficient binding of square planar metals. It is the stability and versatility of the resulting metal complexes that makes the porphyrins such attractive biomimetic targets.

The development of catalytic systems effective at mediating enantioselective functional group transfer to olefins has evolved considerably in this decade. At present, reactions are availible with stereoselectivities at levels not long ago considered beyond the reach of non-enzymatic reactions. In general, the asymmetric transfer depends on substrates which bear specific functionality that directs the reactivity by precoordinating to the metal center, for example, carboxylates or hydroxyls. The development of oxidation reactions of olefinic substrates bearing no coordinating functionality will provide access to many useful organic synthons. This goal can be realized by using nonbonding

interactions, primarily steric effects. In this case, it is the ligand, not the metal center that is the critical player in the enantioselectivity. Primary examples include the salen-type ligands of Jacobsen and Katsuki **I**,[9-13] the dioxo-cyclam catalysts of Burrows **II**,[14-18] the semicorrin complexes of Pfaltz **III**[4] and the bis-oxazolines of Evans and Masamune **IV**.[19-21]

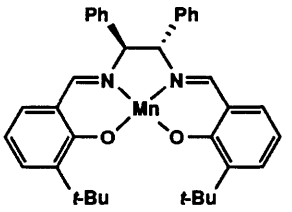

I

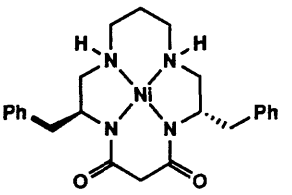

II

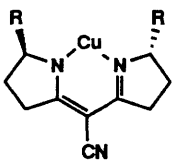

III

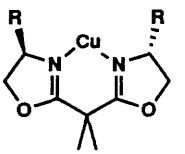

IV

The chiral salen-type manganese complexes **I** have been reported to epoxidize *cis*-olefins with the highest enantioselectivity to date. The authors suggest the advantages of the salen over the porphyrin system is two-fold: 1) The complexes bear the chirotopic carbon groups in the direct vicinity of the approaching olefin, resulting in better stereochemical communication in the epoxidation step. 2) The synthesis of the ligand is much simpler than that of the porphyrins and their steric properties can be modified in a more facile manner from the readily available synthons. On the other hand, it is difficult to introduce and systematically modify the chirality within porphyrin systems, and the known examples to date (Figure 1) require extensive synthesis.[22-25]

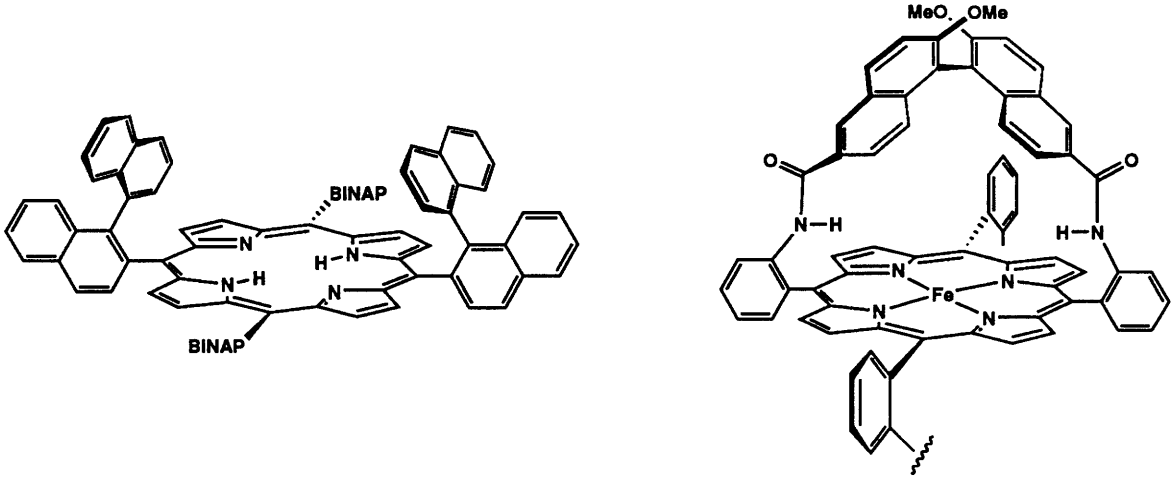

Figure 1. *Examples of asymmetric porphyrins include a BINAP-appended ligand*[25] *and Groves "vaulted" porphyrin complex.*[23]

7.2 Development of Novel Dioxazoline Ligands

The difficulty in modifying the chirality of the porphyrins prompted the development of a series of chiral *C2*-symmetric[26] bis(2-oxazoline) ligands of structure types **1** and **2** based on xanthene and carbazole derivatives. Molecular modeling of the xanthene-based ligands revealed an undesirable geometry of the metal coordination site. The oxazoline nitrogens are angled inwards, towards the ether oxygen, creating a less accessible and more trigonal cavity, not ideally suited for complexing square planar metals.

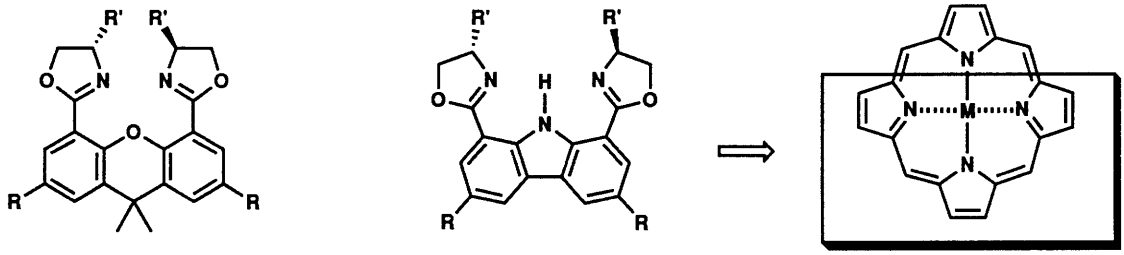

1 **2**

The carbazole skeleton **2** offers more desirable structural features and can be considered a "three-quarter" porphyrin. The central five membered pyrrole ring forces an

enlarging of the angle between the diacid functionality (~36 degrees), and suggests a geometry with the nitrogens positioned perfectly to satisfy three of the four sites necessary to complex square planar metals. Also, the modular design allows for facile introduction and modification of the chirality with regards to size and shape of appending groups.

The substituents at the stereogenic centers are positioned in close proximity to the approaching substrate by the rigid skeleton of the carbazole ligand. This effectively blocks two of the four sides of the catalyst (Figure 2). The result is that the enantiotopic face of the olefin substrate must approach the metal-oxo center from the less hindered side. It is expected that this restriction should have a salubrious effect on the stereochemical outcome of the reaction.

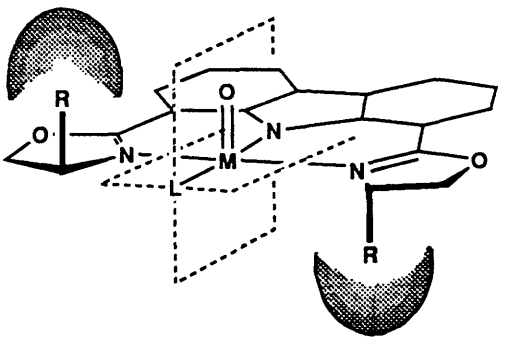

Figure 2. *The approach of an olefinic substrate towards the M=O site is reduced to two of the four quadrants outlined.*

Carbazole ligands **8a-d** were prepared in seven steps through a versatile, organic soluble diacid synthon **6** (Scheme 1). *N*-Benzylation of carbazole followed by Friedel-Crafts alkylation generated compound **4**. The *N*-benzyl protecting group was necessary to avoid a mixture of poly-*tert*-butyl isomers, a resulting reaction mixture that has been well documented.[27] The introduction of the *tert*-butyl groups was advantageous on three accounts. First, they provided organic solubility. They also directed subsequent substitution reactions at the 1,8-positions (adjacent to the carbazole nitrogen). Finally, they effectively blocked approach of the oxidizable substrate over the carbazole system, forcing

the olefin to be exposed to the chiral environment provided by the oxazolines. This substrate trajectory was previously shown for the Schiff base complexes of Jacobsen to be absolutely necessary for efficient stereochemical transfer.[9]

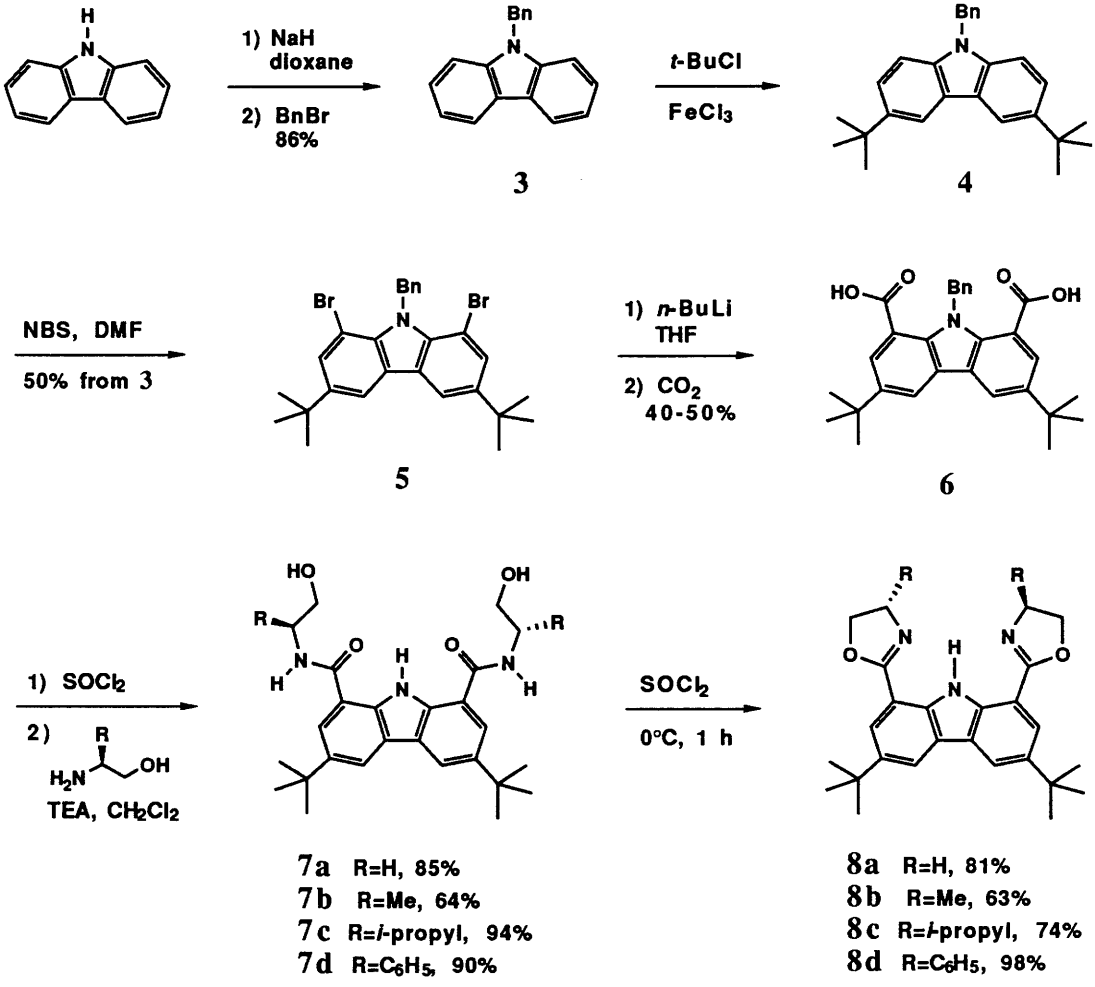

Scheme 1. *Synthesis of bis(2-oxazolines) based on carbazole.*

Attempts to brominate **4** under conditions involving Br_2 resulted in complete *N*-debenzylation due to the large quantities of HBr produced during the bromination. Attempts to neutralize the generated HBr by the addition of organic bases (pyridine, *tetra*-alkyamines) similarly yielded only *N*-deprotected carbazole. However, treating crude **4** under neutral bromination conditions (*N*-bromosuccinimide, *N*,*N*-dimethylformamide)[28]

generated *N*-benzyl-1,8-dibromo-3,6-di-*tert*-butylcarbazole **5**. The dibromide was converted to diacid **6** by quenching its lithium derivative with gaseous CO_2. It was unnecessary to remove the *N*-benzyl protecting group at this stage in a separate step; it was cleaved by the the HCl produced upon treating the diacid with excess thionyl chloride. Treatment of the resulting diacid chloride with chiral amino alcohols followed by thionyl chloride assisted cyclization afforded the chiral bis(2-oxazoline) ligands **8a-d**. It was essential to maintain the temperature below 0°C during the cyclization to avoid the documented HCl-assisted ring opening to the β-chloroamides (Scheme 2).[29,30]

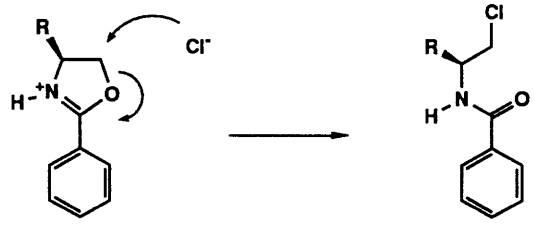

Scheme 2. *Cl^- ion-assisted ring opening of aryl 2-oxazolines.*

The chelating potential of the dioxazoline ligands **8a-d** was initially realized by ^1H NMR spectroscopy. The pyrrole N-H resonance was observed to be significantly further downfield than expected (11.6-11.9 ppm). This can be explained by the strong hydrogen bonding to the pyrazoline nitrogens or oxygens.

7.3 Nickel Catalyzed Epoxidations of Olefins[31,32]

Ligands **8a-d** formed stable nickel(II) complexes when alcoholic solutions of the ligands were heated gently with the metal acetate or acetylacetonate salts. Evaporation of the solvent furnished the nickel complexes which showed catalytic activity towards the epoxidation of both *cis*- and *trans*-β-methylstyrene in a sodium hypochlorite[33-36] two

phase system (Scheme 3). The catalysts showed no activity when iodosylbenzene (PhIO) was used as the oxidant.

Scheme 3. *Catalytic epoxidation of trans-β-methylstyrene with nickel(II) complexes of ligand 8.*

A solution of the complex and the styrene substrate was treated with commercial bleach (Clorox®) in the presence of a phase transfer catalyst (benzyltrimethylammonium chloride). Periodically, (every 15-30 minutes) aliquots were removed and analyzed by gas chromatography using chlorobenzene as an internal standard. After 30 minutes there was complete consumption of $^{-}$OCl, but large quantities of olefin were still present. An excess amount of terminal oxidant was required to completely consume the substrate, and bleach was continually added until no substrate was detected.

In general, disappearance of β-methylstyrene was observed after 3 hours for the *trans*-isomer and 6 hours for the *cis*. Only trace amounts of over-oxidized products were detected (epoxide:benzaldehyde ratios were 19:1) . There was no need for exclusion of O_2 to obtain high epoxide to benzaldehyde ratios (the dioxo-cyclam catalysts of Burrows produced ratios of ~3:1 when oxygen was present).[16] Also, *trans*-β-methylstyrene was consumed faster than the *cis*-isomer and the product of the oxidation was in both cases the *trans*-epoxide. This feature was observed for Burrows' cyclam catalysts, but the opposite was reported for the metalloporphyrin catalysts.[34,36,37]

The epoxide products were isolated by chromatography and analyzed for enantioselectivity by the use of a ^{1}H NMR chiral shift reagent (europium tris[3-(trifluoromethylhydroxymethylene)-(+)-camphorato]). In no case did either enantiomer predominate. This observation can be rationalized by examining similar results using the

dioxo-cyclam nickel complexes reported by Burrows and co-workers.[15] These authors concluded that the lack of stereochemical preference is due to the fact that the mechanism of nickel-catalyzed epoxidations proceeds through a radical intermediate (Figure 3). Of the four possible reaction pathways, the cationic and radical mechanisms **C** and **D** do not allow for enantioselectivity due to the rotational scrambling of these intermediates. Pathway **C** was ruled out from the results of radical quenching studies. The isolation of the *trans*-epoxide from the oxidation of *cis*-β-methylstyrene supported the radical pathway.

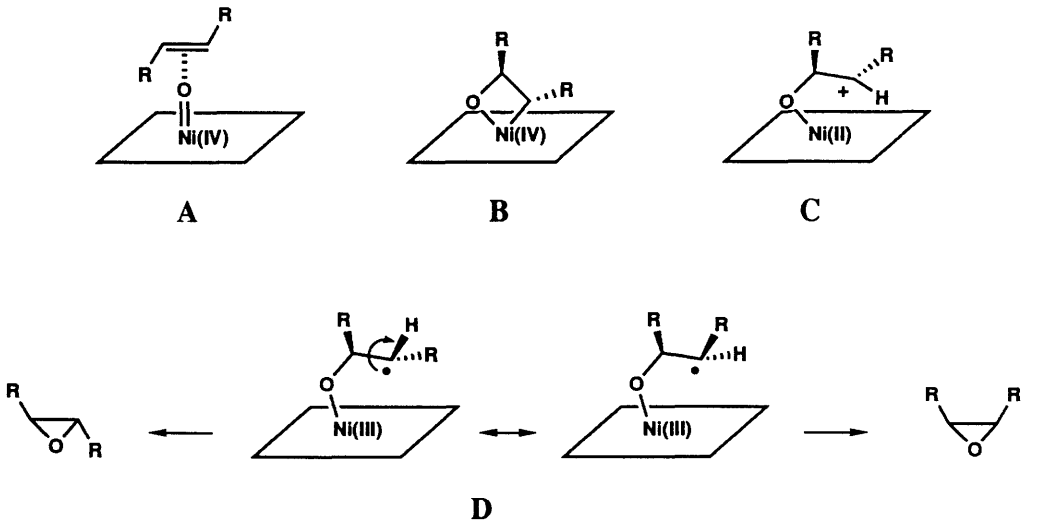

Figure 3. *Possible mechanisms for the nickel-catalyzed epoxidation reaction: a concerted oxygen atom transfer in a π complex **A**, oxa-metallocycle **B**. The radical and cationic pathways **C** and **D** involve a rotational scrambling step and erodes enantioselectivity.*

The synthesis of manganese(III) complexes of ligand **8** would overcome the scrambling problems of the nickel catalysts, because it has been speculated that epoxidations catalyzed by manganese(III) involve an intermediate with less radical character. Instead, a metal-oxo species of metal oxidation state five is the active intermediate which directly transfers an oxygen atom to the olefin in a concerted fashion. Initial progress towards preparing manganese complexes of the carbazole ligand **8** have been promising, although the stablility of the resulting catalysts is questionable. Catalysts

prepared *in situ* consumed ~17% of the olefin substrate in 8 hours (epoxide:benzaldehyde ratios were 8:1). After 20 hours significant quantities of over-oxidized products and decomposition were observed.

7.4 Development of a Xanthene-based Ligand

Other oxidation catalysts developed include the xanthene based diamine **13** (Scheme 4) which is an acyclic analogue of Burrows' dioxo-cyclams. Diphenylphosphoryl azide-assisted[38] modified Curtius-type rearrangement of diacid **9** followed by deprotection of the resulting benzyl carbamate generated diamine **11**. Acylating with Fmoc-protected valine acid chloride and removing the 9-fluorenylmethyl carbamate protecting groups afforded compound **13**.

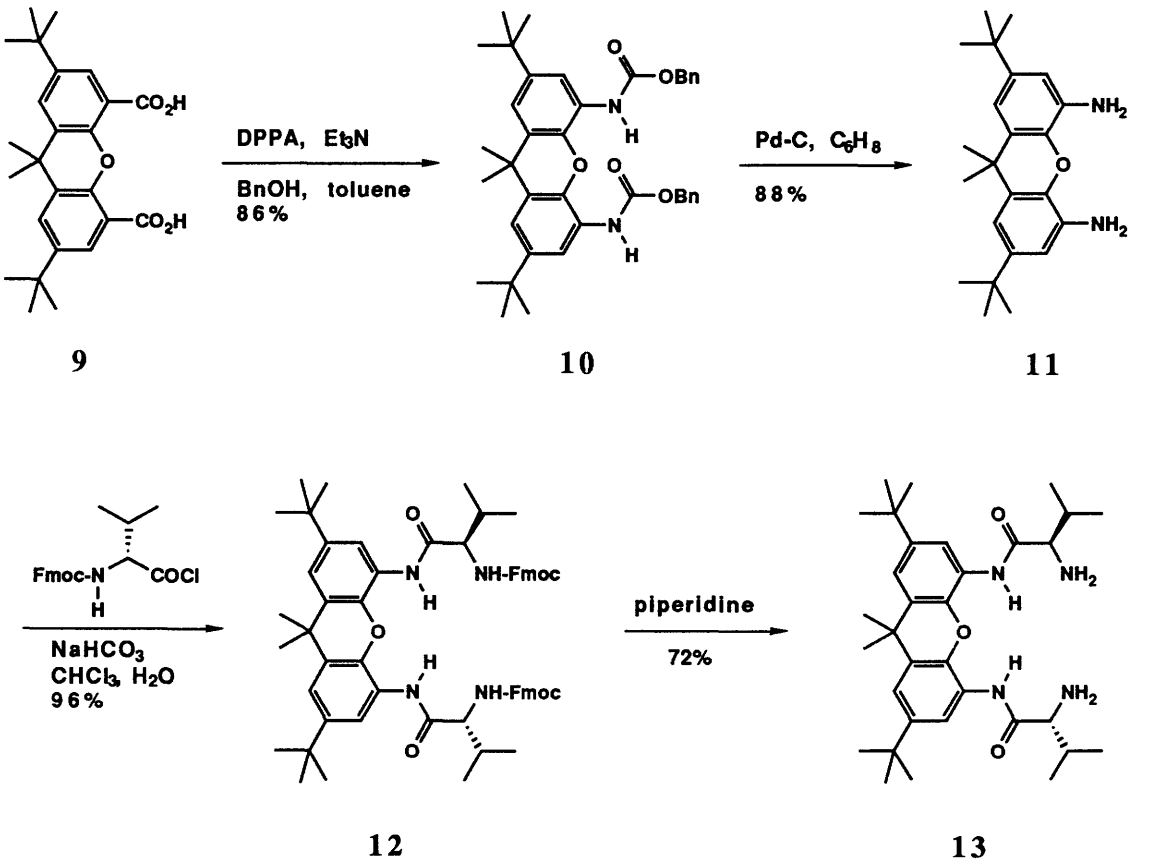

Scheme 4. *Synthesis of a xanthene-based dioxo-cyclam* ***13.***

The nickel(II) and copper(II) complexes of **13** were prepared by heating alcoholic solutions of the ligand with the metal acetate salts (Scheme 5). The two amide groups are deprotonated in the presence of metal salts affording neutral, organic soluble metal complexes. The nickel complex showed no activity in attempted epoxidation reactions of β-methylstyrene with NaOCl or iodosylbenzene as the terminal oxidant. This is most likely due to the distorted square planar geometry adopted by the complex which has been suggested to have no catalytic epoxidation properties.[39] The distortion was demonstrated by the NMR inactivity of the resulting paramagnetic complex and was supported by molecular modeling (CAChe, Tektronix, MM2 force field). If Burrows' catalyst "colour code" can be relied upon (yellow complexes are active, purple are inactive)[39] then it is not unexpected that the blue nickel complexes **14** show no epoxidation power (the yellow complexes of ligand **8** are active).

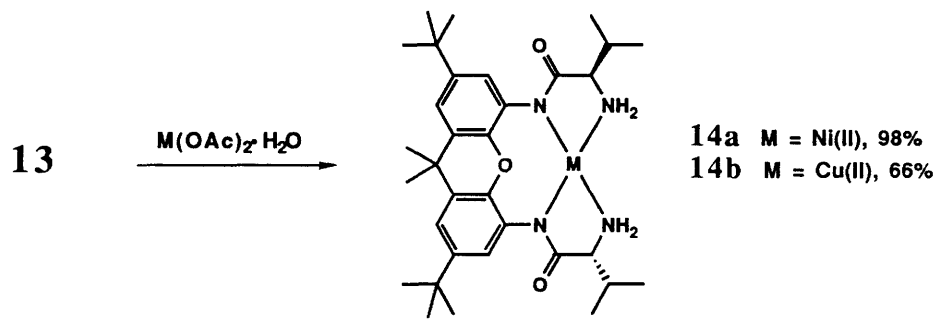

Scheme 5. *Preparation of the nickel(II) and copper(II) complexes of xanthene-based ligand* ***13***.

It should be noted that upon nitrating di-*tert*-butylxanthene **15** (Scheme 6), *ipso* substitution afforded a 4:5 ratio of products **16a** and **16b**. Catalytic reduction (H_2, Pd-C) of **16b** afforded the diamine.

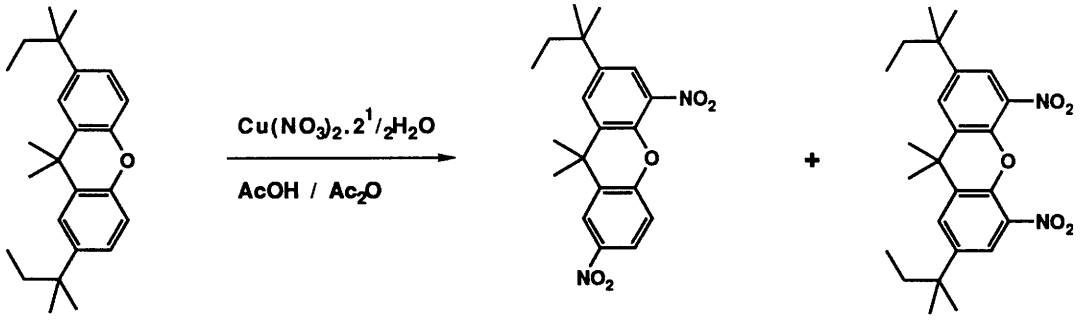

15 16a, 40% 16b, 50%

Scheme 6. *Nitration products of xanthene.*

7.5 Copper Catalyzed Cyclopropanations of Olefins

Another strategy towards efficient stereochemical communication of the chiral metal catalysts is to force a *trans*-olefin substrate to approach a metal active site buried deep within a chiral environment, resembling a canyon (Figure 4). In this geometric structure, the substrate is unconditionally exposed to a chiral *C-2* symmetric environment as it approaches the metal center on the "canyon floor". A reaction in which the reactive intermediate is buried deep within this canyon must be chosen to ensure the desired approach of the substrate. This type of geometry can be realized for metal complexes of ligand **8** if the approach of the substrate is perpendicular to the aromatic surface along the path outlined (**A**). One possibility is the copper catalyzed cyclopropanation of olefins with diazoacetic esters (**B**).

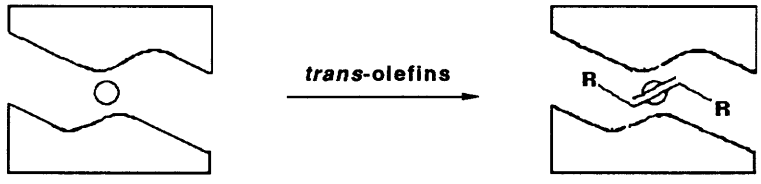

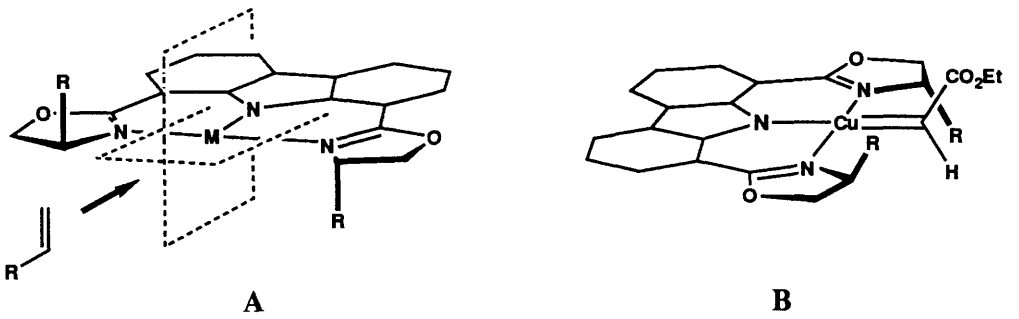

Figure 4. *A "canyon"-like catalyst selective for trans-olefins. Complexes of ligand 8 can be regarded as canyons if the substrate approaches the metal center as shown in A. The cyclopropanation intermediate B is one example.*

It is believed that the catalytic cycle begins with the reaction of the metal and the diazo compound to generate the metal-carbene complex **B**.[3,4,40] It is this complex that subsequently attacks the olefin. The stereochemical transfer results from blocking one face of the enantiotopic carbene carbon atom, forcing the olefin to approach from the less hindered side.

The copper(II) complexes of ligands **8a-d** were prepared by heating the ligands with copper acetate or acetyacetate salts in alcoholic medium. Copper(I) complexes were synthesized *in situ* from the readily prepared copper *tert*-butoxide salt.[41] In one case the metal complex was undesirable from the onset: the glycine-derived ligand **8a** formed a highly stable 2:1 complex with copper as visualized by the electron impact mass spectrum results. A proposed structure for this complex is pictured in figure 5. The stability of the structure was demonstrated by its being chemically inert to reductive conditions such as hydrazines. Dimers of this type have been reported previously for other dioxazoline ligands lacking appending groups.[42]

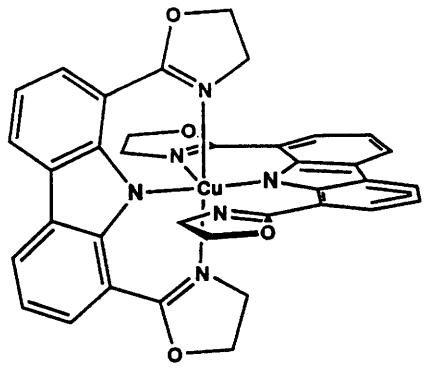

Figure 5. *Proposed dimeric structure of the copper complex of bis(2-oxazoline)* ***8a****. The tert-butyl groups have been omitted for clarity.*

The copper complexes derived from **8** were seen to be ineffective at cyclopropanating olefins such as styrene as evidenced from gas chromatographs of the reaction products. In all cases, unreacted styrene was the only detectable compound. The crystal structure of the bis(2-oxazoline) derived from valinol **8c** provides an explanation (Figure 6). The crystal structure reveals that the appending *iso*-propyl groups are "criss-crossed" over the active site of the metal (Figure 7). This feature blocks any carbene formation and would explain the poor results from the cyclopropanation reactions. This geometry prohibits the formation of a carbene complex in the plane of the carbazole backbone.

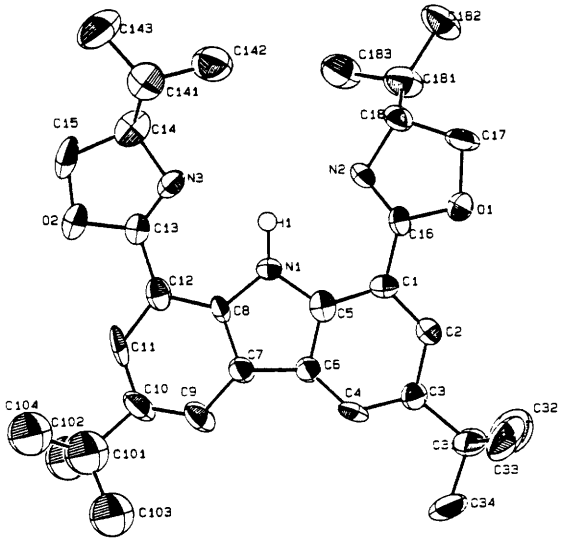

atom pair	distance (Å)
N2-N3	4.185
C141-C181	5.965
C142-C183	3.921
N1-N3	2.865
N1-N2	2.813

Figure 6. *X-ray crystal structure of carbazole ligand* ***8c****.*

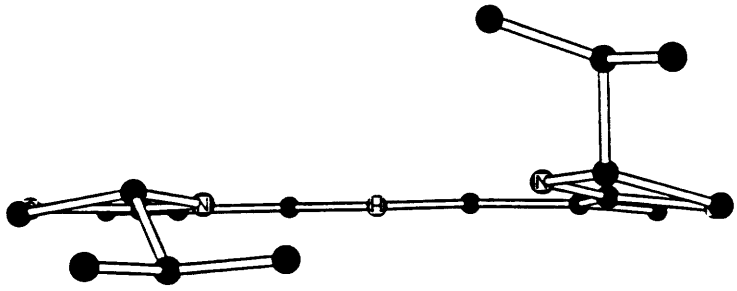

Figure 7. *X-ray structure of carbazole ligand* ***8c*** *looking down the N-H bond through the appending iso-propyl groups of the oxazolines. The structure indicates that there is inadequate space to form the intermediate of the cyclopropanation reaction (the distance between the methine carbon of these groups is ~5.97 Å).*

7.6 Conclusions

It has been shown that nickel complexes are not effective at stereochemical transfer in epoxidation reactions, although they are of unquestionable activity. These results confirm those reported by Burrows. In order to achieve enantioselectivity with the complexes at hand, a reaction involving an intermediate that does not behave as an electrophilic cabenoid must be chosen. One example is the nickel-catalyzed cyclopropanation of olefins via methylene transfer from lithiated *tert*-butyl methyl sulfone.[43]

Also, a balance exists between placing the stereogenic centers on the periphery of the ligand and too close to permit reaction. This must be taken into consideration when designing catalysts. Outlying appending groups may result in no stereochemical communication with the substrate, while those in close proximity may block any possible reaction.

7.7 Experimental

For a general description of apparatus, materials and methods, see chapter 2.

_N_-benzyl carbazole (3).

Carbazole (10 g, 60 mmol) and sodium hydride (1.8 g, 75 mmol) were heated to reflux in dioxane (100 mL) for 2 hours. The mixture was cooled to room temperature and benzyl bromide (10.7 mL, 90 mmol) was added in one portion. The suspension was stirred at 100°C for 2.5 h, cooled to room temperature and poured into ice water (1000 mL). The solid product was collected by vacuum filtration, washed with water then hexane and pump dried affording 13.3 g (86%) of **3** as a beige solid:

mp 122-123°C;

IR (KBr) 3048 (w), 3029 (w), 1595 (m), 1485 (m), 1403 (s), 1307 (s), 749 (s), 721 (s) cm^{-1};

^1H NMR ($CDCl_3$, 250 MHz) δ 8.13 (d, *J*=8.0 Hz, 2H), 7.46-7.13 (m, 11H), 5.52 (s, 2H).

_N_-Benzyl-3,6-di-*tert*-butylcarbazole (4).

$FeCl_3$ (1.26 g, 7.78 mmol) was added in portions over 15 minutes to a solution of *N*-benzylcarbazole (10.0 g, 38.9 mmol) and *tert*-butyl chloride (8.9 mL, 81.6 mmol) in dry CH_2Cl_2 (200 mL) at 0°C under argon. The ice bath was removed and the solution stirred at room temperature under argon for 24 h. The reaction was quenched with water (200 mL), extracted with CH_2Cl_2 (2x100 mL), dried over $MgSO_4$ and evaporated *in vacuo*. The resulting solid (14.65 g) was carried on without further purification:

^1H NMR ($CDCl_3$, 300 MHz) δ 8.13 (d, *J*=2.0 Hz, 2H), 7.46 (dd, *J*=8.0, 2.0 Hz, 2H), 7.26-7.16 (m, 7H), 5.43 (s, 2H), 1.45 (s, 18H).

_N_-Benzyl-1,8-dibromo-3,6-di-*tert*-butylcarbazole (5).

A solution of *N*-benzyl-3,6-di-*tert*-butylcarbazole **4** (13.40 g, 36.3 mmol) in DMF (100 mL) was added to a solution of NBS (13.55 g, 76.1 mmol) in DMF (100 mL). The

resulting mixture was stirred at room temperature for 22 h and poured into water (1 L). The solid was collected by vacuum filtration, dissolved in ether (300 mL), dried over $MgSO_4$ and evaporated. Purification by column chromatography through silica gel (hexanes) afforded 9.6 g (50% from *N*-benzyl carbazole) of **5** as a white solid:

mp 163-164°C;

IR (KBr) 3427 (m), 3134 (m), 3114 (m), 3066 (w), 3034 (w), 2962 (s), 1552 (m), 1449 (s) cm^{-1};

^1H NMR ($CDCl_3$, 250 MHz) δ 8.00 (d, *J*=2.0 Hz, 2H), 7.62 (d, *J*=2.0 Hz, 2H), 7.25-7.20 (m, 3H), 7.05-6.95 (m, 2H), 6.45 (s, 2H), 1.42 (s, 18H).

^{13}C NMR ($CDCl_3$) δ 144.6, 141.5, 138.5, 130.4, 128.3, 126.6, 126.1, 125.9, 115.36, 103.2, 47.9, 34.6, 31.8;

HRMS (EI) Calcd for $C_{27}H_{29}Br_2N$: 525.0667 Found: 525.0665.

_N_-Benzyl-3,6-di-*tert*-butylcarbazole-1,8-diacid (6).

Sec-butyl lithium (7.2 mL, 1.3 M in cyclohexane, 9.36 mmol) was added dropwise to a solution of *N*-benzyl-1,8-dibromo-3,6-di-*tert*-butylcarbazole **5** (1.64 g, 3.11 mmol) in dry THF (30 mL) at -78 °C under argon. After stirring at -78 °C for 45 minutes, dry CO_2 was bubbled through the resulting suspension for 45 minutes. The reaction was allowed to warm to room temperature and stirred for 15 h. The solution was cooled in ice, quenched with 5% HCl (15 mL) and brine (25 mL), extracted with THF (3x20 mL), dried over $MgSO_4$ and evaporated. The solid residue was washed with hexane to afford 1.24 g (87%) of **6** as a white solid:

mp >300°C;

IR (KBr) 3086 (m), 3064 (m), 3029 (m), 2961 (s), 2869 (m), 1683 (s), 1482 (s) cm^{-1};

^1H NMR (acetone-d_6, 300 MHz) δ 8.58 (d, *J*=2.0 Hz, 2H), 8.00 (d, *J*=2.0 Hz, 2H), 7.08-7.01 (m, 3H), 6.58-6.55 (m, 2H), 6.00 (s, 2H), 1.44 (s, 18H);

HRMS (EI) Calcd for $C_{29}H_{31}NO_4$: 457.2253 Found: 457.2257.

3,6-Di-*tert*-butylcarbazole-1,8-diacid.

Anhydrous HBr was bubbled through a solution of *N*-benzyl-3,6-di-*tert*-butylcarbazole-1,8-diacid **6** in $CHCl_3$ (15-20 mg/mL) for 15-30 min.. Evaporation of the solvent and crystallization from ether afforded the diacid as a white solid (78%):

mp >300°C;

IR (KBr) 3456 (m), 2961 (s) 2905 (s), 2570 (w), 1678 (s), 1596 (m), 1483 (s) cm^{-1};

^1H NMR (250 MHz, acetone-d_6) δ 11.07 (s, 1H), 8.64 (d, *J*=2.0 Hz, 2H), 8.22 (d, *J*=2.0 Hz, 2H), 1.47 (s, 18H).

MS (EI) Calcd for $C_{22}H_{25}NO_4$: 367.4 Found: 367.1.

3,6-Di-*tert*-butylcarbazole-1,8-diacid Chloride.

A solution of 3,6-di-*tert*-butylcarbazole-1,8-diacid **6** (570 mg, 1.25 mmol) was refluxed in thionyl chloride for 3 h. Excess thionyl chloride was evaporated under reduced pressure. The residue was suspended in dry toluene and the solvent evaporated *in vacuo* yielding 495 mg (98%) of the product as a white solid:

mp >300°C;

IR (KBr) 3434 (m), 2960 (m), 2907 (w), 2868 (w), 1734 (s), 1583 (m), 1485 (s) cm^{-1};

^1H NMR (250 MHz, $CDCl_3$) δ 10.86 (s, 1H), 8.45 (d, *J*=2.0 Hz, 2H), 8.39 (d, *J*=2.0 Hz, 2H), 1.52 (s, 18H).

General Coupling Procedure of 3,6-Di-*tert*-butylcarbazole-1,8-diacid Chloride with Chiral Amino Alcohols.

A solution of 3,6-di-*tert*-butylcarbazole-1,8-diacid chloride in dry CH_2Cl_2 (50-150 mM) was treated with a solution of the appropriate amino alcohol (2 equiv) and triethyl amine (2 equiv) in 1-2 mL dry CH_2Cl_2. The reaction was stirred under argon overnight and evaporated to dryness under reduced pressure. The solid residue was triturated with 1N

HCl, washed with water and dried *in vacuo* affording the amide alcohols as cream-coloured solids. All amide alcohols were carried on without further purification:

3,6-Di-*tert*-butyl-bis[*N*-(2-hydroxyethyl)]carbazole-1,8-dicarboxamide (7a).

85% yield;

^{1}H NMR ($CDCl_3$/DMSO-d_6, 250 MHz) δ 11.43 (br s, 1H), 8.21 (s, 2H), 7.84-7.82 (m, 4H), 3.83-3.79 (m, 4H), 3.69-3.65 (m, 4H), 1.48 (s, 18H).

3,6-Di-*tert*-butyl-bis[*N*-((S)-2-hydroxy-1-methylethyl)]carbazole-1,8-dicarboxamide (7b).

64% yield;

mp 235-236°C;

IR (KBr) 3438 (s), 3351 (m), 2957 (s), 1590 (s), 1530 (m) cm^{-1};

^{1}H NMR (300 MHz, $CDCl_3$) δ 11.11 (s, 1H), 8.17 (d, *J*=2.0 Hz, 2H), 7.59 (d, *J*=2.0 Hz, 2H), 6.60 (d, *J*=7.0 Hz, 2H), 4.50-4.30 (m, 2H), 3.91 (dd, *J*=8.0 Hz, 2H), 3.77 (dd, *J*=6.0 Hz, 2H), 1.43 (s, 18H), 1.38 (d, *J*=7.0 Hz, 6H).

3,6-Di-*tert*-butyl-bis[*N*-((S)-2-hydroxy-1-*iso*-propylethyl)]carbazole-1,8-dicarboxamide (7c).

94% yield;

mp 145-146°C;

IR (KBr) 3444 (s), 3337 (m), 2960 (s), 1633 (s), 1590 (s), 1529 (s), 1488 (m) cm^{-1};

^{1}H NMR ($CDCl_3$, 300 MHz) δ 10.90 (br s, 1H), 8.02 (d, *J*=2.0 Hz, 2H), 7.57 (d, *J*=2.0 Hz, 2H), 6.92 (d, *J*=9.0 Hz, 2H), 4.15-4.13 (m, 2H), 4.00-3.89 (m, 4H), 2.15-2.00 (m, 2H), 1.35 (s, 18H), 1.09 (dd, *J*=7.0, 1.0 Hz, 12H).

3,6-Di-*tert*-butyl-bis[N-((S)-2-hydroxy-1-phenylethyl)]carbazole-1,8-dicarboxamide (7d).

90% yield;

mp 155-156°C;

IR (KBr) 3335 (m), 3317 (m), 2957 (s), 1641 (s), 1590 (s), 1527 (s) cm^{-1};

^1H NMR ($CDCl_3$, 250 MHz) δ 11.00 (br s, 1H), 8.01 (d, *J*=2.0 Hz, 2H), 7.59 (d, *J*=2.0 Hz, 2H), 7.48-7.27 (m, 10H), 5.50-5.40 (m, 2H), 4.10 (d, *J*=5.0 Hz, 4H), 1.33 (s, 18H).

General Cyclization Procedure.

Solutions of the amide alcohols **7a-7d** in dry CH_2Cl_2 (10-50 mM) at 0°C were treated with thionyl chloride (20 equiv) for 45-60 minutes under argon. The reaction was quenched with cold $NaHCO_3$, extracted with CH_2Cl_2, dried over Na_2SO_4 and evaporated. Purification through a short column of silica gel (5% MeOH/chloroform) afforded the dioxazolines as cream-coloured solids. The glycinol derived oxazoline **8a** was purified by dissolving the crude in ether, filtering any impurities and evaporating the solvent:

3,6-Di-*tert*-butylcarbazole-1,8-bis(2-oxazoline) (8a).

81% yield;

mp 260-262°C;

IR (KBr) 3385 (m), 2959 (s), 2904 (m), 2870 (m), 1646 (s), 1621 (s), 1489 (s), 1463 (m) cm^{-1};

^1H NMR ($CDCl_3$, 250 MHz) δ 11.47 (br s, 1H), 8.25 (d, *J*=2.0 Hz, 2H), 8.00 (d, *J*=2.0 Hz, 2H), 4.48 (dd, *J*=14.0, 5.0 Hz, 2H), 4.41 (dd, *J*=14.0, 5.0 Hz, 2H), 1.48 (s, 18H); MS (EI) Calcd for $C_{26}H_{31}N_3O_2$: 417.8 Found: 417.6.

3,6-Di-*tert*-butylcarbazole-1,8-bis[(S)-5-methyl-2-oxazoline] (8b).

63% yield;

mp 130-135°C;

IR (KBr) 3393 (m), 3366 (m), 2962 (s), 2900 (m), 2361 (w), 1647 (s), 1620 (s), 1488 (s) cm^{-1};

^1H NMR ($CDCl_3$, 250 MHz) δ 11.59 (br s, 1H), 8.22 (d, *J*=2.0 Hz, 2H), 7.97 (d, *J*=2.0 Hz, 2H), 4.65-4.52 (m, 4H), 4.04-3.98 (m, 2H), 1.49-1.44 (m, 24H);

MS (EI) Calcd for $C_{28}H_{35}N_3O_2$ $[M+H]^+$: 446.6 Found: 446.4.

3,6-Di-*tert*-butylcarbazole-1,8-bis[(S)-5-*iso*-propyl-2-oxazoline] (8c):

74% yield;

mp 118-120°C;

IR (KBr) 3351 (w), 2959 (s), 2903 (s), 2871 (m), 1648 (s), 1622 (m), 1488 (s) cm^{-1};

^1H NMR ($CDCl_3$, 250 MHz) δ 11.88 (br s, 1H), 8.22 (d, *J*=2.0 Hz, 2H), 7.95 (d, *J*=2.0 Hz, 2H), 4.50-4.40 (m, 2H), 4.25-4.10 (m, 4H), 1.95-1.87 (m, 2H), 1.47 (s, 18H), 1.08 (dd, *J*=33.0, 7.0 Hz, 12H);

^{13}C NMR ($CDCl_3$) δ 162.7, 141.5, 137.6, 123.4, 123.2, 119.7, 109.7, 72.9, 69.8, 33.4, 32.0, 19.2, 18.7;

MS (EI) Calcd for $C_{32}H_{43}N_3O_2$: 501.7 Found: 501.9.

3,6-Di-*tert*-butylcarbazole-1,8-bis[(S)-5-phenyl-2-oxazoline] (8d):

98% yield;

mp 120-122°C;

IR (KBr) 3363 (w), 2960 (s), 2901 (m), 2867 (w), 1645 (s), 1619 (m), 1603 (m), 1488 (s) cm^{-1};

^{1}H NMR ($CDCl_3$, 300 MHz) δ 11.84 (br s, 1H), 8.27 (d, *J*=2.0 Hz, 2H), 8.03 (d, *J*=2.0 Hz, 2H), 7.39-7.23 (m, 10H), 5.55-5.45 (m, 2H), 4.86 (dd, *J*=10.0, 8.0 Hz, 2H), 4.30 (dd, *J*=8.0, 8.0 Hz, 2H), 1.49 (s, 18H);

MS (EI) Calcd for $C_{38}H_{39}N_3O_2$: 569.8 Found: 569.9.

General Metal Complexation Procedure.

The carbazole dioxazoline **8** and 1 equivalent $Ni(OAc)_2 \cdot 4H_2O$ were heated to reflux in methanol or ethanol (0.03 M) for 30-60 min. A bright green-yellow solution was seen immediately. The solvent was evaporated under reduced pressure and the green-yellow powder pump dried.

3,6-Di-*tert*-butylcarbazole-1,8-bis[(S)-5-methyl-2-oxazoline] Nickel Complex.

Prepared as decribed above from ligand **8b** and used for the catalytic reactions without further purification.

^{1}H NMR ($CDCl_3$, 300 MHz) δ 8.50 (s, 2H), 7.92 (s, 2H), 4.50-4.35 (m, 6H), 1.45 (s, 24H).

^{13}C NMR ($CDCl_3$) δ 168.8, 148.0, 141.0, 130.5, 122.1, 120.8, 106.2, 70.5, 70.0, 32.2, 31.3, 19.4, 14.3.

3,6-Di-*tert*-butylcarbazole-1,8-bis[(S)-5-*iso*-propyl-2-oxazoline] Nickel Complex.

Prepared in quantitiative yield as decribed above from ligand **8c** and used for the catalytic reactions without further purification.

^{1}H NMR ($CDCl_3$, 250 MHz) δ 8.62 (s, 2H), 7.93 (s, 2H), 4.67-4.35 (m, 6H), 2.57 (br m, 2H), 1.47 (s, 18H), 0.85 (dd, *J*=45.0, 5.0 Hz, 12H).

General Epoxidation Procedure.

A solution of 165 μL of 0.05M Na_2HPO_4 and 411 μL of 0.7M Clorox© bleach was adjusted to pH 11.5 with 1N NaOH. The nickel complexes (0.6 M in CH_2Cl_2), β-methylstyrene (0.25 mmol) and benzyltrimethylammonium chloride (0.08 mmol) were added. The reaction mixture was stirred vigorously at room temperature, and aliquots were periodically removed, filtered through a small plug of silica, and analyzed by GC (silicate column, T_1=100°C, T_2=250 °C, t_1=2 min., rate=10 °C/min., flow=60-61 Helium). Equivalent amounts of Na_2HPO_4 and Clorox© were added every 30 minutes until the complete disappearance of olefin was seen. The reaction mixture was extracted with hexane, dried over Na_2SO_4, evaporated and the residue NMR analyzed with tris[3-(heptafluoropropylhydroxymethylene)-(+)-camphorato] europium chiral-shift reagent.

3,6-Di-*tert*-butylcarbazole-1,8-bis(2-oxazoline) Copper Complex.

A solution of the ligand **8a** in THF was treated with *n*-butyl lithium (1 equivalent) at -78°C. After stirring at this temperature for 15 minutes, $CuCl_2$ (1 equivalent) was added. The reaction was stirred for 1 hour. Purification by column chromatography through silica gel (5% MeOH/CH_2Cl_2) afforded the product as a green-brown solid:

IR (KBr) 3624 (m), 2957 (s), 1643 (s), 1612 (m), 1465 (s), 1431 (s) cm^{-1};

MS (EI) Calcd for $C_{52}H_{60}N_6O_4Cu$ [M+H$^+$]: 896.3 Found: 896.1.

2,7-Di-*tert*-butyl-9,9-dimethylxanthene-4,5-bis[benzyloxycarbamate] (10).

2,7-Di-*tert*-butyl-9,9-dimethylxanthene-4,5-diacid **9** (1.0 g, 2.44 mmol), triethylamine (854 μL, 6.08 mmol), benzyl alcohol (630 μL, 6.08 mmol) and diphenylphosphoryl azide (1.31 mL, 6.08 mmol) were heated to reflux in dry toluene (25 mL) under $CaCl_2$ drying tube for 4 h. Evaporation under reduced pressure and purification by column chromatography through silica gel (10% EtOAc/hexanes) afforded 1.3 g (86%) of **10** as a yellow solid:

mp 197-198°C;

IR (KBr) 3330 (s), 3241 (m), 2961 (s), 2937 (m), 1741 (s), 1689 (s), 1623 (m), 1540 (s) cm^{-1};

^1H NMR ($CDCl_3$, 250 MHz) δ 7.77 (br s, 2H), 7.34-7.26 (m, 12H), 7.16 (d, *J*=2.0 Hz, 1H), 5.16 (s, 4H), 1.61 (s, 6H), 1.32 (s, 18H);

^{13}C NMR ($CDCl_3$) δ 155.6, 146.0, 145.4, 138.6, 136.0, 129.8, 128.2, 127.5, 124.8, 117.5, 117.0, 116.7, 67.1, 34.9, 34.7, 31.8, 31.5;

HRMS (EI) Calcd for $C_{39}H_{44}N_2O_5$: 620.3250 Found: 620.3254.

4,5-Diamino-2,7-di-*tert*-butyl-9,9-dimethylxanthene (11).

2,7-Di-*tert*-butyl-9,9-dimethylxanthene-4,5-bis[benzylcarbamate] **10** (1.2 g, 1.93 mmol), Pd-C (450 mg 10%) and cyclohexadiene (915 μL, 9.67 mmol) in ethanol (50 mL) were heated to reflux for 1 h. Filtration through Celite and evaporation under reduced pressure afforded 600 mg (88%) of the free diamine as a cream-coloured solid which was carried on without further purification. Analytical samples were recrystallized from ethanol:

mp 193-194°C;

IR (KBr) 3426 (w), 3351 (m), 3204 (s), 2964 (m), 2903 (m), 1631 (s), 1513 (m), 1487 (s) cm^{-1};

^1H NMR ($CDCl_3$, 250 MHz) δ 6.84 (d, *J*=2.0 Hz, 2H), 6.69 (d, *J*=2.0 Hz, 2H), 3.81 (br s, 4H), 1.61 (s, 6H), 1.30 (s, 18H);

^{13}C NMR ($CDCl_3$) δ 145.5, 136.6, 133.5, 129.7, 112.5, 111.1, 34.6, 34.4, 32.0, 31.5;

MS (EI) Calcd for $C_{23}H_{32}N_2O$: 352.5 Found: 352.2.

2,7-Di-*tert*-butyl-9,9-dimethylxanthene-4,5-bis[(S)-Fmoc-valine] (12).

A solution of 4,5-diamino-2,7-di-*tert*-butyl-9,9-dimethylxanthene **11** (1.45 g, 4.11 mmol) in CH_2Cl_2 (120 mL) was added to a solution of $NaHCO_3$ (8.4 g) in 90 mL water. (S)-Fmoc-valyl chloride (2.96 g, 8.22 mmol) was added in one portion and the reaction stirred

vigorously for 30 minutes. The organic layer was removed, washed with water, dried over Na_2SO_4 and evaporated under reduced pressure yielding 3.91 g (96%) of **12** as a beige solid which was carried on without further purification:

^1H NMR ($CDCl_3$, 250 MHz) δ 8.92 (br s, 2H), 8.02 (d, *J*=3.0 Hz, 2H), 7.69 (dd, *J*=7.0, 3.0 Hz, 4H), 7.48 (dd, *J*=7.0, 3.0 Hz, 4H), 7.36-7.16 (m, 10H), 5.51 (d, *J*=9.0 Hz, 2H), 4.45-4.26 (m, 6H), 4.15-4.09 (m, 2H), 2.25-2.10 (m, 2H), 1.58 (s, 6H), 1.34 (s, 18H), 1.03 (dd, *J*=6.0, 4.0 Hz, 12H).

2,7-Di-*tert*-butyl-9,9-dimethylxanthene-4,5-bis[(S)-valylamide] (13).

2,7-Di-*tert*-butyl-9,9-dimethylxanthene-4,5-bis[(S)-Fmoc-valine] **12** (3.9 g) was deprotected by stirring in piperidine (25 mL) for 2 h at room temperature. The resulting solution was poured into water (200 mL), extracted with ether (2x100 mL), dried over Na_2SO_4 and evaporated under reduced pressure. Purification by column chromatography through silica gel (10% MeOH/$CHCl_3$) yielded 1.64 g (72% from diamine **11**) as a cream-coloured solid:

mp 202-203°C;

$[\alpha]_D$=-20.35°;

IR (KBr) 3375 (w), 3306 (m), 2960 (s), 2905 (m), 1699 (s), 1695 (s), 1685 (s), 1553 (m), 1625 (s), 1545 (s), 1521 (s), 1507 (s) cm^{-1};

^1H NMR ($CDCl_3$, 300 MHz) δ 8.24 (br s, 2H), 8.38 (d, *J*=2.0 Hz, 2H), 7.19 (d, *J*=2.0 Hz, 2H), 3.40 (d, *J*=5.0 Hz, 2H), 2.40-2.30 (m, 2H), 1.75 (br s, 4H), 1.64 (s, 6H), 1.35 (s, 18H), 1.03 (dd, *J*=31.0, 7.0 Hz, 12H);

^{13}C NMR ($CDCl_3$) δ 172.5, 146.0, 137.3, 129.1, 125.0, 117.7, 116.2, 61.78, 34.7, 34.6, 32.4, 31.4, 19.9, 17.0;

MS (EI) Calcd for $C_{33}H_{50}N_4O_3$ [M+H]: 551.8 Found: 551.6.

2,7-Di-*tert*-butyl-9,9-dimethylxanthene-4,5-bis[(S)-valylamide] Nickel Complex (14a).

2,7-Di-*tert*-butyl-9,9-dimethylxanthene-4,5-bis[(S)-valylamide] **13** (100 mg, 0.182 mmol) and $Ni(OAc)_2 \cdot 4H_2O$ (45 mg, 0.182 mmol) were heated to reflux in methanol (5 mL) for 30 minutes. The hot light blue solution was treated with ether to initiate precipitation and cooled to -5°C. The metal complex was collected by vacuum filtration as a pale blue powder (108 mg, 98%):

IR (KBr) 3277 (s), 2963 (s), 2909 (s), 2873 (m), 1690 (m), 1623 (s), 1576 (s), 1544 (s), 1431 (s) cm^{-1};

MS (EI) Calcd for $C_{33}H_{48}N_4O_3$: 607.5 Found: 607.2.

2,7-Di-*tert*-butyl-9,9-dimethylxanthene-4,5-bis[(S)-valylamide] Copper Complex (14b).

2,7-Di-*tert*-butyl-9,9-dimethylxanthene-4,5-bis[(S)-valylamide] **13** (100 mg, 0.182 mmol) and $Cu(OAc)_2 \cdot H_2O$ (22 mg, 0.182 mmol) were heated in refluxing ethanol (5 mL) for 1 h. The colour of the solution immediately turned dark green. The solvent was evaporated under reduced pressure, the residue taken up in minimal THF, and the product was precipitated by the addition of hexanes at -5°C. The metal complex was collected by vacuum filtration as a dark green powder (75 mg, 66%):

IR (KBr) 3327 (m), 3236 (m), 2962 (s), 2907 (m), 1684 (m), 1591 (s), 1559 (s), 1544 (s), 1435 (s);

MS (EI) Calc for $C_{33}H_{48}N_4O_3Cu$ $[M+H]^+$: 613 Found: 613.4.

2-*Tert*-Amyl-4,7-dinitro-9,9-dimethylxanthene (16a).

Copper nitrate (1.33 g, 5.74 mmol) was dissolved in a solution of AcOH (1.7 mL) and Ac_2O (3 mL) at 30°C. 2,7-Di-*tert*-amyl-9,9-dimethylxanthene (1.0 g, 2.85 mmol) was added in portions over 15 minutes. After stirring at 30°C for 3.5 h, the reaction was

poured into water (50 mL). The solid product was filtered, washed with water and dried in vacuo affording 1.23 g (98%) of a mixture of **16a** and **16b** in a 4:5 ratio. Purification by column chromatography through silica gel (5% EtOAc/hexanes) afforded **16a** (40%) as a pale yellow solid:

^{1}H NMR ($CDCl_3$, 300 MHz) δ 8.38 (d, *J*=2.0 Hz, 1H), 8.16 (d, *J*=2.0 Hz, 1H), 8.16 (dd, *J*=9.3, 2.0 Hz, 1H), 7.75 (d, *J*=2.0 Hz, 1H), 7.61 (d, *J*=2.0 Hz, 1H), 7.28, (d, *J*=9.3 Hz, 1H), 1.70 (m, 8H), 1.35 (s, 6H), 0.70 (m, 3H).

2,7-Di-*tert*-amyl-4,5-dinitro-9,9-dimethylxanthene (16b).

The product was isolated from the reaction described above (650 mg, 52%) as a pale yellow solid:

^{1}H NMR ($CDCl_3$, 300 MHz) δ 7.72 (d, *J*=1.9 Hz, 2H), 7.59 (d, *J*=2.0 Hz, 2H), 1.70 (m, 10H), 1.35 (s, 12H), 0.70 (m, 6H).

^{13}C NMR ($CDCl_3$) δ 145.52, 140.05, 138.73, 131.63, 127.62, 121.36, 38.14, 36.71, 35.12, 32.10, 28.26, 9.02.

X-ray Crystallography

Crystal data was collected using a Rigaku AFC6R diffractometer and solved using Texsan-Texray Structure Analysis Package.

3,6-Di-*tert*-butylcarbazole-1,8-bis[(S)-5-*iso*-propyl-2-oxazoline] (8c).

Crystal data: $C_{32}H_{31}N_3O_2$, formula weight 489.62, colourless orthorhombic parallelpiped crystals, 0.28 x 0.24 x 0.18 mm, space group $P2_12_12_1$, a = 12.120(1), b = 13.289(1), c = 19.006(2) Å, V = 3061(8) Å^3, D_{calc} = 1.062 g/cm^3, Z = 4, μ(MoKα) = 0.62 cm^{-1}, T = 23°C.

The crystals were stable at room temperature. A total of 7893 reflections were measured in ω-2θ scan mode (scan width (ω) 0.80 + 0.35 tanθ) at a rate of 1.9-

16.5°/minutes, of which 3945 were unique. The structure was solved by direct methods and refined with full-matrix least-squares methods. The final R factors were 10.1% and Rw = 12.2%. The structure suffered from poor data quality. While the integrity, read connectivity, is not compromised, as well as the gross structural characteristics, the fine structural details should be viewed with some discretion. The probable cause of this problem is in the disorder of one of the *tert*-butyl groups. For atom coordinates, see appendix 5.

References and Notes

(1) Noyori, R. *Chem. Soc. Rev.* **1989**, *18*, 187-208.

(2) Noyori, R. *Science* **1990**, *248*, 1194-1199.

(3) Doyle, M. P. *Chem. Rev.* **1986**, *86*, 919-936.

(4) Pfaltz, A. *Modern Synthetic Methods* **1989**, *5*, 199-248.

(5) Ojima, I.; Clos, N.; Bastos, C. *Tetrahedron* **1989**, *45*, 6901-6939.

(6) Finn, M. G.; Sharpless, K. B. In *Asymmetric Synthesis: Chiral Catalysts*; Morrison, J. D., Ed.; Academic Press: Orlando, 1985; Vol 5, pp 247-308.

(7) Meunier, B. *Chem. Rev.* **1992**, *92*, 1411-1456.

(8) Chance, B.; Estabrook, R. W.; Yonetan, T. *Hemes and Hemoproteins* Academic Press: New York, 1966.

(9) Zhang, W.; Loebach, J. L.; Wilson, S. R.; Jacobsen, E. N. *J. Am. Chem. Soc.* **1990**, *112*, 2801-2803.

(10) Zhang, W.; Lee, N. H.; Jacobsen, E. N. *J. Am. Chem. Soc.* **1994**, *116*, 425-426.

(11) Irie, R.; Noda, K.; Matsumoto, N.; Katsuki, T. *Tetrahedron Lett.* **1990**, *31*, 7345-7348.

(12) Irie, R.; Noda, K.; Ito, Y.; Katsuki, T. *Tetrahedron Lett.* **1991**, *32*, 1055-1058.

(13) Irie, R.; Ito, Y.; Katsuki, T. *Synlett* **1991**, 265-266.

(14) Kinneary, J. F.; Wagler, T. R.; Burrows, C. J. *Tetrahedron Lett.* **1988**, *29*, 877-880.

(15) Kinneary, J. F.; Albert, J. S.; Burrows, C. J. *J. Am. Chem. Soc.* **1988**, *110*, 6124-6129.

(16) Wagler, T. R.; Burrows, C. J. *Tetrahedron Lett.* **1988**, *29*, 5091-5094.

(17) Wagler, T. R.; Fang, Y.; Burrows, C. J. *J. Org. Chem.* **1989**, *54*, 1584-1589.

(18) Yoon, H.; Wagler, T. R.; O'Connor, K. J.; Burrows, C. J. *J. Am. Chem. Soc.* **1990**, *112*, 4568-4570.

(19) Lowenthal, R. E.; Abiko, A.; Masamune, S. *Tetrahedron Lett.* **1990**, *31*, 6005-6008.

(20) Lowenthal, R. E.; Masamune, S. *Tetrahedron Lett.* **1991**, *32*, 7373-7376.

(21) Evans, D. A.; Woerpel, K. A.; Hinman, M. M.; Faul, M. M. *J. Am. Chem. Soc.* **1991**, *113*, 726-728.

(22) Groves, J. T.; Viski, P. *J. Am. Chem. Soc.* **1989**, *111*, 8537-8538.

(23) Groves, J. T.; Visli, P. *J. Org. Chem.* **1990**, *55*, 3628-3634.

(24) Bolm, C.; Zehnder, M.; Bur, D. *Angew. Chem. Int. Ed. Engl.* **1990**, *29*, 205-207.

(25) Bolm, C. *Angew. Chem. Int. Ed. Engl.* **1991**, *30*, 403-404.

(26) For a review on *C2*-symmetry and chiral induction, see: Whitesell, J. K. *Chem. Rev.* **1989**, *89*, 1581-1590.

(27) Neugebauer, F. A.; Fischer, H. *Chem. Ber.* **1972**, *105*, 2686-2693.

(28) Mitchell, R. H.; Lai, Y.; Williams, R. V. *J. Org. Chem.* **1979**, *44*, 4733-4735.

(29) Fry, E. M. *J. Org. Chem.* **1949**, *14*, 887-894.

(30) For reviews on oxazolines, see: Frump, J. A. *Chem. Rev.* **1971**, *71*, 483-505. Meyers, A. I.; Mihelich, E. D. *Angew. Chem. Int. Ed. Engl.* **1976**, *15*, 270-281. Reuman, M.; Meyers, A. I. *Tetrahedron* **1985**, *41*, 837-860.

(31) Koola, J. D.; Kochi, J. K. *Inorg. Chem.* **1987**, *26*, 908-916.

(32) Jørgensen, K. A. *Chem. Rev.* **1989**, *89*, 431-458.

(33) Krishnan, S.; Kuhn, D. G.; Hamilton, G. A. *J. Am. Chem. Soc.* **1977**, *99*, 8121-8123.

(34) Guilmet, E.; Meunier, B. *Tetrahedron Lett.* **1982**, *23*, 2449-2452.

(35) Fonouni, H. E.; Krishnan, S.; Kuhn, D. G.; Hamilton, G. A. *J. Am. Chem. Soc.* **1983**, *105*, 7672-7676.

(36) Meunier, B.; Guilmet, E.; De Carvalho, M.; Poilblanc, R. *J. Am. Chem. Soc.* **1984**, *106*, 6668-6675.

(37) Guilmet, E.; Meunier, B. *Tetrahedron Lett.* **1980**, *21*, 4449-4450.

(38) Shioiri, T.; Nimomiya, K.; Yamada, S.-I. *J. Am. Chem. Soc.* **1972**, *94*, 6203-6204.

(39) Burrows, C. J. In *Inclusion Phenomena and Molecular Recognition*; Atwood, J. L., Ed., Plenum Press: New York, 1990, pp 199-207.

(40) Aratani, T.; Yoneyoshi, Y.; Nagase, T. *Tetrahedron Lett.* **1982**, *23*, 685-688.

(41) Tsuda, T.; Hashimoto, T.; Saegusa, T. *J. Am. Chem. Soc.* **1972**, *94*, 658-659.

(42) Masamune, S., private comunication.

(43) Gai, Y.; Julia, M.; Verpeaux, J. *Synlett* **1991**, 56-57.

Appendix 1

X-ray Crystalography: Atom Coordinates

Methanetricarboxamide (Part I, Chapter 1.2, structure 1).

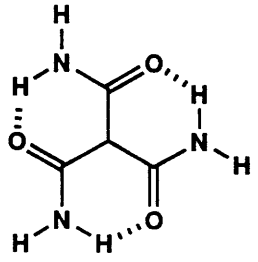

atom	x	y	z
O(1)	-0.0893(1)	0.30358(9)	0.856
O(2)	0.0128(1)	0.3554(1)	1.2941(6)
O(3)	-0.0862(1)	0.4422(1)	1.0262(6)
N(1)	0.0216(1)	0.2739(1)	0.8163(7)
N(2)	-0.0710(1)	0.4406(1)	0.6241(7)
N(3)	0.0857(1)	0.4220(1)	1.1346(8)
C(1)	-0.0262(1)	0.3146(1)	0.8440(8)
C(2)	0.0018(1)	0.3774(1)	0.8705(8)
C(3)	-0.0563(1)	0.4233(1)	0.8468(9)
C(4)	0.0341(1)	0.3839(1)	1.1215(8)
H(1)	0.040	0.387	0.748
H(2)	0.017	0.235	0.801
H(3)	0.067	0.279	0.805
H(4)	-0.052	0.426	0.479
H(6)	0.102	0.432	1.294
H(5)	-0.112	0.463	0.585
H(7)	0.095	0.452	1.026

Appendix 2

X-ray Crystalography: Atom Coordinates

***Trans*-cyclopropanetricarboxamide (Part I, Chapter 1.2, structure 2a).**

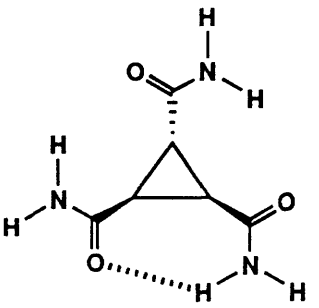

atom	x	y	z
O(2)	0.1881(2)	0.2844(1)	0.9654(1)
O(3)	0.3237(2)	0.4100(1)	0.4954(1)
O(4)	0.2633(2)	0.5792(1)	0.9710(2)
N(1)	-0.0275(2)	0.5804(2)	0.8198(2)
N(2)	-0.0371(2)	0.1955(2)	0.7678(2)
N(3)	0.5863(2)	0.3839(1)	0.6984(2)
C(1)	0.1672(2)	0.4836(2)	0.7177(2)
C(2)	0.1472(2)	0.3408(2)	0.7034(2)
C(3)	0.3271(2)	0.4031(2)	0.7538(2)
C(4)	0.1398(2)	0.5519(2)	0.8492(2)
C(5)	0.1019(2)	0.2708(2)	0.8230(2)
C(6)	0.4127(2)	0.3995(1)	0.6386(2)
H(1)	0.123(3)	0.524(2)	0.620(2)
H(2)	0.095(2)	0.309(2)	0.596(2)
H(3)	0.401(3)	0.396(2)	0.856(2)
H(4)	-0.077(3)	0.151(2)	0.834(2)
H(5)	-0.100(3)	0.189(2)	0.673(2)
H(6)	0.643(3)	0.384(2)	0.799(3)
H(7)	0.639(3)	0.378(2)	0.638(3)
H(8)	-0.046(3)	0.623(2)	0.891(2)
H(9)	-0.110(4)	0.572(2)	0.721(3)

Appendix 3

X-ray Crystalography: Atom Coordinates

Cis-cyclopropanetricarboxamide (Part I, Chapter 1.2, structure 2b).

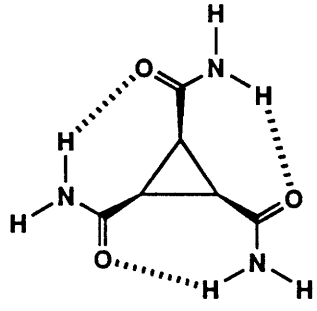

atom	x	y	z
O(1)	-0.2369(8)	0.0029(4)	0.5979(4)
O(2)	0.1439(7)	0.1597(4)	0.7680(3)
O(3)	0.0380(8)	0.3747(4)	0.5684(3)
N(1)	-0.090(1)	0.1496(4)	0.5015(4)
N(2)	-0.043(1)	0.1189(5)	0.9172(4)
N(3)	0.0571(9)	0.4425(4)	0.7434(4)
C(1)	-0.361(1)	0.1940(5)	0.6382(4)
C(2)	-0.290(1)	0.2156(5)	0.7614(4)
C(3)	-0.284(1)	0.3109(5)	0.6775(4)
C(4)	-0.217(1)	0.1073(6)	0.5790(4)
C(5)	-0.046(1)	0.1640(5)	0.8163(4)
C(6)	-0.042(1)	0.3765(5)	0.6593(5)
H(1)	-0.5413	0.1876	0.6162
H(2)	-0.4248	0.2177	0.8043
H(3)	-0.4253	0.3618	0.6752
H(6)	-0.0223	0.4481	0.8157
H(4)	-0.0574	0.2357	0.4968
H(7)	0.1604	0.4955	0.7312
H(5)	0.0237	0.0870	0.4688
H(8)	0.1186	0.0833	0.9581
H(9)	-0.1380	0.1366	0.9775

Appendix 4

X-ray Crystalography: Atom Coordinates

Tennis Ball (Part I, Chapter 4, structure 1).

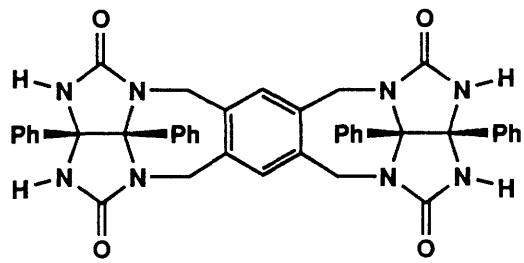

ATOM	x	y	z	<u Squared>
C(1)	0.2711(21)	0.3282(19)	0.2087(12)	0.040(8)
N(2)	0.2405(17)	0.2599(16)	0.2413(10)	0.050(8)
C(3)	0.2228(20)	0.2056(21)	0.2119(12)	0.039(9)
O(4)	0.2038(14)	0.1344(14)	0.2289(8)	0.054(6)
N(5)	0.2217(15)	0.2501(15)	0.1568(9)	0.036(7)
C(6)	0.2528(20)	0.3273(19)	0.1466(11)	0.040(8)
N(7)	0.3449(16)	0.3128(15)	0.1164(9)	0.038(7)
C(8)	0.4064(25)	0.3055(22)	0.1513(14)	0.064(10)
O(9)	0.4931(16)	0.2850(14)	0.1349(8)	0.061(7)
N(10)	0.3642(17)	0.3236(16)	0.2031(10)	0.048(7)
C(11)	0.2288(20)	0.1885(19)	0.1096(11)	0.046(9)
H(11A)	0.2018	0.2328	0.0739	0.060
H(11B)	0.1866	0.1441	0.1253	0.060
C(12)	0.3250(19)	0.1318(18)	0.0932(10)	0.028(8)
C(13)	0.3468(22)	0.0373(21)	0.1021(12)	0.053(10)
H(13)	0.2924	0.0077	0.1208	0.060
C(14)	0.4351(20)	-0.0226(18)	0.0882(11)	0.028(8)
C(15)	0.5090(20)	0.0133(18)	0.0662(11)	0.034(8)
C(16)	0.4850(21)	0.1107(19)	0.0575(11)	0.045(9)
H(16)	0.5399	0.1403	0.0403	0.070
C(17)	0.3916(20)	0.1724(19)	0.0707(11)	0.036(9)
C(18)	0.3715(21)	0.2704(19)	0.0611(11)	0.041(9)
H(18A)	0.4330	0.2860	0.0389	0.050
H(18B)	0.3150	0.2989	0.0364	0.050
C(19)	0.4532(19)	-0.1199(18)	0.1028(11)	0.035(8)
H(19A)	0.3881	-0.1325	0.1206	0.050
H(19B)	0.4799	-0.1514	0.0646	0.050
N(20)	0.5232(17)	-0.1629(15)	0.1442(9)	0.042(7)
C(21)	0.4874(22)	-0.1593(19)	0.2003(12)	0.038(9)
O(22)	0.4085(15)	-0.1387(13)	0.2181(8)	0.056(6)
N(23)	0.5671(18)	-0.1899(16)	0.2255(10)	0.050(8)
C(24)	0.6468(20)	-0.1847(19)	0.1923(11)	0.032(8)
N(25)	0.6723(16)	-0.1055(16)	0.1907(10)	0.047(7)

C(26)	0.6699(23)	-0.0545(23)	0.1417(14)	0.062(11)
O(27)	0.6823(14)	0.0249(14)	0.1284(8)	0.058(7)
N(28)	0.6429(15)	-0.0937(14)	0.1032(9)	0.029(6)
C(29)	0.6066(20)	-0.0402(19)	0.0544(11)	0.043(9)
H(29A)	0.6464	0.0060	0.0374	0.030
H(29B)	0.6131	-0.0857	0.0242	0.030
C(30)	0.6170(22)	-0.1725(20)	0.1300(12)	0.043(9)
C(2P)	0.2449(13)	0.5058(19)	0.2114(8)	0.092(14)
C(3P)	0.1918(13)	0.5884(19)	0.2319(8)	0.108(15)
C(4P)	0.1107(13)	0.5933(19)	0.2695(8)	0.102(14)
C(5P)	0.0827(13)	0.5156(19)	0.2866(8)	0.122(16)
C(6P)	0.1358(13)	0.4330(19)	0.2661(8)	0.099(14)
C(1P)	0.2169(13)	0.4281(19)	0.2285(8)	0.047(9)
H(2P)	0.3078	0.5020	0.1823	0.100
H(3P)	0.2135	0.6486	0.2188	0.100
H(4P)	0.0696	0.6573	0.2855	0.100
H(5P)	0.0199	0.5194	0.3157	0.100
H(6P)	0.1141	0.3728	0.2793	0.100
C(12P)	0.0922(15)	0.4123(12)	0.1222(7)	0.052(10)
C(13P)	0.0276(15)	0.4896(12)	0.0994(7)	0.078(13)
C(14P)	0.0560(15)	0.5637(12)	0.0725(7)	0.066(11)
C(15P)	0.1491(15)	0.5604(12)	0.0684(7)	0.080(12)
C(16P)	0.2137(15)	0.4830(12)	0.0913(7)	0.053(10)
C(11P)	0.1852(15)	0.4090(12)	0.1182(7)	0.033(8)
H(12P)	0.0702	0.3549	0.1431	0.070
H(13P)	-0.0444	0.4921	0.1025	0.070
H(14P)	0.0060	0.6236	0.0548	0.070
H(15P)	0.1711	0.6177	0.0476	0.070
H(16P)	0.2857	0.4805	0.0881	0.070
C(22P)	0.6325(11)	-0.3243(15)	0.1042(7)	0.054(10)
C(23P)	0.6808(11)	-0.4038(15)	0.0789(7)	0.085(12)
C(24P)	0.7668(11)	-0.4115(15)	0.0460(7)	0.059(11)
C(25P)	0.8047(11)	-0.3398(15)	0.0383(7)	0.066(11)
C(26P)	0.7564(11)	-0.2603(15)	0.0635(7)	0.079(12)
C(21P)	0.6704(11)	-0.2526(15)	0.0965(7)	0.040(8)
H(22P)	0.5659	-0.3183	0.1297	0.100
H(23P)	0.6515	-0.4593	0.0849	0.100
H(24P)	0.8042	-0.4731	0.0264	0.100
H(25P)	0.8713	-0.3458	0.0127	0.100
H(26P)	0.7857	-0.2048	0.0576	0.100
C(32P)	0.8176(18)	-0.2674(14)	0.1886(8)	0.076(12)
C(33P)	0.8899(18)	-0.3484(14)	0.1974(8)	0.120(16)
C(34P)	0.8696(18)	-0.4288(14)	0.2197(8)	0.092(13)
C(35P)	0.7769(18)	-0.4282(14)	0.2330(8)	0.145(18)
C(36P)	0.7046(18)	-0.3472(14)	0.2242(8)	0.069(12)
C(31P)	0.7249(18)	-0.2668(14)	0.2019(8)	0.042(9)
H(32P)	0.8333	-0.2052	0.1713	0.070
H(33P)	0.9617	-0.3489	0.1870	0.070
H(34P)	0.9256	-0.4915	0.2265	0.070
H(35P)	0.7612	-0.4905	0.2503	0.070
H(36P)	0.6328	-0.3468	0.2346	0.070
C(51)	0.7081(20)	0.1920(19)	0.2249(11)	0.034(8)
N(52)	0.6132(18)	0.2535(16)	0.2217(10)	0.051(8)
C(53)	0.5602(25)	0.2750(22)	0.2730(14)	0.053(10)
O(54)	0.4813(16)	0.3160(14)	0.2819(8)	0.061(7)
N(55)	0.6280(17)	0.2444(15)	0.3104(9)	0.042(7)

C(56)	0.7170(22)	0.1898(21)	0.2902(12)	0.049(9)
N(57)	0.7335(15)	0.0928(15)	0.3065(9)	0.043(7)
C(58)	0.7290(21)	0.0322(22)	0.2659(13)	0.049(9)
O(59)	0.7289(14)	-0.0402(15)	0.2736(8)	0.061(7)
N(60)	0.7191(17)	0.0957(17)	0.2178(10)	0.056(8)
C(61)	0.5870(20)	0.2417(18)	0.3717(11)	0.044(9)
H(61A)	0.6397	0.2431	0.3950	0.060
H(61B)	0.5260	0.3004	0.3785	0.060
C(62)	0.5608(21)	0.1542(20)	0.3926(11)	0.040(9)
C(63)	0.4675(23)	0.1629(22)	0.4121(12)	0.054(10)
H(63)	0.4194	0.2315	0.4114	0.070
C(64)	0.4312(22)	0.0913(21)	0.4315(12)	0.039(9)
C(65)	0.5012(21)	-0.0005(19)	0.4299(11)	0.038(8)
C(66)	0.5915(21)	-0.0103(20)	0.4101(11)	0.041(9)
H(66)	0.6408	-0.0783	0.4116	0.050
C(67)	0.6254(22)	0.0651(22)	0.3899(12)	0.052(9)
C(68)	0.7249(19)	0.0529(19)	0.3655(11)	0.040(9)
H(68A)	0.7533	0.0873	0.3892	0.060
H(68B)	0.7632	-0.0191	0.3688	0.060
C(69)	0.3330(20)	0.1034(20)	0.4469(12)	0.046(9)
H(69A)	0.3246	0.0702	0.4887	0.070
H(69B)	0.2946	0.1752	0.4464	0.070
N(70)	0.2934(16)	0.0619(16)	0.4113(10)	0.040(7)
C(71)	0.2597(23)	0.1136(25)	0.3653(14)	0.068(11)
O(72)	0.2550(14)	0.1919(14)	0.3539(8)	0.055(6)
N(73)	0.2437(19)	0.0535(20)	0.3351(11)	0.071(9)
C(74)	0.2831(21)	-0.0418(20)	0.3535(12)	0.035(9)
N(75)	0.3692(19)	-0.0851(16)	0.3254(10)	0.059(8)
C(76)	0.4445(27)	-0.1142(23)	0.3532(14)	0.063(11)
O(77)	0.5268(17)	-0.1499(15)	0.3413(9)	0.077(8)
N(78)	0.4048(17)	-0.0900(15)	0.4094(9)	0.043(7)
C(79)	0.4681(22)	-0.0845(20)	0.4455(13)	0.057(10)
H(79A)	0.4356	-0.0852	0.4883	0.060
H(79B)	0.5301	-0.1430	0.4413	0.060
C(80)	0.3144(22)	-0.0331(21)	0.4127(12)	0.044(9)
C(42P)	0.8582(18)	0.1657(12)	0.1555(10)	0.091(14)
C(43P)	0.9229(18)	0.1992(12)	0.1185(10)	0.111(16)
C(44P)	0.9107(18)	0.2927(12)	0.1101(10)	0.098(13)
C(45P)	0.8337(18)	0.3528(12)	0.1388(10)	0.095(13)
C(46P)	0.7690(18)	0.3194(12)	0.1758(10)	0.075(11)
C(41P)	0.7812(18)	0.2258(12)	0.1842(10)	0.061(11)
H(42P)	0.8676	0.0933	0.1620	0.110
H(43P)	0.9825	0.1526	0.0963	0.110
H(44P)	0.9608	0.3186	0.0814	0.110
H(45P)	0.8242	0.4253	0.1323	0.110
H(46P)	0.7094	0.3659	0.1980	0.110
C(52P)	0.8875(16)	0.1610(10)	0.2897(7)	0.057(10)
C(53P)	0.9603(16)	0.1918(10)	0.2963(7)	0.066(11)
C(54P)	0.9407(16)	0.2787(10)	0.3122(7)	0.083(12)
C(55P)	0.8484(16)	0.3349(10)	0.3215(7)	0.088(12)

C(56P)	0.7757(16)	0.3041(10)	0.3149(7)	0.062(10)
C(51P)	0.7952(16)	0.2171(10)	0.2990(7)	0.041(9)
H(52P)	0.9026	0.0936	0.2773	0.090
H(53P)	1.0317	0.1483	0.2890	0.090
H(54P)	0.9970	0.3026	0.3173	0.090
H(55P)	0.8333	0.4022	0.3339	0.090
H(56P)	0.7042	0.3476	0.3221	0.090
C(62P)	0.2797(11)	-0.1622(13)	0.4836(8)	0.057(10)
C(63P)	0.2231(11)	-0.1949(13)	0.5274(8)	0.092(13)
C(64P)	0.1385(11)	-0.1358(13)	0.5498(8)	0.073(11)
C(65P)	0.1105(11)	-0.0440(13)	0.5284(8)	0.072(12)
C(66P)	0.1671(11)	-0.0113(13)	0.4846(8)	0.063(11)
C(61P)	0.2517(11)	-0.0704(13)	0.4622(8)	0.044(8)
H(62P)	0.3452	-0.2080	0.4663	0.080
H(63P)	0.2448	-0.2660	0.5440	0.080
H(64P)	0.0947	-0.1611	0.5837	0.080
H(65P)	0.0450	0.0018	0.5457	0.080
H(66P)	0.1454	0.0598	0.4681	0.080
C(72P)	0.1183(17)	-0.0430(11)	0.3598(8)	0.085(13)
C(73P)	0.0576(17)	-0.0933(11)	0.3615(8)	0.100(14)
C(74P)	0.0930(17)	-0.1872(11)	0.3580(8)	0.104(15)
C(75P)	0.1891(17)	-0.2307(11)	0.3529(8)	0.140(18)
C(76P)	0.2499(17)	-0.1804(11)	0.3513(8)	0.083(12)
C(71P)	0.2145(17)	-0.0866(11)	0.3548(8)	0.036(9)
H(72P)	0.0909	0.0297	0.3625	0.120
H(73P)	-0.0169	-0.0595	0.3654	0.120
H(74P)	0.0459	-0.2261	0.3592	0.120
H(75P)	0.2165	-0.3034	0.3502	0.120
H(76P)	0.3244	-0.2142	0.3474	0.120
C(4S)	0.1329(47)	-0.1336(45)	0.2099(25)	0.167(24)
C(8S)	0.4508(34)	0.5386(34)	0.2361(20)	0.128(18)
CL(1S)	0.1108(14)	-0.0103(13)	0.1996(7)	0.231
CL(2S)	-0.0026(15)	-0.1107(13)	0.2177(7)	0.229
CL(3S)	0.1698(20)	-0.1707(13)	0.1484(9)	0.331
CL(5S)	0.4957(11)	0.5046(11)	0.1683(6)	0.175
CL(6S)	0.4136(11)	0.6527(9)	0.2336(7)	0.169
CL(7S)	0.5607(12)	0.5025(10)	0.2686(8)	0.211
CL(9S)	0.6381(27)	0.2649(26)	-0.0347(16)	0.179(16)
CL(10)	0.7016(20)	0.3391(21)	0.0428(11)	0.123(10)
CL(12)	0.5575(36)	0.4410(32)	0.0067(21)	0.236(23)
CL(13)	0.6467(26)	0.4074(24)	0.0328(13)	0.110(11)
CL(14)	0.7611(38)	0.2260(36)	0.0239(21)	0.202(22)
CL(16)	0.5905(19)	0.3193(19)	-0.0392(10)	0.106(9)
C(17S)	0.7390(59)	0.1755(53)	0.0112(31)	0.057(26)
C(18S)	0.6782(71)	0.2454(68)	0.0308(37)	0.121(33)
C(19S)	0.6172(50)	0.3127(51)	0.0280(27)	0.000(19)
C(1F)	0.2801(37)	0.2527(36)	0.6386(20)	0.131(19)
C(2F)	0.2183(49)	0.3274(51)	0.6462(26)	0.186(27)
C(3F)	0.1712(35)	0.3924(35)	0.6207(21)	0.139(20)
C(4F)	0.1154(39)	0.2459(34)	0.6685(21)	0.113(21)

C(5F)	0.1849(43)	0.2306(36)	0.6529(22)	0.149(20)
C(1U)	0.2745(32)	0.3947(30)	0.3771(18)	0.115(17)
C(2U)	0.3318(26)	0.4349(25)	0.3662(15)	0.079(12)
C(3U)	0.3168(54)	0.5255(51)	0.4079(30)	0.281(36)
C(4U)	0.1915(47)	0.5383(43)	0.4200(25)	0.207(28)
C(1E)	0.0610(**)	0.3873(**)	0.4775(**)	0.792(**)
CL(2E)	0.9493(34)	0.4310(31)	0.4278(18)	0.165(18)
CL(3E)	0.0511(43)	0.2581(40)	0.4410(26)	0.196(25)
CL(5E)	-0.0322(**)	0.3439(**)	0.5002(73)	0.728(**)
CL(6E)	0.0060(**)	0.2503(79)	0.4918(57)	0.221(66)
CL(7E)	0.0854(42)	0.2976(44)	0.4248(25)	0.212(28)
CL(8E)	-0.0827(96)	0.3097(**)	0.5262(61)	0.731(83)
CL(9E)	-0.1095(50)	0.3887(46)	0.4520(30)	0.274(30)
C(1G)	0.1298(67)	0.0721(65)	0.9566(39)	0.174(35)
CL(4G)	0.0977(36)	-0.0192(37)	0.9537(22)	0.312(26)
CL(1G)	0.1464(12)	0.0597(11)	0.0213(7)	0.086(5)
CL(2G)	0.0253(13)	0.1785(12)	0.9538(7)	0.122(6)
CL(3G)	0.0789(21)	0.0666(21)	0.9213(12)	0.191(11)
O(4W)	0.1737(24)	0.1969(22)	0.5809(14)	0.169(14)
O(7W)	0.5386(32)	0.3767(29)	0.5947(18)	0.214(20)
C(7W)	0.4676(38)	0.3518(35)	0.6049(21)	0.144(20)
O(8W)	0.4680(22)	0.3523(21)	0.5216(13)	0.155(12)
O(9W)	0.6277(25)	0.5188(24)	0.4118(14)	0.169(14)
H(9W1)	0.3346	0.4528	0.6125	0.210
H(9W2)	0.3940	0.5317	0.5747	0.210
O(10W)	0.2707(27)	0.2649(26)	0.5581(16)	0.201(16)
O(12W)	0.2477(32)	0.3965(30)	0.4608(19)	0.255(20)

Appendix 4

X-ray Crystalography: Atom Coordinates

3,6-Di-*tert*-butylcarbazole-1,8-bis[(S)-5-*iso*-propyl-2-oxazoline] (Part II, Chapter 7, structure 8a).

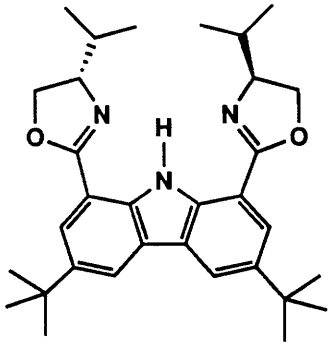

atom	x	y	z
O(1)	0.3509(5)	0.1760(5)	1.0433(3)
O(2)	0.7859(6)	0.2938(6)	0.7102(4)
N(1)	0.5812(6)	0.1476(5)	0.8679(4)
N(2)	0.4723(7)	0.2589(6)	0.9767(4)
N(3)	0.6718(7)	0.3180(6)	0.8018(4)
C(1)	0.4584(7)	0.0778(7)	0.9635(5)
C(2)	0.4151(7)	-0.0092(7)	0.9889(4)
C(3)	0.4479(8)	-0.1072(7)	0.9625(5)
C(4)	0.5203(8)	-0.1106(7)	0.9079(5)
C(5)	0.5332(7)	0.0690(8)	0.9070(5)
C(6)	0.5628(8)	-0.0257(7)	0.8796(5)
C(7)	0.6349(8)	-0.0019(7)	0.8211(5)
C(8)	0.6456(7)	0.1021(7)	0.8170(4)
C(9)	0.6916(8)	-0.0619(8)	0.7733(6)
C(10)	0.759(1)	-0.022(1)	0.7239(7)
C(11)	0.7661(8)	0.082(1)	0.7207(5)
C(12)	0.7100(8)	0.1492(8)	0.7656(5)
C(13)	0.7180(8)	0.2594(8)	0.7618(5)
C(14)	0.7107(9)	0.4195(9)	0.7848(6)
C(15)	0.773(1)	0.399(1)	0.7152(7)
C(16)	0.4299(7)	0.1748(7)	0.9931(5)
C(17)	0.3324(8)	0.2816(7)	1.0604(6)
C(18)	0.4250(8)	0.3367(7)	1.0222(5)
C(31)	0.392(1)	-0.2015(8)	0.9967(7)
C(32)	0.432(2)	-0.209(1)	1.0711(7)
C(33)	0.269(1)	-0.201(1)	0.9944(9)
C(34)	0.420(1)	-0.2971(8)	0.9593(8)
C(141)	0.616(1)	0.496(1)	0.7787(6)

C(142)	0.546(1)	0.4980(9)	0.8432(6)
C(143)	0.658(1)	0.595(1)	0.7511(8)
C(181)	0.508(1)	0.3828(8)	1.0745(7)
C(182)	0.452(1)	0.464(1)	1.1204(7)
C(183)	0.609(1)	0.419(1)	1.0379(7)
H(1)	0.571	0.217	0.877
H(2)	0.360	-0.008	1.024
H(3)	0.538	-0.176	0.890
H(4)	0.677	-0.137	0.777
H(5)	0.811	0.115	0.688
H(6)	0.761	0.442	0.822
H(7)	0.735	0.428	0.679
H(8)	0.845	0.432	0.720
H(9)	0.340	0.289	1.112
H(10)	0.261	0.303	1.048
H(11)	0.392	0.387	0.993
H(12)	0.392	-0.270	1.092
H(13)	0.403	-0.154	1.098
H(14)	0.504	-0.219	1.075
H(15)	0.240	-0.186	0.949
H(16)	0.243	-0.139	1.024
H(17)	0.236	-0.254	1.015
H(18)	0.394	-0.294	0.914
H(19)	0.382	-0.350	0.985
H(20)	0.496	-0.308	0.963
H(21)	0.572	0.471	0.742
H(22)	0.490	0.539	0.838
H(23)	0.596	0.517	0.882
H(24)	0.526	0.429	0.852
H(25)	0.688	0.596	0.711
H(26)	0.704	0.625	0.790
H(27)	0.591	0.642	0.754
H(28)	0.533	0.331	1.103
H(29)	0.421	0.517	1.089
H(30)	0.501	0.493	1.151
H(31)	0.391	0.435	1.144
H(32)	0.644	0.369	1.009
H(33)	0.661	0.448	1.068
H(34)	0.590	0.474	1.002
C(101)	0.8180(7)	-0.0773(6)	0.6644(4)
C(102)	0.9392(8)	-0.089(1)	0.6874(6)
C(103)	0.7659(9)	-0.1822(8)	0.6555(6)
C(104)	0.813(1)	-0.0203(7)	0.5940(6)